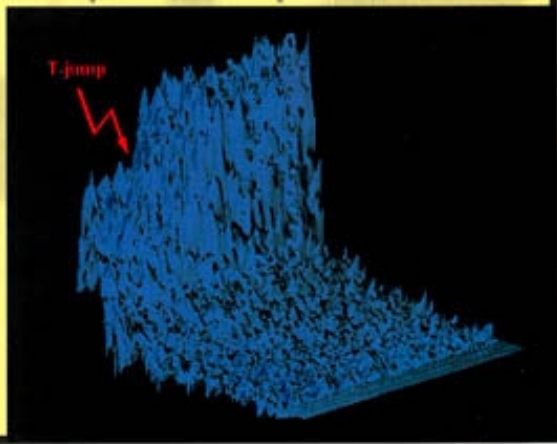
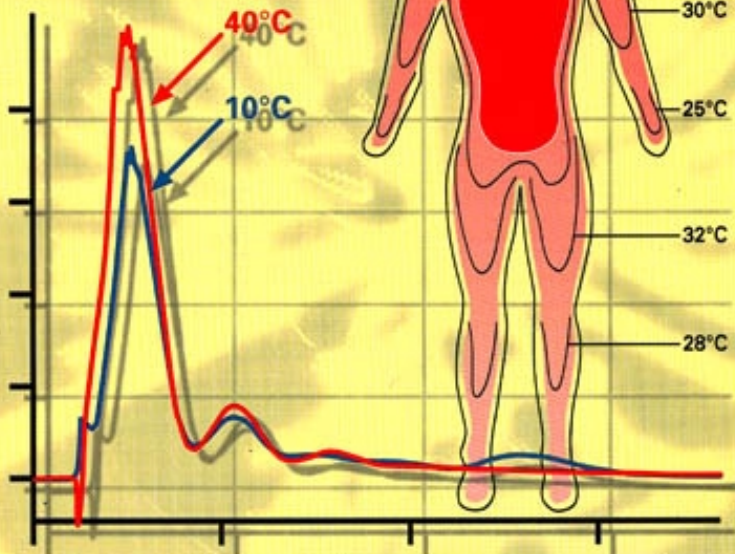
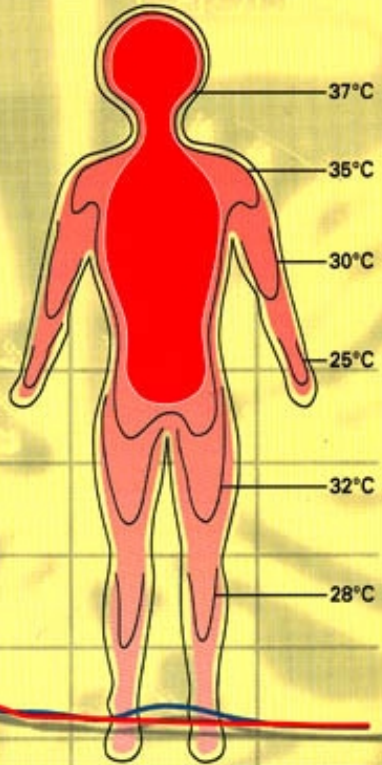




# ANNUAL REPORT 1998



AUSTRIAN SAXS BEAMLIN AT 

Extracted from the user contribution Pregetter et al.: *Time-Resolved X-ray diffraction of the Core Lipid Transition of Human Low Density Lipoproteins*

# **Austrian Small Angle X-ray Scattering (SAXS) Beamline at ELETTRA**

## **Annual Report 1998**

Compiled by the SAXS-Group:

- for IBR: M. Rappolt & H. Amenitsch
- for ELETTRA: S. Bernstorff

## Table of Contents

	<i>page</i>
➤ <b>Preface</b>	<i>1</i>
➤ <b>The SAXS-Group</b>	<i>3</i>
➤ <b>The SAXS-Beamline in General</b>	<i>4</i>
➤ <b>Application for Beamtime at ELETTRA</b>	<i>8</i>
➤ <b>List of Institutes Participating in Experiments</b>	<i>10</i>
➤ <b>List of Performed Experiments</b>	<i>17</i>
➤ <b>User Statistics</b>	<i>21</i>
➤ <b>Experimental Possibilities at the SAXS-beamline</b>	<i>25</i>
1. Installation of a 2D CCD-camera system	<i>25</i>
2. Accessible SAXS and WAXS ranges	<i>27</i>
3. Available sample manipulation stages	<i>28</i>
➤ <b>User Contributions</b>	<i>32</i>
1. Material Sciences	<i>33</i>
2. Life Sciences	<i>43</i>
3. Physics	<i>82</i>
4. Chemistry	<i>97</i>
5. Instrumentation	<i>102</i>
➤ <b>Publications</b>	<i>114</i>
➤ <b>Author Index</b>	<i>130</i>

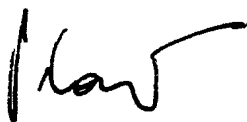
## PREFACE

Thanks to the efforts of all parties and individuals involved - in the end it is always the individuals our SAXS station at ELETTRA has established itself as a recognized, internationally visible player. In this Annual Report we present the abstracts of achievements by the users, the Italian and Austrian station staff and, last but not least, the ELETTRA machine division, who provide US with excellent and reliable beam conditions.

The Austrian ELETTRA/SAXS project is on target. This is best visible from the user statistics showing a remarkable increase in the number and quality of projects. The station has become a point of reference for the European scientific community in the field of nanostructure research, and attracts increasingly also colleagues from beyond Europe.

At about mid-time of the original five-years' plan it is time to think about the future development. It appears that the versatility in terms of optical properties for different needs and in terms of different sample treatments (temperature, pressure, magnetic field, etc.) has reached a satisfactory level and calls for intense exploitations. It seems that increasing demands in the future will arise from high-throughput screening projects following the approach of combinatorial chemistry and materials research. This has been first expressed at the Workshop on Antimicrobial Peptides, organized jointly by ELETTRA and IBR in November 1997, co-chaired by Prof. Paolo Fasella we sincerely miss him - and myself.

The search for new properties and tailored activities in pharmaceuticals, cosmetics, etc. will certainly boost the demand for automation. This goes along with better detectors and artificial-intelligence supported data evaluation. We believe that this will be one focal point of new activities, and the users are invited to express their opinions and wishes on that issue, to make the SAXS station a continuing source of successful work.



Peter Laggner  
Director  
Institute of Biophysics and X-Ray Structure Research  
Austrian Academy of Sciences



It is a pleasure for me to congratulate all the people involved in the day to day management of the Austrian SAXS beamline at Elettra for one more year of smooth operation, outstanding scientific results and satisfied users.

The best evidence of the success of the SAXS beamline is the very heavy user demand: in 1998, 2.5 times more shifts were requested than the available ones. Requests come from a very wide geographical distribution of users and cover a variety of disciplines in the biomedical and in the physical and chemical sciences.

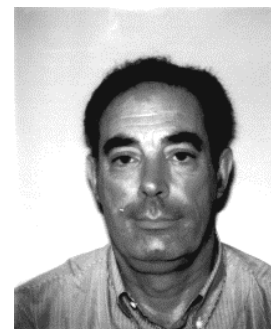
In addition, the beamline also serves for significant instrumentation developments, especially as far detectors and sample environment are concerned. This work is certainly challenging, because it is not easy to have instrumentation at the very top level for the wide variety of scientific fields and techniques that the beamline can serve. It is also very important, because the challenges from the worldwide competition from other third generation synchrotron light sources are growing, and no one can afford to sit down and relax in contemplation in what has been achieved.

The reader of this report will appreciate the scientific output of the beamline, which is in my opinion very satisfactory from the qualitative as well as from the quantitative point of view. I would like to add that, as a late evening and week-end visitor in the Elettra experimental hall, I always found the SAXS beamline as busy as a beehive, with good humoured and enthusiastic staff and users.

I cannot conclude without mentioning that this successful scientific enterprise, realised through the daily side-by-side hard work of people from many different countries, makes me even more optimistic about the future of Europe.



Massimo Altarelli  
Director  
Elettra Synchrotron Light Source



# The SAXS-Group

- HEAD OF PROJECT: Peter Laggner<sup>1)</sup>  
e-mail: fibrlagg@mbox.tu-graz.ac.at
- SCIENTISTS: Heinz Amenitsch<sup>1), 3)</sup>  
e-mail: Amenitsch@Elettra.Trieste.It  
Sigrid Bernstorff <sup>2)</sup>  
e-mail: Bernstorff@Elettra.Trieste.It
- POSTDOCS: Pavo Dubcek<sup>2)</sup>  
e-mail: Pavo.Dubcek@Elettra.Trieste.It  
Ralf Menk<sup>2)</sup>  
e-mail: Ralf.Menk@Elettra.Trieste.It  
Michael Rappolt<sup>1), 3)</sup>  
e-mail: Michael.Rappolt@Elettra.Trieste.It
- PhD-STUDENTS: Georg Pabst<sup>1), 3)</sup>  
e-mail: Georg.Pabst@Elettra.Trieste.It

- 1) Institute for Biophysics and X-ray Structure Research, Austrian Academy of Sciences, Steyrergasse 17, 8010 Graz, Austria.  
*Tel 0043-316-812 004*  
*Fax 0043-316-812 367*
- 2) Sincrotrone Trieste, Strada Statale 14, km 163.5, 34012 Basovizza (TS), Italy.  
*Tel 0039-040-375 81*  
*Fax 0039-040-938 0902*
- 3) Institute for Biophysics and X-ray Structure Research, Austrian Academy of Sciences  
c/o Sincrotrone Trieste

# The SAXS-Beamline in General

Small Angle X-ray Scattering has become a well known standard method to study the structure of various objects in the spatial range from 1 to 1000 nm, and therefore instruments capable to perform such experiments are installed at most of the synchrotron research centers. The high-flux SAXS beamline at ELETTRA is mainly intended for time-resolved studies on fast structural transitions in the sub-millisecond time region in solutions and partly ordered systems with a SAXS-resolution of 1 to 140 nm in real-space.

The photon source is the 57-pole wiggler whose beam is shared and used simultaneously with a Macromolecular Crystallography beamline. The wiggler delivers a very intense radiation between 4 and 25 keV of which the SAXS-Beamline accepts 3 discrete energies, namely 5.4, 8 and 16 keV. The beamline optics consists of a flat double crystal monochromator and a double focusing toroidal mirror.

A versatile SAXS experimental station has been set-up, and an additional wide-angle X-ray scattering (WAXS) detector monitors simultaneously diffraction patterns in the range from 0.1 to 0.9 nm. The sample station is mounted move-able onto an optical table for optimising the sample detector distance with respect to SAXS resolution and sample size.

Besides the foreseen sample surrounding the users have the possibility to install their own specialised sample equipment. In the design phase, besides technical boundary conditions, user friendliness and reliability have been considered as important criteria.

The optimisation of the beamline with respect to high-flux and consequently high flux density, allows to perform the following experiments:

- Low Contrast Solution Scattering
- Grazing Incidence Surface Diffraction
- Micro-Spot Scanning
- X-ray Fluorescence Analysis
- Time-Resolved Studies  $\geq 11 \mu\text{s}$
- Simultaneously Performed Small- and Wide-Angle Measurements (SWAXS) on:
  - Gels
  - Liquid Crystals
  - (Bio) Polymers
  - Amorphous Materials
  - Muscles

Furthermore, using 5.4 and 16 keV energies, the beamline is widely applicable also to very thin, e.g. single muscle fibers, and optically thick (high Z) specimen, as often used in e.g., material science and solid state physics.

## THE INSERTION DEVICE

The wiggler for the SAXS beamline consists of three 1.5 m long segments, each having 19 poles. The device can work with a minimum gap of 20 mm, which corresponds to  $K=20$  at 2 GeV. The main parameters of the wiggler are:

- Critical Energy 4.1 keV
- Radiation Power 8.6 kW
- Flux  $3.5 \times 10^{14}$  ph/s/mrad/0.1%BW (at 400 mA)

The wiggler radiation cone has a horizontal width of 9 mrad. From this the SAXS-beamline accepts vertically 0.3 mrad, and horizontally +/-0.5 mrad at a 1.25 mrad off-axis position. The resulting source size for 8 keV photons is  $3.9 \times 0.26 \text{ mm}^2$  (horiz. x vert.).

## THE OPTICS

The optics common with the diffraction beamline consists of:

- C-Filter and Beryllium window assembly to reduce the power load on the first optical elements by a factor of 2 and to separate the beamline vacuum from the storage ring.
- Beam defining slit chamber which allows to define the SAXS beam on three sides before the monochromator in order to reduce the straylight in the downstream beamline sections.

The SAXS beamline optics consists of:

- A double-crystal monochromator consisting of four individual chambers, in which three interchangeable asymmetric Si(111) crystal pairs are used to select one of three fixed energies. Each of the crystal pairs is optimised for the corresponding energy to accomplish a grazing angle of  $2^\circ$ . The energy resolution  $\Delta E/E$  of the monochromator is in the range of  $0.7 - 2.5 \cdot 10^{-3}$ .
- A baffle chamber after the monochromator is used as an adjustable straylight fenditure.
- A segmented toroidal mirror focuses the light in horizontal and vertical direction with a 1/2.5 magnification onto the SAXS-detector.
- An aperture slit reduces the straylight after the monochromator and the toroidal mirror.
- A guard slit defines the illuminated region around the focal spot. The spot size on the detector is 1.6 mm horizontally and 0.6 mm vertically. The calculated flux at the sample is in the order of  $10^{13}$  ph/s at 400 mA. For a maximum sample size of  $5.4 \times 1.8 \text{ mm}^2$  correspondingly a flux density of  $10^{12}$  ph/s/ $\text{mm}^2$  has been calculated.

## SAMPLE STAGE

The multipurpose sample stage allows to perform fast time-resolved relaxation studies based on temperature- or pressure-jumps as well as stopped flow experiments. Shear jump relaxation experiments are planned. Specifically, T-jumps can be induced by an infra-red light pulse (2 ms) from an Erbium-Glass laser, raising the temperature about  $20^\circ \text{C}$  in an aqueous sample volume of  $10 \mu\text{l}$ . A newly designed hydrostatic pressure cell with a maximal accessible angular range of  $30^\circ$  for simultaneous SAXS and WAXS measurements is available. P-jumps are realised by switching fast valves between a low and a high pressure reservoir, increasing or decreasing the hydrostatic pressure in the range from 1 bar to 1.7 kbar (in future 3 kbar) within a few ms. Also a 1.5 T magnet has been installed. In an overview, the following sample manipulations are possible:

- Temperature Manipulations: Ramps, Jumps and Gradient Scans
- Pressure Manipulation: Scan and Jumps
- Stopped Flow Experiments
- SWAXS Measurements Applying Mechanical Stress
- SWAXS Measurements Applying Magnetic Fields

(For further details see also Experimental Possibilities part 1.-3.)



<b>Scientific applications</b>	<p>Low Contrast Solution Scattering, Grazing Incidence Surface Diffraction, Micro-Spot Scanning, X-ray Fluorescence Analysis, Time-Resolved Studies <math>\geq 11 \mu\text{s}</math> and Simultaneously Performed Small- and Wide-Angle Measurements (SWAXS) on:</p> <p>Gels Liquid Crystals (Bio) Polymers Amorphous Materials Muscles</p>																								
<b>Source characteristics</b>	<p><u>Wiggler (NdFeB Hybrid):</u></p> <table border="0"> <tr> <td>Period</td> <td>140 mm</td> </tr> <tr> <td>No. full poles</td> <td>57</td> </tr> <tr> <td>Gap</td> <td>20 mm</td> </tr> <tr> <td><math>B_{\text{max}}</math></td> <td>1.607 T</td> </tr> <tr> <td>Critical Energy <math>\epsilon_c</math></td> <td>4.27 keV</td> </tr> <tr> <td>Power (9 mrad)</td> <td>8.6 kW</td> </tr> <tr> <td>Effective source size FWHM</td> <td><math>3.9 \times 0.26 \text{ mm}^2(\text{HxV})</math></td> </tr> </table>	Period	140 mm	No. full poles	57	Gap	20 mm	$B_{\text{max}}$	1.607 T	Critical Energy $\epsilon_c$	4.27 keV	Power (9 mrad)	8.6 kW	Effective source size FWHM	$3.9 \times 0.26 \text{ mm}^2(\text{HxV})$										
Period	140 mm																								
No. full poles	57																								
Gap	20 mm																								
$B_{\text{max}}$	1.607 T																								
Critical Energy $\epsilon_c$	4.27 keV																								
Power (9 mrad)	8.6 kW																								
Effective source size FWHM	$3.9 \times 0.26 \text{ mm}^2(\text{HxV})$																								
<b>Optics</b>	<table border="0"> <tr> <td><u>Optical elements:</u></td> <td>Double crystal monochromator: Si (111) asym. cut, water cooled.</td> <td>Mirror: two-segment, toroidal, Pt coated.</td> </tr> <tr> <td><u>Distance from source:</u></td> <td>18.4 m</td> <td>26.5 m</td> </tr> <tr> <td>Acceptance</td> <td colspan="2">1 mrad/0.3 mrad (HxV)</td> </tr> <tr> <td>Energy (3 selectable)</td> <td colspan="2">5.4, 8, 16 keV (0.077, 0.154, 0.23 nm)</td> </tr> <tr> <td>Energy resolution <math>\Delta E/E</math></td> <td colspan="2"><math>0.7\text{-}2.5 \times 10^{-3}</math></td> </tr> <tr> <td>Focal spot size FWHM</td> <td colspan="2"><math>1.2 \times 0.6 \text{ mm}^2(\text{HxV})</math></td> </tr> <tr> <td>Spot at Sample FWHM</td> <td colspan="2"><math>5.4 \times 1.8 \text{ mm}^2(\text{HxV})</math></td> </tr> <tr> <td>Flux at sample</td> <td colspan="2"><math>5 \times 10^{12} \text{ ph s}^{-1}(2 \text{ GeV}, 200 \text{ mA}, 8 \text{ keV})</math></td> </tr> </table>	<u>Optical elements:</u>	Double crystal monochromator: Si (111) asym. cut, water cooled.	Mirror: two-segment, toroidal, Pt coated.	<u>Distance from source:</u>	18.4 m	26.5 m	Acceptance	1 mrad/0.3 mrad (HxV)		Energy (3 selectable)	5.4, 8, 16 keV (0.077, 0.154, 0.23 nm)		Energy resolution $\Delta E/E$	$0.7\text{-}2.5 \times 10^{-3}$		Focal spot size FWHM	$1.2 \times 0.6 \text{ mm}^2(\text{HxV})$		Spot at Sample FWHM	$5.4 \times 1.8 \text{ mm}^2(\text{HxV})$		Flux at sample	$5 \times 10^{12} \text{ ph s}^{-1}(2 \text{ GeV}, 200 \text{ mA}, 8 \text{ keV})$	
<u>Optical elements:</u>	Double crystal monochromator: Si (111) asym. cut, water cooled.	Mirror: two-segment, toroidal, Pt coated.																							
<u>Distance from source:</u>	18.4 m	26.5 m																							
Acceptance	1 mrad/0.3 mrad (HxV)																								
Energy (3 selectable)	5.4, 8, 16 keV (0.077, 0.154, 0.23 nm)																								
Energy resolution $\Delta E/E$	$0.7\text{-}2.5 \times 10^{-3}$																								
Focal spot size FWHM	$1.2 \times 0.6 \text{ mm}^2(\text{HxV})$																								
Spot at Sample FWHM	$5.4 \times 1.8 \text{ mm}^2(\text{HxV})$																								
Flux at sample	$5 \times 10^{12} \text{ ph s}^{-1}(2 \text{ GeV}, 200 \text{ mA}, 8 \text{ keV})$																								
<b>Experimental apparatus</b>	<p><u>Resolution in real space:</u> 1-140 nm (small-angle), 0.1- 0.9 nm (wide-angle)</p> <p><u>Sample stage:</u> temperature manipulations: ramps, jumps and gradient scans, pressure manipulation: scan and jumps, flow jump experiments, SWAXS measurements applying mechanical stress, SWAXS measurements applying magnetic fields.</p> <p><u>Detectors:</u> 1D gas-filled detectors for simultaneous small- and wide-angle (Gabriel type), 2D CCD-detector for small-angle.</p>																								
<b>Experiment control</b>	<p><u>Beamline control:</u> Program-units written in LabView for Windows</p> <p><u>1 D detector control:</u> PC-card and software from Hecus &amp; Braun, Graz.</p> <p><u>2 D detector control:</u> Software from Photonic Science, Oxford.</p>																								

## CURRENT STATUS

The beamline has been built by the Institute for Biophysics and X-ray structure Research (IBR), Austrian Academy of Science in collaboration with staff members from Sincrotrone Trieste, and is in user operation since September 1996. The set-up of the beamline started at the beginning of January 1995 with the installation of the support structure. Until the end of 1995, the 8 keV single energy system had been realised. The upgrade to the full three energy system was finished in spring 1998. Time resolved experiments require fast X-ray detectors and data acquisition hard- and software. Depending on the desired resolution in time and in reciprocal space, on isotropic or anisotropic scattering of the sample, one-dimensional position sensitive (delay-line type) or two-dimensional area detectors (CCD-type, available since October 1998) are employed.

In conclusion, due to wide tuneability of the beamline and the highly variable kept sample stage, there are nearly no limits for the realisation of an experiment, and you are welcome by our team to propose any interesting and highlighting investigation for the benefit of material and life sciences.

# **Application for Beamtime at ELETTRA**

## **1. Beamtime Policy at SAXS beamline**

The agreement of setting-up a collaborating research group, and the co-operation between the Austrian Academy of Sciences and Sincrotrone Trieste concerning the SAXS beamline, has been signed on the 20th March 1998. It defines also the beamtime distribution between the partners and the beamtime policy.

The following points are of interest for users:

The available beamtime of 5000 hours/year is distributed as follows:

- 35% for Austrian Users, type: "CRG" (Collaborating Research Group)
- 50% for Users of Sincrotrone Trieste (ST)
- 15% is reserved for beamline maintenance

In both user beamtime contingents also any industrial, proprietary and confidential research can be performed according to the "General User Policy" of Sincrotrone Trieste.

To apply for CRG and ST user beamtime proposals must be submitted according to the rules of Sincrotrone Trieste. The international review committee at ELETTRA will rank the proposals according to their scientific merit assessment. Based on this decision beamtime will be allocated according to the specific quotes for the beamtimes (CRG/ST).

## **2. How to apply for beamtime**

There are two deadlines each year for proposals, namely August 31<sup>st</sup> and February 28<sup>th</sup>. Accepted proposals will receive beamtime either in the then following first or second half year period, respectively. The Application Form has been modified. Now it must be completed on-line according to the following instructions. In addition, one printed form is also required and must be send their to:

ELETTRA USERS OFFICE

Strada Statale 14 - km 163.5

34012 Basovizza (Trieste), ITALY

Tel: +39 040 3758628 - fax: + 39 040 3758565

email: useroffice@elettra.trieste.it

### **INSTRUCTIONS GIVEN BY THE USERS OFFICE**

In case of emergency you can also download the old application form (download at: <http://www.elettra.trieste.it/Documents/Users/CallForProposal.html>)

1. Read carefully the following Guidelines.

2. Connect to the virtual Users' Office: <http://users.elettra.trieste.it> (or <http://brain.elettra.trieste.it>) using your favorite browser (Netscape 3.0 or above, Internet explorer 4.0 or above, etc.) with JavaScript enabled.
3. Select the Virtual Users Office link.
4. When prompted, insert your ID and password. If you are a new user fill in the registration form with your data and choose your institution with the search button; in case your institution does not appear in the list, please contact [useroffice@elettra.trieste.it](mailto:useroffice@elettra.trieste.it) giving all the details about it. When registered, you will receive an acknowledgment, i.e. your ID and password, and you will be able to continue. In case you do not remember your password, please don't register again but contact [useroffice@elettra.trieste.it](mailto:useroffice@elettra.trieste.it). At any moment you can select the help button and view more detailed instructions.
5. Select the proposals button in the User functions group.
6. Select add and fill in on-line the proposal form. Please, type your proposal in English. Repeat this procedure for each proposal you intend to submit.
7. When finished, submit the proposal electronically, selecting the save button.
8. In case of continuation proposal: a) attach the experimental report of previous measurements; b) give your previous proposal number.
9. Print the proposal form together with each related safety form.
10. Sign the safety form(s).
11. Mail one complete printed copy to the Users Office.

#### NOTE

For further information, e.g., financial support for travel expenses, please have a look into the web-pages <http://www.elettra.trieste.it/Documents/Users/ProceduraEU.html> or contact the USERS OFFICE.

# List of Institutes Participating in Experiments

## Austria

Austrian Academy of Science, Erich Schmid Institut für  
Materialwissenschaft, Leoben

*Fratzl Peter*

*Grabner Barbara*

*Hebesberger H.*

*Pippan R.*

*Zizak Ivo*

Institut für Metallphysik, Montanuniversität, Leoben

*Paris Oskar*

Austrian Academy of Science, Institute for Biophysics and X-ray Structure  
Research, Graz

*Amenitsch Heinz*

*Farkas Rita*

*Kriechbaum Manfred*

*Krenn Christian*

*Laggner Peter*

*Latal Angelika*

*Lohner Karl*

*Pabst Georg*

*Prassl Ruth*

*Pregetter Magdalena*

*Rappolt Michael*

*Schwarzenbacher Robert*

*Staudegger Erich*

Hecus Braun, Graz

*Leingartner Werner*

Ludwig Boltzmann Institut für Osteologie, Wien

*Roschger Paul*

Ludwig Boltzmann-Institut für Osteologie, und UKH-Meidling & Hanusch-  
Krankenhaus, Wien

*Klaushofer Klaus*

Technische Universität Wien, Institut für Physikalische Chemie, Wien

*Jentys Andreas*

Universität Wien, Institut für Materialphysik, Wien

*Karnthaler H.P.*

*Kopacz Ireneusz*

*Loidl Dieter*

*Mingler B.*

*Peterlik Herwig*

*Schafler Erhard*  
*Zehetbauer Michael*

Zentrum für Ultrastrukturforschung, Wien

*Pum Dietmar*  
*Schuster Bernhard*  
*Sleyter Uwe B.*

## Belgium

Catholic University of Leuven, Laboratory of Macromolecular Structural  
Chemistry, Heverlee

*Bisbano Stefania*  
*Bongaerts Karin*  
*Evmenenko Guennady*  
*Mischenko Nicolai*  
*Rheynaers Harry*  
*Theunissen Elisabeth*

## Croatia

"Ruder Boskovic" Institute, Zagreb

*Etlinger Bozidar*  
*Pivac B.*  
*Turkovic Aleksandra*

University of Split, Faculty of Technology, Split

*Lucic-Lavcevic Magdi*

University of Zagreb, Institute for Physics, Zagreb

*Milat Ognjen*

## Czech Republic

Academy of Sciences of the Czech Republic, Institute of Macromolecular  
Chemistry, Prague

*Baldrian Josef*  
*Horky Martin*  
*Steinhart Milos*  
*Vlèek P.*

## Finland

Åbo Akademi University, Dept. of Physical Chemistry, Materials  
Research Group, Turku

*Ågren Patrik  
Lindin Mika  
Rosenholm Jarl B.*

## Germany

European Molecular Biology Laboratory (EMBL) - Outstation Hamburg, Hamburg  
*Rapp Gert  
Woo David*

Fraunhofer Institute for Non-Destructive Testing, Saarbrücken  
*Altpeter I.*

J. W. Goethe Universität, Institut für Anorganische Chemie und Analytische  
Chemie, Frankfurt  
*Blanchard Juliette  
Schüth Ferdi*

Max-Planck-Institut für Biochemie, Abtl. Membran- und Neurophysik, Martinsried  
*Heumann Hermann  
Manakova Elena  
Roessle Manfred*

Techn. Universität München, Dept. of Physics, E22 Biophysics, Garching and  
EMBL - Outstation Hamburg, Hamburg  
*Richter Frank*

Universität Mainz, Institut für Biochemie, Mainz  
*Lauer Iris  
Gebhardt Ronald  
Nawroth Thomas*

Universität Siegen, Walter Flex Strasse, 57068 Siegen  
*Besch Hans-Juergen  
Meissner Wolf  
Orthen Andre  
Pavel Nikolaj  
Sarvestani Amir  
Sauer Norbert  
Walenta Albert Heinrich*

Universitätsklinik Eppendorf (UKE), c/o EMBL - Outstation Hamburg, Hamburg  
*Funari Sergio*

## Hungary

Eötvös University, Institute for General Physics, Budapest

*Hanak Peter*  
*Ungár Tamás*

Hungarian Academy of Sciences, Biological Research Center, Institute of Plant  
Biology, Szeged

*Cseh Zoltán*  
*Garab Gyozo*  
*Jávorfi Tamás*  
*Mustárdy L.*

## India

Bhabha Atomic Research Centre, Materials Science Division, Trombay, Mumbai,  
India

*Banerjee S.*  
*Batra I. S.*  
*Tewari R.*  
*Malhotra N.*

Bhabha Atomic Research Centre, Solid State Physics Division, Trombay, Mumbai,  
India

*Mazumder Subhasish*  
*Sequeira A.*

Inter University Consortium for DAE Facilities, Univ. Campus, Khandwa Road,  
Univ. Campus, Indore, India

*Bhagat Neeru*  
*Dasannacharya B.A.*  
*Gupta Ajay*

Solid State Physics Division, BARC, Trombay, Bombay, India

*Goel P.S.*

## Italy

Fondazione El.B.A., Genova

*Erokhin Viktor*  
*Paddeu S.*

ICGEB, Area di Ricerca, Trieste

*Kühne Christian*

INFN UdR Milano, Dip. di Fisica

*Beretta Sabrina*  
*Chirico Giuseppe*

POLYbios Research Center, Area di Ricerca, Trieste



*Navarini Luciano*

Sincrotrone Trieste, Trieste

*Bernstorff Sigrid*

*Dubcek Pavo*

*Menk Ralf*

Università di Ancona, INFN-Istituto di Scienze Fisiche, Ancona

*Ciuchi Federica*

*Carsughi Flavio*

*Maccioni Elisabetta*

*Mariani Paolo*

*Pisani Michaela*

*Romanzetti Sandro*

*Rustichelli Franco*

*Saturni Letizia*

*Spinozzi Francesco*

*Yang Bin*

Università di Ancona, Dipartimento di Scienze dei Materiali, Sezione Chimica,  
Ancona

*Bruni P.*

*Iacussi Marco*

*Maurelli E.*

*Marzocchini Renato*

Università di Ancona, Dipartimento di Scienze dei Materiali e della Terra, e Istituto  
Nazionale per la Fisica della Materia, Ancona

*Caciuffo Roberto*

*Francescangeli Oriano*

Università di Firenze, Dip. Scienze Fisiologiche, Firenze

*Bagni Maria Angela*

*Balducci Gianni*

*Cecchi Giovanni*

*Colombini Barbara*

*Linari Marco*

*Lombardi Vincenzo*

*Lucii Leonardo*

*Piazzesi Gabriella*

Università di Genova, Istituto di Biofisica, Genova Sestri Ponente

*Carrara Sandro*

*Nicolini Claudio*

*Paternolli C.*

Università di Genova, Dip. di Fisica, e INFN, Sez. di Genova, Genova

*Ottonello Pasquale*

*Rottigni Giovanni Antonio*

Università di Padova, Dip. di Biologia, Padova  
*Salvato B.*

Università di Padova, Dip. di Fisica, e Istituto Nazionale di Fisica Nucleare,  
Sezione di Padova, Padova  
*Zannella Giovanni*  
*Zanoni Roberto*

Università di Padova, Dep. of Mechanical Engineering, Padova  
*Maddalena A.*  
*Ponza A.*  
*Principi Giovanni*

Università di Parma, Dip. di Fisica, e INFN Parma  
*Del Signore F.*  
*Favilla R.*

Università di Roma-II-Tor Vergata, Dip. Chim. Science Techn.  
*Paradossi Gaio*

Università di Roma-La Sapienza, Dip. Di Chimica  
*La Mesa Camillo*

Università di Trieste, Cattedra di Chirurgia Plastica, c/o Ospitale di Cattinara,  
Trieste  
*Guarneri Gianfranco*  
*Papa Giovanni*  
*Pascone Michele*  
*Sabatti Morena*

Università di Trieste, Dip. Biochimica, Biofisica, Chimica delle Macromole  
(BBCM), Trieste  
*Cesàro Attilio*  
*Fabri Deborah*  
*Gamini Amelia*  
*Paoletti Sergio*  
*Sussich Fabiana*  
*Urbani Ranieri*  
*Vetere Amedeo*

Università di Trieste, Dip. di Fisica, Trieste  
*Arfelli Fulvia*

## Japan

Kyoto University, Institute for Chemical Research, Kyoto  
*Hiragi Yuzuru*

## Poland

Institute of Nuclear Chemistry and Technology, Warsaw  
*Chmielewski A.G.*  
*Griegoriew Helena*

Institute of Physics PAS, Warsaw  
*Domagala Jaroslaw*

## Russia

Moscow State Univ., Dept. Mechanics, Moscow  
*Tsaturyan Andreij*  
*Koubassova Natalia*

Ivanovo State University, Ivanovo  
*Valkova L.*

## United Kingdom

University Laboratory of Physiology, Oxford  
*Ashley Christopher C.*  
*Griffiths Peter J.*

# List of Performed Experiments

**1998 (first half year):**

Proposal	Proposer	Institution	Country	Title	Research Area
<i>Pilot</i>	Baldrian Josef	Czech Acad. of Sciences Inst. of Macromol. Chemistry, Prague Czech Republic	Czech Republic	Time resolved SAXS and WAXS studies on macromolecular materials	Chemistry
<i>029/97</i>	Mariani Paolo	Univ. di Ancona Istituto di Scienze Fisiche	Italy	Phase behaviour, molecular conformation and compressibility of the monoolein-water lyotropic system	Biophysics
<i>170/97</i>	Carrara Sandro	Univ. di Genova I. Biofisica, Sestri Ponente	Italy	Thermal Kinetics Characterisation of Proteins Langmuir-Blodgett Films.	Physics
<i>173/97</i>	Turkovic Aleksandra	"Ruder Boskovic" Institute, Zagreb	Croatia	SAXS study of grain sizes and porosity in TiO <sub>2</sub> , CeO <sub>2</sub> and CeO <sub>2</sub> /SnO <sub>2</sub> nanophases.	Physics
<i>174/97</i>	Cecchi Giovanni	Università di Firenze Dip. di Scienze Fisiologiche	Italy	Time resolved mechanical and X-ray diffraction studies on single muscle cells.	Life Sciences
<i>186/97</i>	Grigoriev Helena	Institute of Nuclear Chemistry and Technology, Warsaw	Poland	Kinetics of structural changes in polymer membrane.	Physics
<i>199/97</i>	Gupta Ajay	Inter University Consortium for DAE Facilities, Indore	India	Small angle x-ray scattering study of amorphous to nanocrystalline transformation in Fe-Cu-Nb-Si-B and Fe-Cu-Zr-B alloys.	Physics
<i>203/97</i>	Menk Ralf-Hendrik	Sincrotrone Trieste	Italy	Measurements of System Performance and Saturation Behaviour of a new High Rate Multi Element Imaging Detector.	Technology Instrumentation
<i>206/97</i>	Paoletti Sergio	Univ. di Trieste Dip. Biochimica, Biofisica, Chimica della Macromolecole	Italy	Structural Studies of Physical Gel Networks and Supramolecular Structures.	Chemistry / Life sciences
<i>216/97</i>	Mariani Paolo	Univ. di Ancona Istituto di Scienze Fisiche	Italy	Phase behaviour, molecular conformation and compressibility of the monoolein-water lyotropic system.	Biophysics
<i>230/97</i>	Bin Yang	Univ. di Ancona Istituto di Scienze Fisiche	Italy	Determination of the amplitudes of smectic layer fluctuation in some oriented LC polyesters by measuring intensity of X-ray diffuse scattering.	Chemistry
<i>236/97</i>	Lombardi Vincenzo	Università di Firenze Dip. di Scienze Fisiologiche	Italy	Structural changes accompanying development of force in single musclefibres:	Life sciences

				combined mechanical & X-ray diffraction study on the molecular aspect of muscle contraction.	
251/97	Rappolt Michael	Austrian Academy of Sciences IBR, Graz	Austria	Realtime X-ray Diffraction Studies on the Formation of Intermediates in Phospholipids induced by Laser Temperature Jump.	Biophysics
259/97	Kriechbaum Manfred	Austrian Academy of Sciences IBR, Graz	Austria	Time-resolved small-angle scattering studies of protein denaturations.	Life sciences
260/97	Schwarzenbacher Robert	Austrian Academy of Sciences IBR, Graz	Austria	Kinetic studies of the polyphosphate based MCM-41 and MCM-48 synthesis, a continuation of proposal nr. 125/97.	Chemistry
261/97	Garab Gyözö	Hungarian Academy Sciences Biological Research Centre Inst. of Plant Biol., Szeged	Hungary	Structure and dynamics of thylakoid membranes and lamellar aggregates of LHCII.	Life sciences
278/97	Francescangeli Oriano	Univ.di Ancona Dip. Scienze Mat. e Terra	Italy	X-ray Diffraction Study of the Structure of DNA-Liposome-Metal Complexes	Physics
283/97	Heumann Hermann	Max Planck Institute für Biochemie, Planegg-Martinfried	Germany	Time resolved small angle scattering studies on the refolding process of substrate protein mediated by the E. coli chaperonin system GroEL-GroES.	Life sciences
289/97	Zehetbauer Michael	Universität Wien Institut für Materialphysik	Austria	Microscale Spatial Distribution of Dislocations & Long Range Internal Stresses in Cold Worked bcc Fe.	Physics
312/97	Mazumder Subhasish	Bhabha Atomic Research Centre Solid State Physics Division, Mumbai	India	SAXS Investigation of Phase Separation in Maraging Steel.	Materials science
313/97	Nawroth Thomas	Univ. Mainz Inst. für Biochemie	Germany	Transient structural changes and cooperativity in the nucleotide reaction cycle of ATP-synthase.	Life sciences
98-032	Pregetter Magdalena	Austrian Academy of Sciences IBR, Graz	Austria	Time-resolved measurements of the apolar lipid core transition of Human Low Density Lipoproteins (LDL).	Life Sciences
98/087	Schwarzenbacher Robert	Austrian Academy of Sciences IBR, Graz	Austria	In Situ Synchrotron SAXS Study of the Formation of MCM-41 and MCM-50	Chemistry

**1998 (second half year):**

Proposal	Proposer	Institution	Country	Title	Research Area
175/97	Fratzl Peter	Universität Wien Institut für Materialphysik	Austria	High-Resolution Scanning-SAXS of Connective Tissue	Life Sciences
98-001	Rustichelli Franco	Univ. di Ancona, Istituto di Scienze Fisiche	Italy	Ligand Effects and Structural Properties of Tissue Transglutaminase by Small Angle X-ray Scattering.	Biophysics
98-016	Mazumder Subhasish	Bhabha Atomic Research Centre, Solid State Physics Division	India	Kinetics of spinodal decomposition in Cu-9Ni-6Sn.	Materials Science
98-017	Bradshaw Jeremy P.	University of Edinburgh, Dept. Preclinical Veterinary Sciences, R.(D.) S.V.S	UK	Perturbation of Phospholipid Phase Transitions by Viral Fusion Peptides.	Biophysics
98-022	Baldrian Josef	Czech Academy of Sciences, Inst. of Macromolecular Chemistry	Czech Republic	Time-resolved SAXS and WAXS Studies on Macromolecular Materials: Phase Transformation and Crystallization of PEO/PMMA Blends.	Chemistry
98-023	Baldrian Josef	Czech Academy of Sciences, Inst. of Macromolecular Chemistry	Czech Republic	Time resolved SAXS and WAXS Studies on Macromolecular Materials: High-pressure Crystallization of PEO and its Blends.	Chemistry
98-034	Prassl Ruth	Austrian Academy of Sciences IBR, Graz	Austria	In Situ 2D-SAXS Studies on the Crystallisation of Low Density Lipoprotein (LDL).	Biophysics
98-044	Cesaro Attilio	Università degli Studi di Trieste, Dip. Biochimica, Biofisica, Chim. Macromol.	Italy	Time-resolved temperature- induced changes in the nano- structure of biodegradable poly- hydroxybutyrate solutions.	Chemistry
98-061	Woo David	European Molecular Biology Laboratory, Outstation Hamburg	Germany	Time-resolved X-ray studies on the sorption of volatile liquids into phospholipid multilayers.	Biophysics
98-068	Pabst Georg	Austrian Academy of Sciences IBR, Graz	Austria	Realtime X-ray Diffraction Studies on the Trapping of Ordered Intermediates in Phospholipid Phase Transitions.	Biophysics
98-069	Rappolt Michael	Austrian Academy of Sciences IBR, Graz	Austria	Highly Temperature Resolved (<10 mK) Phase Boundary Studies in Phospholipid/Water Systems.	Biophysics
98-072	Laggner Peter	Austrian Academy of Sciences IBR, Graz	Austria	Kinetics and mechanism of apo A-I adsorption and insertion into phospholipid bilayers.	Biophysics
98-074	Carrara Sandro	Fondazione EL.B.A.	Italy	Thermal Kinetics Characterisation of solutions and thin films of mutated proteins.	Physics

<b>98-077</b>	Heumann Hermann	Max Planck Institute für Biochemie	Germany	Time dependent small angle scattering studies on the refolding process of substrate protein mediated by the E. coli Chaperonin system GroEL- GroES.	Biophysics
<b>98-087</b>	Schwarzen- bacher Robert	Austrian Academy of Sciences, Inst. of Biophysics and X- Ray Structure Research	Austria	Kinetic studies of the MCM- synthesis under varying sample compositions and reaction conditions, a continuation of proposal nr.: 260/97	Chemistry
<b>98-088</b>	Lohner Karl	Austrian Academy of Sciences, Inst. of Biophysics and X- Ray Structure Research	Austria	Kinetics of Membrane Perturbation and Disruption by Antimicrobial Peptides.	Biophysics
<b>98-089</b>	Kriechbaum Manfred	Austrian Academy of Sciences IBR, Graz	Austria	Kinetics and dynamics of the formation of S-layers.	Life Sciences
<b>98-104</b>	Lombardi Vincenzo	Università di Firenze, Dip. di Scienze Fisiologiche, Dip. di Scienze Fisiologiche	Italy	Structural changes accompanying development of force in single muscle fibres: combined mechanical and X-ray diffraction study on the molecular aspect of muscle contraction.	Biophysics
<b>98-112</b>	Fratzl Peter	Austrian Academy of Sciences, Erich Schmid Institute, Leoben	Austria	In Situ Measurements of Visco- elastic Processes in Collagen.	Life Sciences
<b>98-113</b>	Zehetbauer Michael	Universität Wien, Institut für Materialphysik	Austria	High Lateral Resolution Peak Profile Analysis of Cell Wall Transformation during Torsional Plastic Deformation of Commercial Al.	Material Science
<b>98-114</b>	Paoletti Sergio	Uni. degli Studi di Trieste, Dip. Biochim., Biofis., Chim. Macromol.	Italy	Structural Studies of Physical Gel Networks and Supramolecular Structures.	Chemistry / Life Sciences
<b>98-147</b>	Amenitsch Heinz	Austrian Academy of Sciences IBR, Graz	Austria	Structure Determination with SAXS measurements of various modified P70S6kinase at very low concentrations.	Life Sciences
<b>98-152</b>	Sarvestani Amir	Universität Siegen	Germany	Measurements of System Performances of new one and two dimensional gaseous detectors.	Technology / Instrumen- tation
<b>Pilot</b>	Papa Giovanni	Univ. degli Studi di Trieste, Cattedra di Chirurgia Plastica	Italy	Ultrasonic liposculpturing effects on the human tissue.	Medical Sciences
<b>Pilot</b>	Zanella Giovanni	Università di Padova	Italy	CCD detector research & development	Technology/ Instrumen- tation

# User Statistics

## 1. Number of submitted proposals and assigned shifts from 1995 until June 1999

The Austrian SAXS-beamline at ELETTRA opened to users in September 1996. Since then many experiments have been made on it related to the fields of life science, material science, physics, biophysics, chemistry, technology and instrumentation.

The users gained access to the SAXS-beamline on the basis of the proposals received for the five periods September 1996 - February 1997, March 1997 - August 1997, September 1997 - December 1997, January 1998 - June 1998, and July 1998 - December 1998. The assignment of beamtime at this beamline is done separately for the group of "General Users" (GU) and the "Collaborating Research Group" (CRG), i.e., the Research Team of the Austrian Partner. Beamtime was assigned to the proposals of each group in the order of the rating received by the Scientific Committee, and up to the maximum number of shifts available to each group according to the contract between "The Austrian Academy of Sciences" and the "Sincrotrone Trieste". Until December 1997 up to 55 % of the beamtime was given to CRG, up to 30 % to GU, and 15% was reserved for maintenance purposes. From January 98 on the quota for beamtime is 35 % for CRG and 50 % for GU.

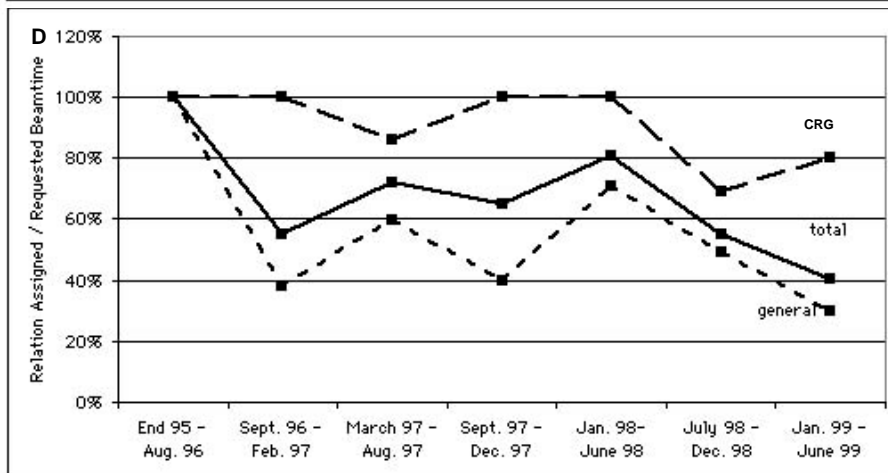
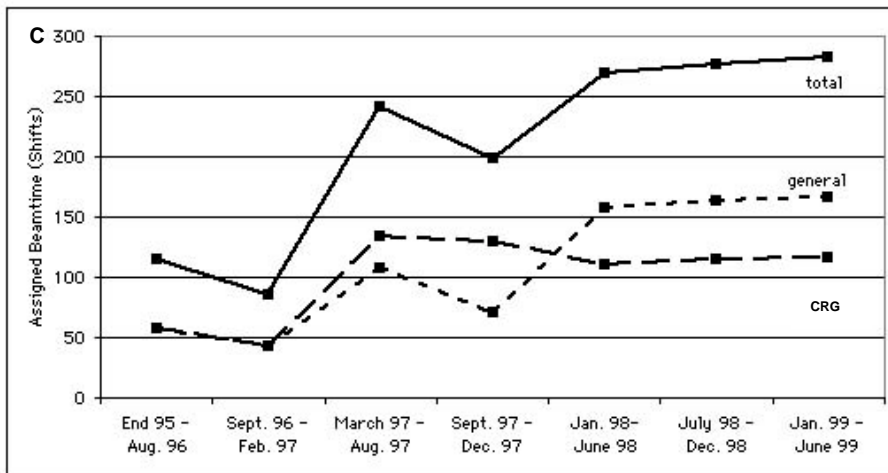
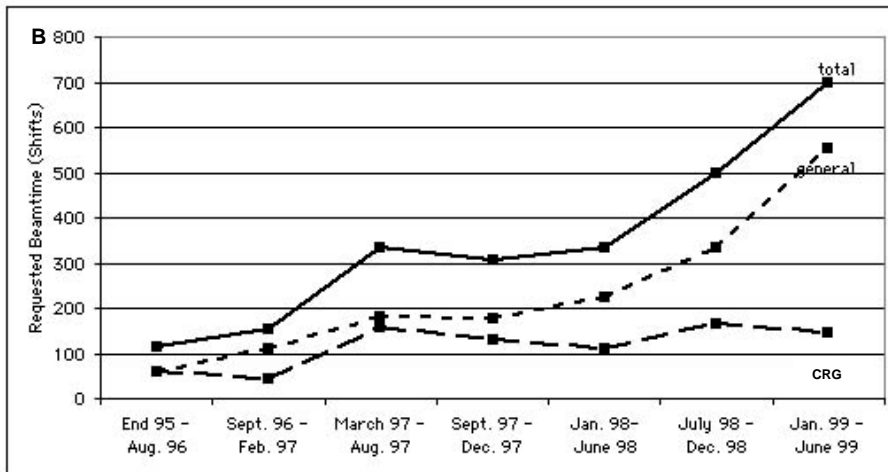
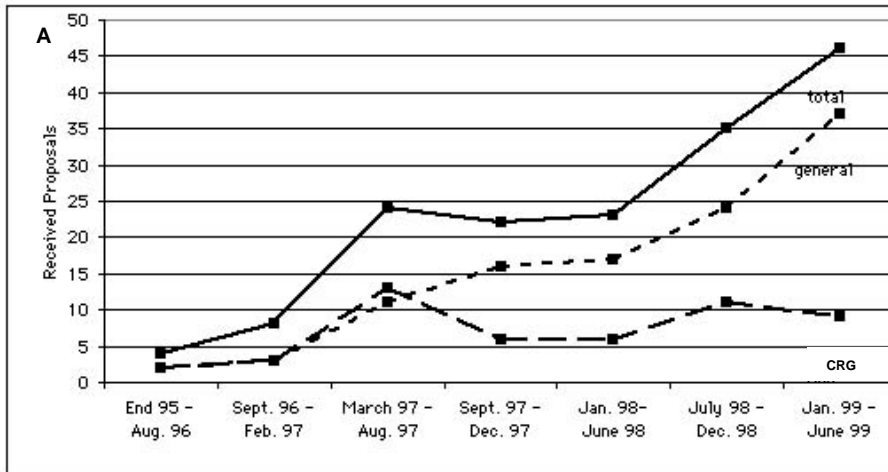
Fig. 1 gives an overview of the numbers of received proposals, the numbers of requested and assigned shifts, as well as the percentage between assigned and requested shifts. Included in the figure are also the same data for the period End 1995 - August 1996, during which some beamtime had been given already to users in order to perform first pilot- and test-experiments together with the beamline staff. These first experiments during the commissioning phase were not yet based on proposals, since the goal was mostly to evaluate and improve the performance of the beamline and the equipment of its experimental station. As can be seen in Fig. 1, the request for beamtime at the SAXS-beamline is continuously and strongly increasing (also during the period Sept.-Dec. 1997, if one takes into account that this period was only 4 instead 6 month long and therefore less proposals were submitted).

**Fig1. (Next Page):** Shown are, for all 6 beamtime periods, respectively:

- (a) Number of received proposals
- (b) Number of requested shifts
- (c) Number of assigned shifts
- (d) Relation between assigned and requested shifts

These informations are given both separately for the groups "CRG", and "GU", as well as for both together ("Total").





## 2. Provenience of Users

In 1998, 156 users from 55 institutes in 13 countries have performed experiments on it. In Fig. 2 are shown both the provenience of the SAXS users, and of their respective institutes. Each user or institute was counted only once, even though most users performed experiments in both beamtime periods of 1998.

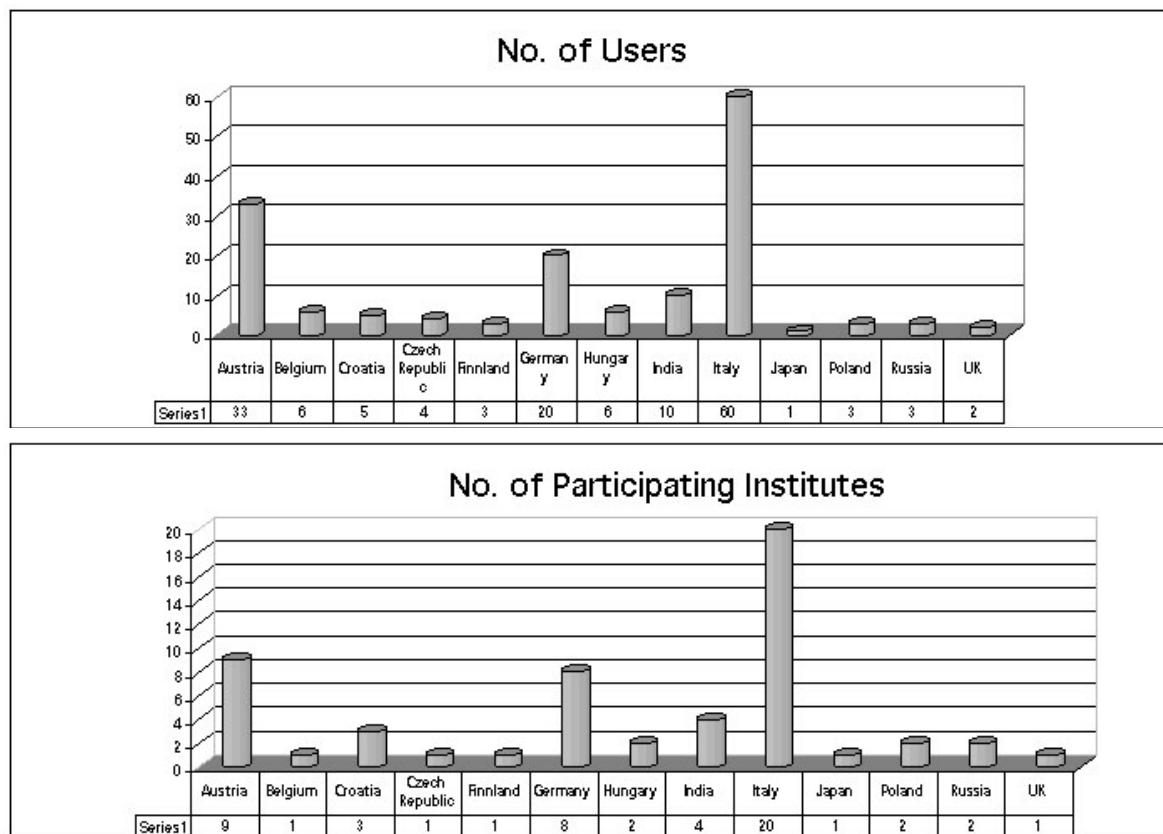
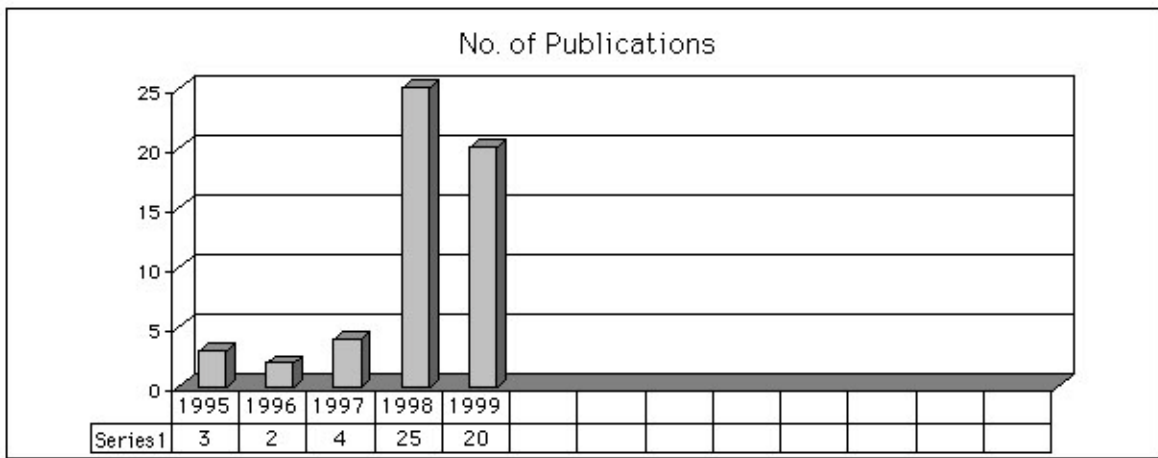
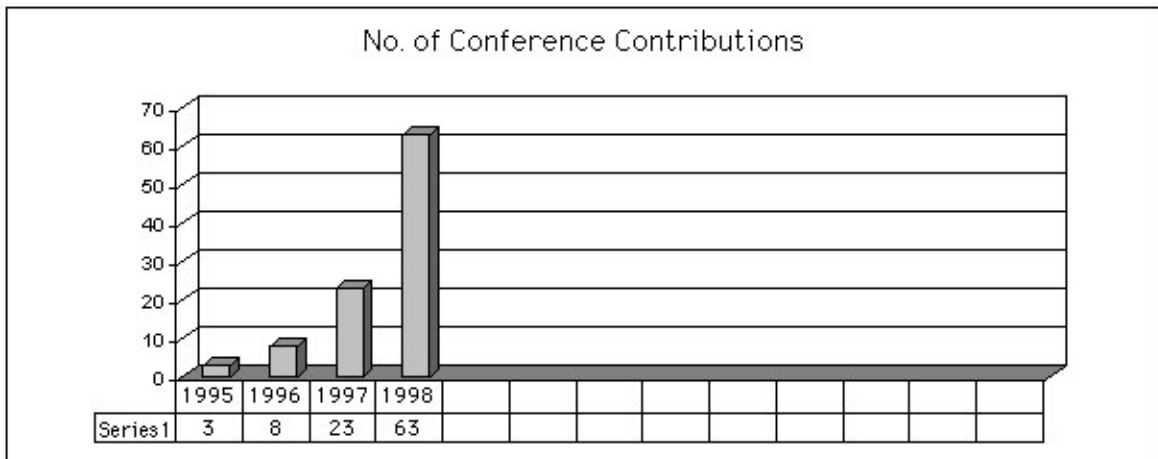


**Fig. 2:** Provenience of users (above) and of their corresponding institutes (below).

## 3. Documentation of experimental results

As could be expected, with the start of user-operation at the SAXS-beamline the number of contributions to conferences started to increase strongly, up to 63 for the year 1998 alone. With a delay of one year - the average time needed for paper publications - also the number of publications started to increase accordingly, as can be seen in Fig. 3.

**Fig. 3 (Next Page):** Number of conference contributions (above) and of refereed paper publications (below) for the years 1995-1998. Also refereed papers, which have been published in 1999, or were in press until 10.3.99, are included.



In addition, until December 1998, the following documentations based on instrumentation of the SAXS-beamline, or on data taken with it, have been produced.

- Non-refereed publications:
  - Technical Reports on Instrumentation: 5
  - Contributions to Elettra Newsletters: 9
  - Contributions to Elettra Highlights: 4
- PhD Thesis: 6
- Diploma Thesis : 2

# **Experimental Possibilities at the SAXS-beamline**

## 1. Installation of a 2D CCD-camera system

Beginning of July 98 a CCD system purchased from Photonic Science, type X-ray L.A. 1024/12, has been installed at the SAXS beamline to cover the needs for non isotropic scattering samples and medium time-resolutions (in the order of 100 ms).

The CCD has a 115 mm diameter input phosphor screen made of a gadolinium oxysulphide polycrystalline layer. The screen is coupled by means of a fiber optic to the image intensifier. The image intensifier is coupled again with an additional taper to the CCD itself. The achieved spatial resolution of a pixel is 79  $\mu\text{m}$  for the whole set-up.

The number of pixels is 1024 x 1024 and they can be pinned down to 2 x 2 and 4 x 4. The dynamic range of the CCD is 12 bit. The dark current of the CCD is in the order of 100 ADU (off-set) and the readout noise (read out speed: 10 MHz) is in the order of 6 ADU. (The CCD is cooled by multistage Peltier element for reducing the dark noise.) The intensifier gain is adjustable between 200 and 20000 photons full dynamic range. Typical readout times and exposure times are 150 ms and 100 ms, respectively. The readout times can be reduced down to 100 ms by using the pinning mode of the CCD. Between the frames additional wait times can be programmed e.g. for reducing the radiation damage in the sample or to extend the time for measuring long time processes.

For the external control a TTL trigger signal is provided (active low, when the CCD is accumulating an image), which is used to control the electromagnetic fast shutter of the beamline on one hand. On the other hand this signal can be used also to trigger processes as requested by the user.

The CCD is controlled by Image Pro+, which also includes non too sophisticated data treatment capabilities. The program is featuring a comprehensive set of functions, including:

- flat fielding/background corrections
- enhanced filters and FFT
- calibration utilities (spatial and intensity)
- segmentation and thresholding
- arithmetic logic operations
- various measurements, like surface, intensity, counts, profiles
- advanced macro management

The data are stored in 12 bit – TIFF format. At the present state up to 300 full images (1024 x 1024) can be recorded by the system, but a strict conservation of the timing sequence is maintained only for the first 15 - 17 frames until the RAM memory is full. Afterwards the images are stored in the virtual memory on the hard disk. At present a software development for the CCD readout system is under way to improve the stability of the readout cycles.

For the complete treatment of the 2D data Fit2D available from the ESRF is used, which is able to perform both interactive and "batch" data processing (homepage: [http://www.esrf.fr/computing/expg/subgroups/data\\_analysis/FIT2D/index.html](http://www.esrf.fr/computing/expg/subgroups/data_analysis/FIT2D/index.html), programmed by Dr. Andy Hammersley), which supports a complete spatial correction, flat field correction and background correction. Furthermore more elevated data-treatment can be performed within this software package, like circular integration, segment integration and similar.

The diffraction pattern of a single fibre of dry rat tail collagen (diameter 0.2 mm) is given as test measurement for the CCD. The beam size was 0.5 x 4 mm (vertical x horizontal) and the fiber was mounted vertically. The sample-CCD distance was 2370 mm and the exposure time

was 10 x 0.1 s and the images were added to achieve a exposure of 1 s in total. The CCD settings were: image intensifier 10, gain 1 and pinning 1x1.

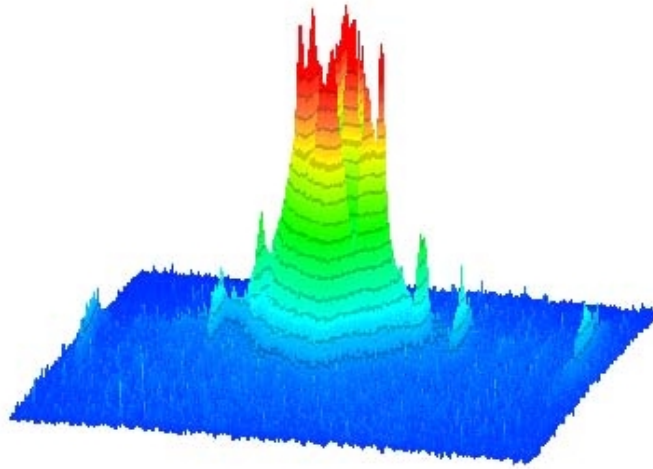


Fig. 1: Diffraction Pattern of a single dry rat tail collagen fibre with 10 x 0.1s = 1 s exposure time (CCD settings: intensifier gain 10, gain 10, pinning 1x1). Representation is  $\ln(I)$  versus channels. An additional pinning of 4 x 4 has been performed by software, but no further correction has been applied.

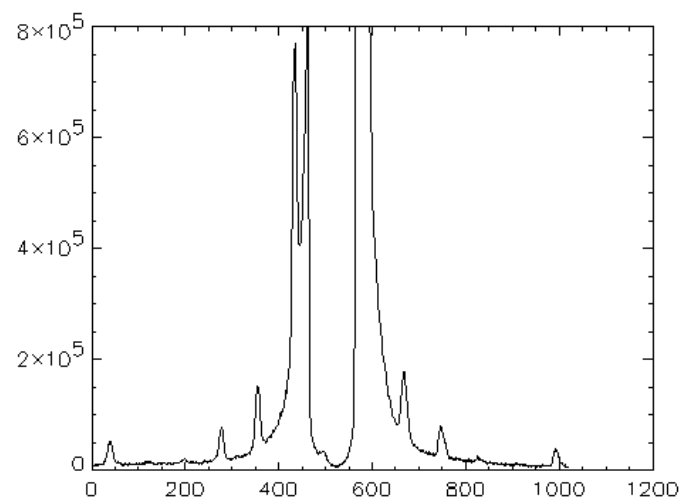


Fig. 2: Integrated Intensity versus channels of the diffraction pattern in Fig 2. The diffraction pattern has been integrated between column 500 – 580 corresponding approximately to the standard Gabriel detector (linear detector, width: 6.8 mm)

## 2. Accessible SAXS and WAXS ranges

Simultaneous SAXS- and WAXS-measurements can be performed using a linear sensitive gas detector (Gabriel type, active length 10 cm) for the WAXS-range, and either a second linear Gabriel type detector (with active length 15 cm), or the new 2D CCD-system for the SAXS-range. A specially designed vacuum chamber (SWAXS-nose, see Annual Report of 1996/97, p. 32) allows to use both scattering areas below (for SAXS) and above (for WAXS) the direct beam, respectively.

The available possible WAXS-ranges are summarised in Table 1. The overall length of the SWAXS-nose in the horizontal direction, measured from the sample position, is 512 mm and the fixed sample to WAXS-detector distance is 324 mm. At the shortest SAXS camera-length an overlap in the d-spacings covered by the SAXS- and WAXS-detectors, respectively, is possible: then, the common regime lies around 9 Å.

Range	$2\theta$ [deg]	d-spacing (Å)		
		8 keV	5.4 keV	16 keV
<b>1</b>	9.4	<i>9.40</i>	14.03	4.27
	27.6	<i>3.23</i>	4.82	1.47
<b>2</b>	27.4	3.25	4.86	1.48
	45.6	1.99	2.97	0.90
<b>3</b>	45.4	2.00	2.98	0.91
	63.6	1.46	2.18	0.66
<b>4</b>	63.4	1.47	2.19	0.67
	81.6	1.18	1.76	0.54

Table 1: Possible d-spacing ranges in the WAXS-regime at the SAXS-beamline at ELETTRA. Since the WAXS-detector can be mounted at four different fixed positions on the SWAXS-nose (range 1-4), with the three possible energy choices (5.4, 8 and 16 keV) this results in 12 different d-spacing regimes. In italic the most common choice (8 keV, range 1) is highlighted. This range is suited for experiments, e.g., on lipid-systems and (bio)polymers.

Depending on the photon energy maximum SAXS resolutions of 2000 Å (5.4 keV), 1400 Å (8 keV) or 630 Å (16 keV) are available.

### 3. Available sample manipulations stages

#### 1. General

Usually the sample is mounted onto the sample alignment stage which allows the user to place the sample into the beam with a precision of 5  $\mu\text{m}$  (resolution: 1  $\mu\text{m}$ ). In fig. 3 the ranges for vertical and horizontal alignment as well as the maximum dimensions of the sample holders are given. The maximum weight on the sample stage is limited to 10 kg. In case the envelope dimensions of a sophisticated sample station provided by the users are slightly larger than those given in fig. 3, the user can ask the beamline responsible for a check up of his space requirements. If it does not fit at all to these specifications, user equipment can also be mounted directly onto the optical table, which allows much larger spatial dimensions.

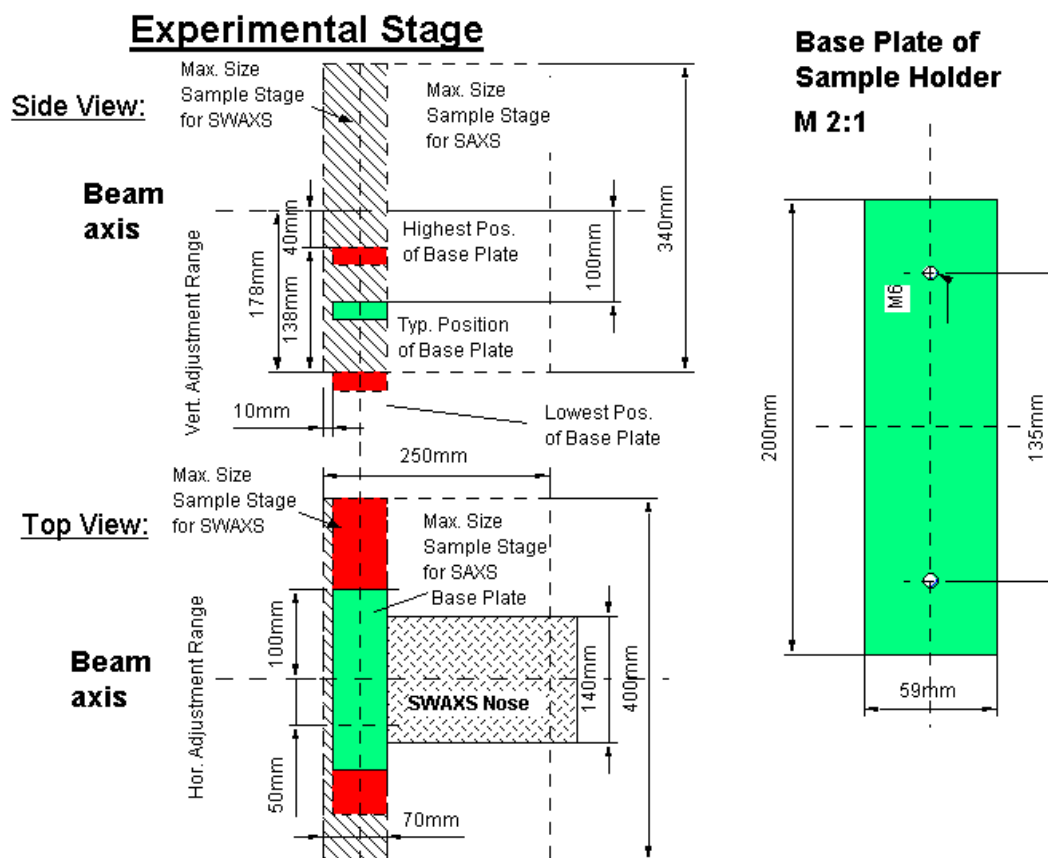


Fig. 3: Maximum dimensions and alignment range of the sample holder to be mounted via a base-plate onto the standard alignment stage (left), and dimensions of the base-plate (right).

#### 2. Sample holders

As standard equipment for liquid samples Paar capillaries (diameter: 1 and 2 mm) are used thermostated with the KHR (electrical heating) or KPR (Peltier heating/cooling) sample holders (Anton Paar, Graz, Austria). For use in these sample holders flow through capillaries and Gel holders are standard equipment. Temperature scans can be performed with KHR and/or KPR in the range from 0 to 150  $^{\circ}\text{C}$ , typically the precision and the stability of this systems is  $< 0.1$   $^{\circ}\text{C}$ . Additionally thermostats for temperature control or cooling proposes can

be used at the beamline (0-95 °C, at present). Helium and Nitrogen gas bottles are available at the beamline, for other gases please contact the beamline responsible.

Multiple-sample holders can be mounted onto the standard sample manipulator. At present a holder is available for measuring in automatic mode up to 30 solid samples at ambient temperature or up to 4 liquid samples in the temperature range 0 – 95 °C.

### **3. Magnet System**

For studying magnetic effects in samples, capillaries or sample holders with suitable dimensions can be mounted inside an electromagnet. Up to now a sample holder for standard Paar capillaries (Anton Paar, Graz, Austria) is available for ambient temperature only. The alignment of the magnetic field is horizontal or vertical (transversal to the photon beam). For short times the maximum magnetic field can be up to 1.5 T, and 1.0 T for continuous operation, respectively, assuming a pole gap of 10 mm for both.

### **4. Stopped Flow Apparatus**

A commercial stopped flow apparatus (Unisoku Co., Ltd, Osaka, Japan) is presently available particularly designed for SAXS investigations of conformation changes of proteins, nucleic acids and macromolecules. The process is triggered by the rapid mixing of two solutions and typically the observation time is ranging from ms to minutes.

The main parameter of the system are:

- dead time: about 1 ms
- mixing ratio: 1:1 (at present)
- reservoir volume: 4 ml each
- syringe volume: 0.3 ml each
- shot volume: 0.1 ml - 0.25 ml each solution
- optical path length: 1 mm; X-ray windows: sapphire 2 x 50  $\mu\text{m}$
- temperature range: by means of a thermostat water bath (0 - 60 °C)

Both solutions are filled in the reservoirs and the syringes are pulled up remote controlled. The syringes are pushed by a pneumatic system and consequently the liquids are rapidly mixed in a sphere mixer and filled into the rectangular observation cell within 1 ms. This process generates the trigger for starting the data acquisition system. The mixing can be repeated about 15 times before the reservoirs must be refilled. Depending on the diffraction power of the sample time resolutions of up to 10 ms can be obtained.

### **5. Grazing Incidence Small Angle X-ray Scattering**

A special set-up has been designed to perform grazing incidence studies on solid samples, thin film samples or Langmuir-Blodgett-films. The samples can be mounted onto a sample holder, which can be rotated around 2 axes transversal to the beam. Furthermore the sample can be aligned by translating it in both directions transversal to the beam. The precisions are 0.001 deg for the rotations and 5  $\mu\text{m}$  for the translations. Usually the system is set to reflect the beam in the vertical direction. According to the required protocol and the



actual assembly of the rotation stages  $\omega$ ,  $\theta$ ,  $2\theta$  and  $\varphi$  scans can be performed. For further information see the experimental reports enclosed.

## 6. Temperature Gradient Cell

A temperature gradient cell for X-ray scattering investigations on the thermal behaviour of soft matter manybody-systems, such as in gels, dispersions and solutions, has been developed. Depending on the adjustment of the temperature gradient in the sample, on the focus size of the X-ray beam and on the translational scanning precision an averaged thermal resolution of a few thousands of a degree can be achieved.

## 7. IR-Laser T-Jump System for Time-Resolved X-ray Scattering on Aqueous Solutions and Dispersions.

The Erbium-Glass Laser available at the SAXS-beamline (Dr. Rapp Optoelektronik, Hamburg, Germany) delivers a maximum of 4 J per 2ms pulse with a wavelength of  $1.54 \mu\text{m}$  onto the sample. The laser-beam is guided by one prism onto the sample, which is filled in a glass capillary (1 or 2 mm in diameter) and Peltier or electronically thermostated in a metal sample holder (A. Paar, Graz, Austria). With a laser spotsize of maximal 7 mm in diameter a sample-volume of maximal  $5.5 \mu\text{l}$  or  $22 \mu\text{l}$ , respectively, is exposed to the laser-radiation. In a water-solutions/dispersions with an absorption coefficient of  $A = 6.5 \text{ cm}^{-1}$  T-jumps up to  $20 \text{ }^\circ\text{C}$  are possible.

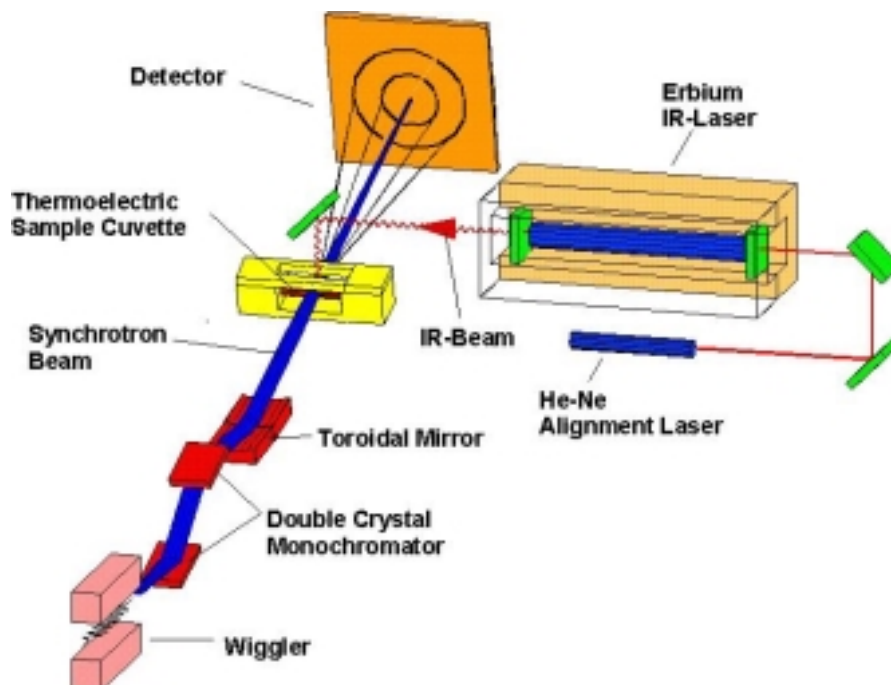


Fig. 4: Sketch of the T-jump set-up.

## 8. High-Pressure Cell for Static and Time-Resolved SAXS-Experiments

A compact X-ray sample cell allows to measure diffraction patterns at hydrostatic pressures up to 3 kbar. Both the entrance and the exit-window for the X-rays are made of 1.5 mm thick Be-discs (3.0 mm diameter), coated with 5m polyimide with a total transmission of 55% for X-rays at a wavelength of 1.54 Å. The sample thickness can be 1.5 mm with a volume of approximately 1mm<sup>3</sup> completely irradiated by pin-hole collimated (1.0 mm diameter) X-rays. The cone-shaped exit window allows detection of scattered X-rays from the sample within a maximal angular range of 30°. The hydrostatic pressure is generated by using water as the pressure transmitting liquid, directly connected via a high-pressure control network with the cell interior. The temperature in the pressure cell can be regulated in the range from 0°C to 80°C.

The large accessible angular range in the reciprocal space makes the cell well suited for scattering/diffraction measurements in the small- (SAXS) and wide-angle (WAXS) region of samples like solid polymers, liquid-crystalline probes and biological model-membrane systems. Static measurements of lipid samples at different pressures show an excellent signal/noise ratio of the diffraction patterns at exposure times of 10 s. Alternatively, this system can be used for time-resolved measurements of dynamic processes (pressure-jump relaxation experiments) with a time resolution of the diffraction patterns in the millisecond range and with jump amplitudes up to 3kbar (1 kbar/10 ms) in both directions (pressurizing and depressurizing jumps). Diffraction patterns of p-jump induced barotropic phase-transitions of lipid samples could be measured with 5 ms time-resolution.

# **User Contributions**

# 1. Material Sciences

## TIME-RESOLVED SAXS/WAXS STUDY OF PHASE BEHAVIOUR AND NUCLEATION IN POLYMER BLENDS

J. Baldrian<sup>1</sup>, M. Horký<sup>2</sup>, M. Steinhart<sup>1</sup>, P. Laggner<sup>3</sup>, P. Vlček<sup>1</sup>, H. Amenitsch<sup>3</sup>, S. Bernstorff<sup>4</sup>

<sup>1</sup>Institute of Macromolecular Chemistry, Academy of Sciences of the Czech Republic, Heyrovsky Sq.2, 162 06 Prague, Czech Republic

<sup>2</sup>Faculty of Nuclear Science and Engineering, Czech Technical University, V Holešovičkách 2, 180 00 Prague 8, Czech Republic

<sup>3</sup>Institute of Biophysics and X-ray Structure Research, Austrian Academy of Sciences, Steyergasse 17, 8010 Graz, Austria

<sup>4</sup>Sincrotrone Trieste, Basovizza, 34012 Trieste, Italy

Whereas the reliable theories for prediction and description of the kinetics of polymer crystallization are well established, the initiation or nucleation stage is not completely understood. The main reason for this is very difficult experimental access to the nucleation step in comparison with relatively simple possibilities of crystal growth study. It is not known whether the phase separation proceeds via *spinodal decomposition* and subsequent crystallization or if isolated lamellar crystals are developed prior to their stacking to the periodical systems. Previous attempts in this field using pure polymers were not successful, since the time lag between beginning of these two processes, if it exists, was too short for measurement. Resolving between these two processes needs the simultaneous measurements of WAXS and SAXS in high time-resolution. The WAXS is sensitive for crystal nucleation and SAXS for long range order arising during spinodal decomposition. The aim of our measurements was to contribute to clarify this problem.

Our previous experiments at the SAXS-Beamline at ELETTRA have shown strong retardation effect of amorphous diluent (PMMA) on the structure development of PEO in PEO/PMMA blends [1,2]. This effect can increase the delay between phase separation and crystallization, which makes our system suitable for studying of these processes.

Blends of PEO (Mw 3000) with PMMA (Mw 1170, 3950) in 8/2 composition were measured after temperature jump from homogenous melt (80°C) to crystallization temperature 40°C using simultaneous SAXS/WAXS measurements consisted from 512 frames each 5s long. The detailed description of experimental conditions are published elsewhere [1]. Fig.1 shows time-resolved SAXS/WAXS diffractograms of PEO/PMMA blend. SAXS part shows development of the NIF lamellae formation and its subsequent recrystallization to the stable IF and EC structures. WAXS part indicates the development of crystalline structure. Fig.2 summarizes development of SAXS and WAXS parameters for PEO blends with PMMA (Mw 1170, 3950) during early stages of crystallization.

The SAXS/WAXS experiments on both kinds of blends show development of the SAXS peak, reflecting periodic electron density fluctuations, prior to the development of WAXS peaks, which indicate the beginning of crystallization. This behaviour shows, that structure development starts with the process of spinodal decomposition which is followed by crystallization after a certain time.

## References

- [1] Baldrian J., Horký M., Steinhart M., Sikora A., Vlček P., Amenitsch H., Bernstorff S: Polymer 40, 439 1999
- [2] Baldrian J., Horký M., Steinhart M., Sikora A., Vlček P., Amenitsch H., Bernstorff S: SPIE Proceedings, in press

*Research supported by the Grant Agency of the Academy of Sciences of the Czech Republic (No. K2050602/12)*

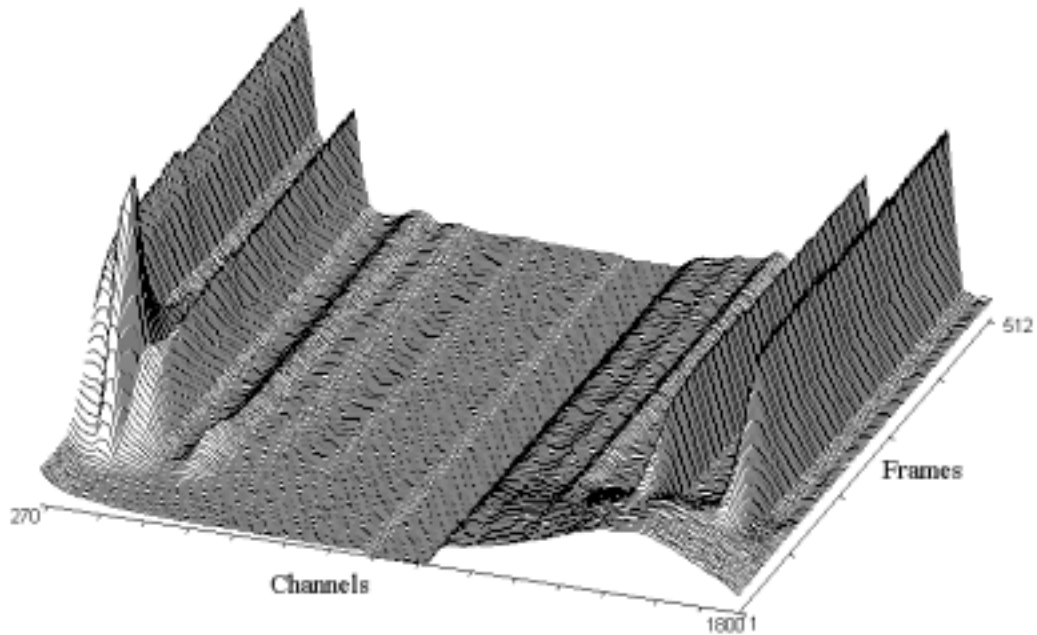


Fig.1. Time resolved SAXS/WAXS curves of PEO/PMMA 3950 blend crystallized at 40°C

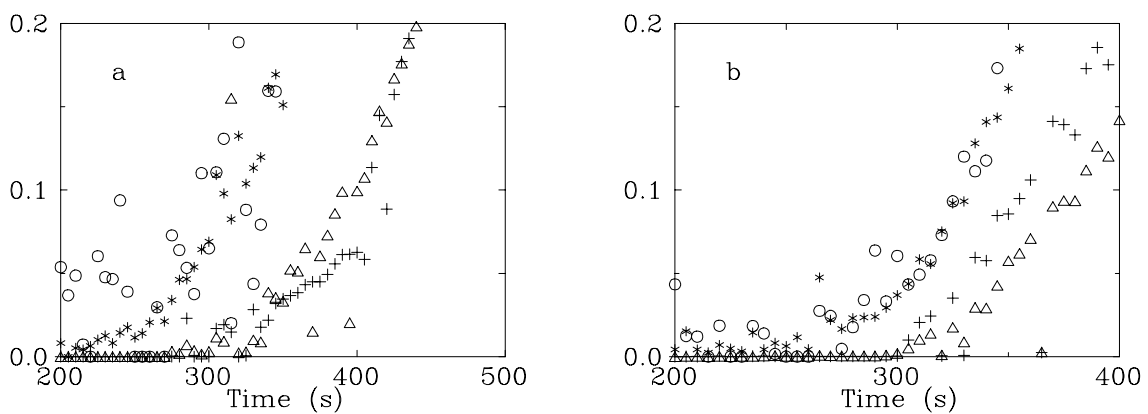


Fig.2. Changes of SAXS scattering invariant (\*) and intensity of dominant NIF reflection (o) and WAXS crystallinity ( $\Delta$ ) and intensity of (120) reflection (+) in early stages of crystallization of PEO3000 blends with PMMA 1170(a) and 3950(b)

## SIMPLE TEMPERATURE DEPENDENT PHASE SEPARATION BEHAVIOR OF A MULTICOMPONENT COMPLEX ALLOY

S. Mazumder<sup>1</sup>, I.S. Batra<sup>2</sup>, R. Tewari<sup>2</sup>, S. Banerjee<sup>2</sup>, A. Sequeira<sup>1</sup>, H. Amenitsch<sup>3</sup> and S. Bernstorff<sup>4</sup>

<sup>1</sup> Solid State Physics Division, Bhabha Atomic Research Centre, Trombay, Mumbai 400 085, INDIA

<sup>2</sup> Materials Science Division, Bhabha Atomic Research Centre, Trombay, Mumbai 400 085, INDIA

<sup>3</sup> Institute of Biophysics and X-ray Structure Research, Austrian Academy of Sciences, Steyrerg. 17, 8010 Graz, Austria

<sup>4</sup> Sincrotrone Trieste, SS 14, Km 163.5, 34012 Basovizza (TS), Italy

Maraging steels, well known for their high strength to weight ratio, high toughness and easy machinability in the solution annealed condition are extensively used in strategic applications. As the name indicates high strength in these steels is developed by precipitation hardening of the relatively soft martensitic matrix. Precipitation hardening of this alloy is, therefore, an important processing step to achieve the desired properties for a specific end use. The evolution of microstructure of the material with aging treatments has been extensively investigated [1-4] primarily by TEM. These studies have helped in the identification of crystallography of the precipitating phases.

In the present study, we were interested in the issue of the competition between displacive/replacive ordering vis-a-vis precipitation of intermetallic phases through classical nucleation and growth. For this, the phase separation behavior of a multi-component 350-grade Maraging steel has been studied simultaneously by small-angle x-ray scattering (SAXS) and wide angle x-ray scattering (WAXS) measurements using the 16 KeV ( $\lambda = 0.077$  nm) branch of the ELETTRA SAXS beamline. The measurements were performed on samples, which previously had been aged at two different temperatures, viz. 430 and 510 °C for different aging times (ranging from 5 minutes to 18 hours at 510 °C, and from 30 minutes to 72 hours at 430 °C). The two specific temperatures, viz. 430 °C and 510 °C, have been suitably chosen in order to study the competition between the formation of the ordered  $\omega$  phase and the intermetallic precipitates, the former known to occur at lower temperatures. The selection of higher aging temperature has also been governed by the fact that the chosen steel (composition 18wt. % Ni, 4.2wt. % Mo, 12.5wt. % Co, 1.7wt. % Ti, 0.1wt. % Al, 0.02wt. % Mn, 0.004wt. % C and rest Fe) is conventionally hardened by vacuum aging at 510 °C for use in strategic applications. Figure 1 shows the time dependent structure factor  $S(q,t)$  ( $q = 4 \pi \sin(\theta) / \lambda$ , where  $2\theta$  is the scattering angle) at 430 °C. It is evident, that with increasing aging time the structure factor becomes sharp with the position of the maxima shifting towards small wave vector and with the peak intensity increasing quite sharply. These observations indicate that both growth and the spatial correlation of the secondary phase intensify with aging. The initial stages of the formation of the  $\omega$ -phase could also be seen in

electron diffraction patterns, which were obtained on the same samples by the complementary method of transmission electron microscopy (TEM).

At 430 °C, the phase separation is attributed to the formation of an ordered  $\omega$  phase - Fe<sub>7</sub>Mo<sub>6</sub> through a mechanism involving a combination of chemical ordering and the  $\omega$ -like lattice collapse in the bcc structure. Time (t) dependent population averaged precipitate size follows  $t^{1/5}$  power law indicating cluster diffusion mechanism of Binder-Staufffer type for the entire range, 30 minutes to 72 hours of aging time. At 510 °C, the phase separation is attributed to the formation of Ni<sub>3</sub>(Ti,Mo) with DO<sub>24</sub> structure through the process of nucleation and growth. Average precipitate size follows  $t^{1/3}$  Lifshitz-Slyozov power law for the entire range, 5 minutes to 18 hours, of aging time. The system, despite being multicomponent and complex, exhibits two distinct time-temperature-transformation curves. Effect of cold work on the phase separation behavior has also been studied. It is observed that cold work facilitates the growth of the precipitates. Also, it narrows down the size distribution and enforces strong spatial correlation of the precipitates.

From the present investigations, we conclude that the nature of the final precipitates and the routes through which these transformations occur appear to be different at the two temperatures. It could be due to different thermodynamic stability criterion at the two temperatures. From SAXS results, it is evident that kinetics of phase separation is different at the two specified temperatures. From TEM experiments with specimens aged at 430 °C, the phase separation is attributed to the formation of  $\omega$  phase through an instability in the bcc matrix. At 510 °C, the phase separation is attributed to the formation of Ni<sub>3</sub> (Ti, Mo) (DO<sub>24</sub> structure) through the process of nucleation & growth. The system appears to follow two different time-temperature-transformation curves. The present study will contribute significantly to design a material with improved properties.

## Acknowledgments

The authors are grateful to Technical Physics & Prototype Engg. Division of BARC for helping to vacuum seal some specimens. The help rendered by Dr. R. K. Fotedar towards rolling some material is also thankfully acknowledged.

## References

- [1] V. K. Vasudevan, S. J. Kim and C. M. Wayman, Metall. Trans., **21A**, 2655 (1990).
- [2] U. K. Viswanathanan, G. K. Dey and M. K. Asundi, Metall. Trans., **24A**, 2429 (1993).
- [3] S. Floreen, Metall. Rev., **126**, 115 (1968).
- [4] D. T. Peters and C. R. Cupp, Trans. Metall. Soc. A. I. M. E., **236**, 1420 (1966).



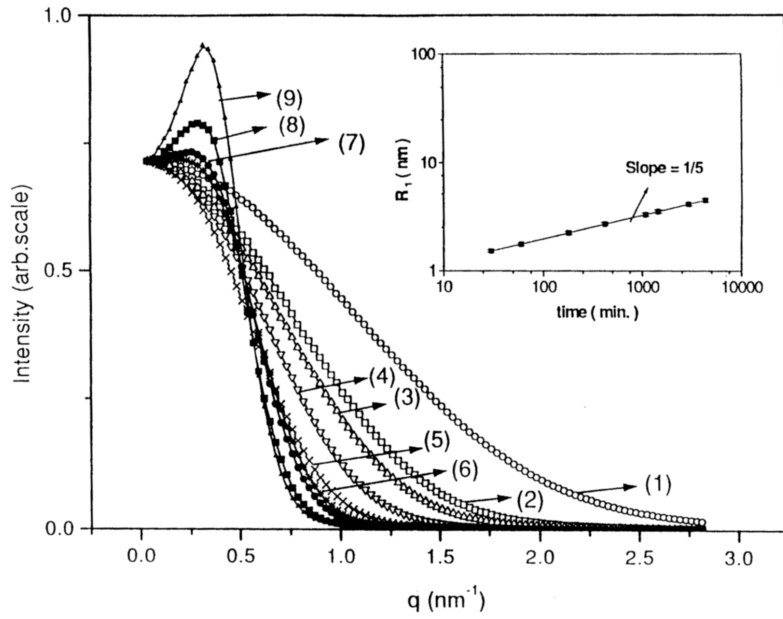
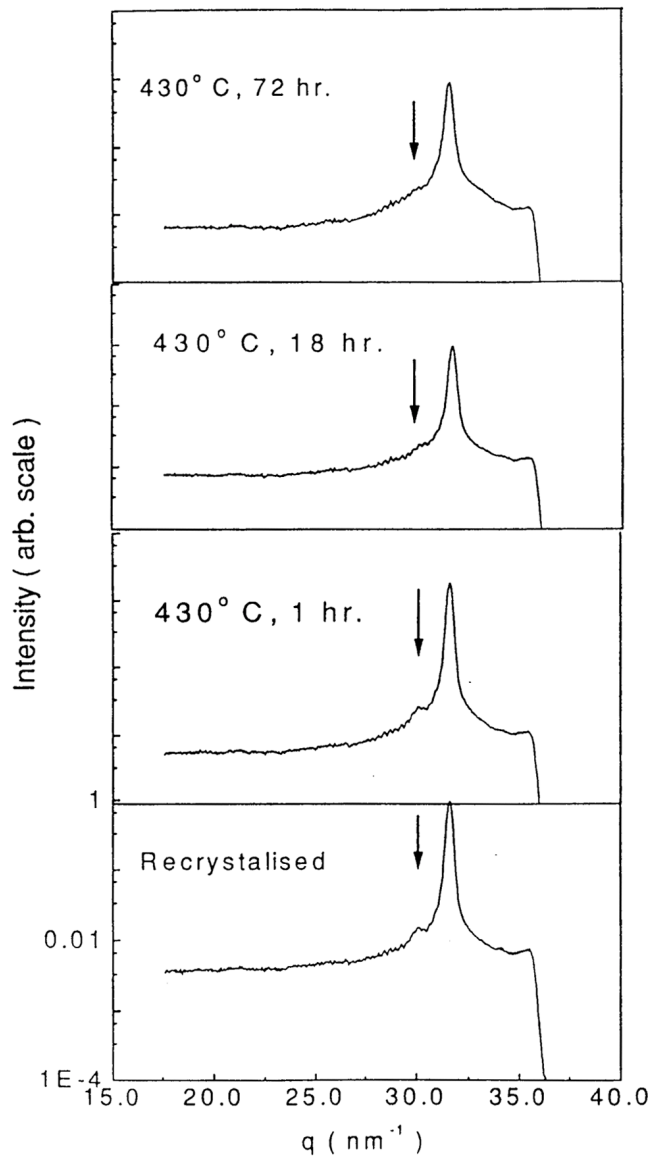


**Fig.1.** Time evolution of the structure factor  $S(q,t)$  of 350-grade Maraging steel aged at 430 °C for different durations of time, namely (1)-recrystallized, (2)-30 mts., (3)-1.0 hr., (4)-3.0 hr., (5)-7.0 hr., (6)-18.0 hr., (7)-24.0 hr., (8)-48.5 hr., (9)-72.0 hr.. The inset shows the time evolution of average precipitate size showing  $t^{1/5}$  law.

**Fig.2.** WAXS profiles of specimens aged at 430 °C for 25 hours. The side peak is indicated by the arrow. The strong peak is due to reflection from (110) of the martensite bcc matrix.



# FRAGMENTATION IN LARGE STRAIN COLD ROLLED ALUMINIUM AS OBSERVED BY SYNCHROTRON X-RAY BRAGG PEAK PROFILE ANALYSIS (SXPA), ELECTRON BACK SCATTER DIFFRACTION (EBSD) AND TRANSMISSION ELECTRON MICROSCOPY (TEM) [1]

E. Schafner<sup>1</sup>, M. Zehetbauer<sup>1</sup>, B. Mingler<sup>1</sup>, H.P. Karnthaler<sup>1</sup>, P. Hanak<sup>2</sup>, T. Ungar<sup>2</sup>, T. Hebesberger<sup>3</sup>, R. Pippan<sup>3</sup>, H. Amenitsch<sup>4</sup> and S. Bernstorff<sup>5</sup>

- 1.) Institute of Materials Physics, University of Vienna, Austria
- 2.) Institute of General Physics, Eötvös University Budapest, Hungary
- 3.) Erich Schmid Institute for Materials Science, Austrian Academy of Sciences, Leoben, Austria
- 4.) Institute of Biophysics & X-Ray Structure Research, Austrian Academy of Sciences, Graz, Austria
- 5.) Sincrotrone ELETTRA, Trieste, Italy

Samples of Al 99.99% Aluminium were cold rolled in steps of  $\Delta\varepsilon = 0.1$  up to true strains of about  $\varepsilon = 1$ . Then they were subjected to substructural analyses by SXPA, EBSD and TEM to study the microstructural changes occurring during cold work. While the SXPA allows local measurements of the variations of dislocation density and/or long range internal stresses within the substructure of a single grain, the EBSD and TEM are capable of identifying the size distribution of both misoriented and equally oriented cells. In deformation stages II and III ( $\varepsilon < 0.7$ ) the dislocation arrange in areas with slightly changing dislocation density showing almost no misorientation (Fig. 1). However, at the transition to stage IV ( $\varepsilon \cong 0.7$ ), local maxima of dislocation density paired with local minima of long range internal stresses are observed. At the same time, some of the cells start tilting relative to neighbouring ones with misorientation angles of 2-10 degrees. Within stage IV ( $\varepsilon > 0.7$ ) the number of these fluctuations is markedly increased, leaving only single local minima of dislocation density paired with local maxima of long range internal stresses (Fig. 3). The misorientation between shrinking subgrains reaches 20 degrees. The results can be interpreted as follows: With the onset of stage IV, a few number of cell walls transform into tilt walls, situated between families of cells ('cell blocks') with equal orientation. With increasing deformation in stage IV, more and more cell walls experience this transformation; they form subgrain-like zones which shrink in size but grow in misorientation, and thus restrict the free movement of dislocations. - The results resemble to those found in cold worked polycrystalline Cu [2], with the difference that the dislocations' tendency to form high-stress pile-ups in the wake of the grain boundaries prevails in large strain deformation rather than in small strain range. Since the same tendency has been observed in cold rolled Ni [3], this seems to arise from the high stacking fault energy in Ni and Al as compared with the low one in Cu, allowing for an easier integration of dislocations in the grain boundaries.

## References

1. Proc. NATO Advanced Research Workshop „Investigations and Applications of Severe Plastic Deformation“, August 2-6 (1999, Moscow, Russia); to be published
2. M.Zehetbauer, T.Ungar, R.Kral, A.Borbely, E.Schafner, B.Ortner, H.Amenitsch, S.Bernstorff, Acta mater. 47, 1053 (1999)
3. E.Schafner, M.Zehetbauer, I.Kopacz, B.Ortner, S.Bernstorff, H.Amenitsch, T.Ungar Proposal 088/97 at ELETTRA (1997), in preparation for Scripta mater.

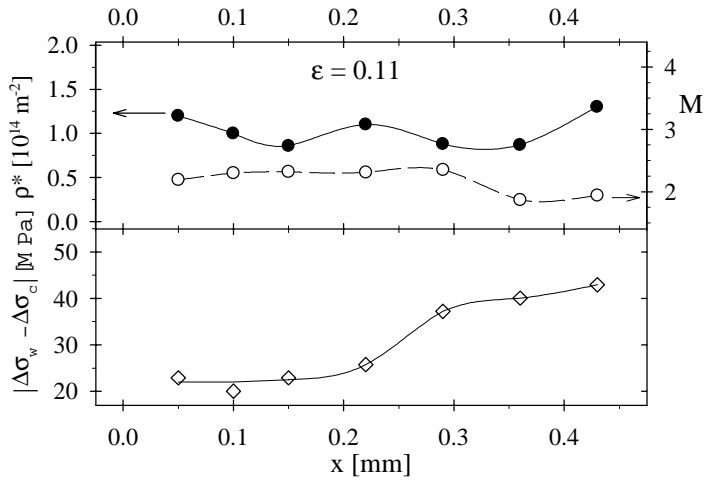


**Fig. 1.**

Variation of dislocation density  $\rho^*$ , and long range internal stresses  $|\Delta(\Delta\sigma_i)|$  within one grain, at small plastic deformation. The quantity  $M$  describes the extent of local strains connected with dislocation density considered [2].

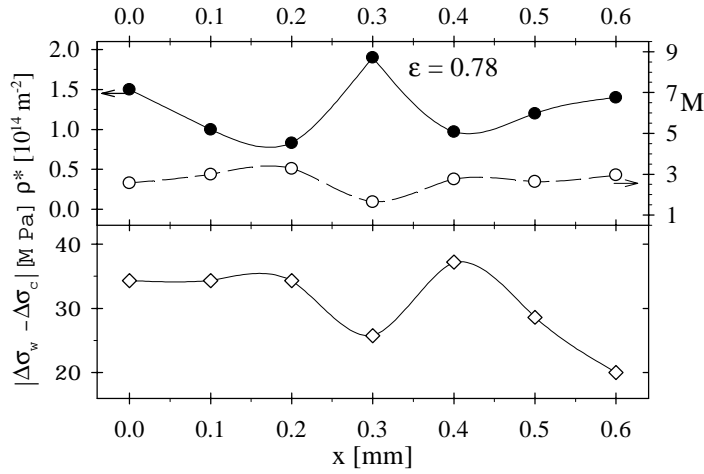


**Fig. 2.**

Same as in Fig. 1, but for samples being plastically deformed up to the beginning of stage IV.

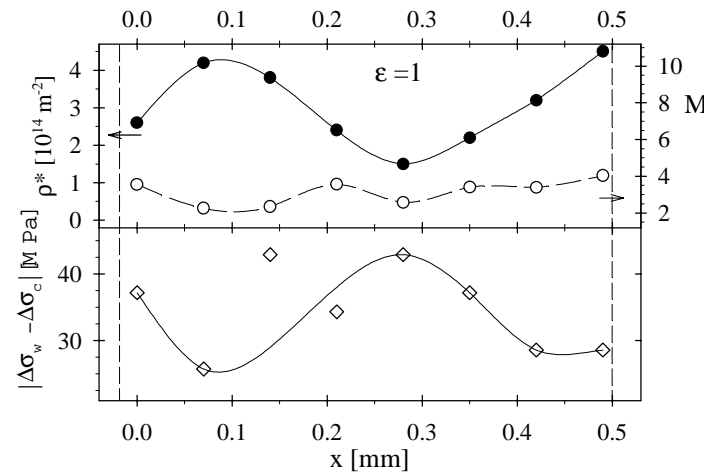


**Fig. 3**

Same as in Fig. 1, but for samples being plastically deformed far into stage IV. The vertical dashed lines denote the site of grain boundaries.

## MICROSCALE SPATIAL DISTRIBUTION OF DISLOCATIONS AND LONG RANGE INTERNAL STRESSES IN COLD WORKED BCC FE

M. Zehetbauer<sup>1</sup>, E. Schafler<sup>1</sup>, I. Kopacz<sup>1</sup>, T. Ungar<sup>2</sup>, P. Hanak<sup>2</sup>, I. Altpeter<sup>3</sup>, S. Bernstorff<sup>4</sup> and H.Amenitsch<sup>5</sup>

- 1.) Institute of Materials Physics, University of Vienna, Austria
- 2.) Institute of General Physics, Eötvös University Budapest, Hungary
- 3.) Fraunhofer Institute for Non-Destructive Testing, Saarbrücken, Germany
- 4.) Sincrotrone ELETTRA, Trieste, Italy
- 5.) Institute of Biophysics & X-Ray Structure Research, Austrian Academy of Sciences, Graz, Austria

Samples of b.c.c. Fe have been investigated on the SAXS Beamline of ELETTRA operated at 16 keV, by means of Synchrotron X-Ray Profile Analysis (SXPA, [1]): Profiles of Bragg reflections were measured in individual grains from grain boundary to grain boundary in a scanning mode, by means of a beam spot size of 50 $\mu$ m. The understanding of the kinetics of microstructural evolution in large strain cold worked bcc metals on a local scale is very important because of industrial interest in these materials. At present, the deformation stage IV gets into focus of the international research on plasticity since it governs the strength of ultrafine-grained and nanocrystalline metals as they are produced by severe plastic deformation [2]. The results shown in Fig. 1 confirm previous ones from home laboratory experiments [3,4] where a break-down of long range internal stresses  $|\Delta\sigma_w - \Delta\sigma_c|$  occurs at the onset of stage IV. This suggests a transformation of high stress - dipolar cell walls (PDW) into low stress - polarized tilt walls (PTW) where the dislocations can arrange to higher densities. Although glide mechanisms of dislocations in Fe are quite different from those in Cu because of specific atomic lattice, the local evolutions of dislocation density and internal stresses with increasing strain are quite similar: at small deformations, these quantities show no significant variation within one grain (Fig. 2). However, they start to fluctuate markedly when reaching the deformation stage IV at a shear strain of (Fig. 3): Local maxima of the dislocation density are strongly correlated with local minima of the internal stresses indicating the development of tilt walls (PTW's) at these sites. At strain values exceeding  $\gamma \cong 1.5$  which is well in stage IV of deformation, the fluctuations are represented by minima of dislocation density paired with maxima of internal stresses, due to the spreading & multiplication of the tilt walls at the cost of original dipolar walls. - These SXPA results shall serve as a calibration basis to magnetic properties such as coercivity force and Barkhausen amplitude, in order to use them as additional quantities to characterize the dislocation density and the long range internal stress, respectively [5].

### References

1. M.Zehetbauer, T.Ungar, R.Kral, A.Borbely, E.Schafler, B.Ortner, H.Amenitsch, S.Bernstorff, Acta mater. 47, 1053 (1999)
2. R.Z.Valiev, Yu.V.Ivanisenko, E.F.Rauch, B.Baudelet, Acta mater. 44, 4705 (1996)
3. T. Ungar, M. Zehetbauer, Scripta Mater. 35, 1467 (1996)
4. E.Schafler, M.Zehetbauer, A.Borbely, T.Ungar, Mater.Sci.Eng. A 234-236, 445 (1997)
5. I.Altpeter, R.Kern, N.Meyendorf, M.Berveiller, Proc. 4th Int.Conf. on Residual Stresses, Baltimore, USA, p. 434 (1994)

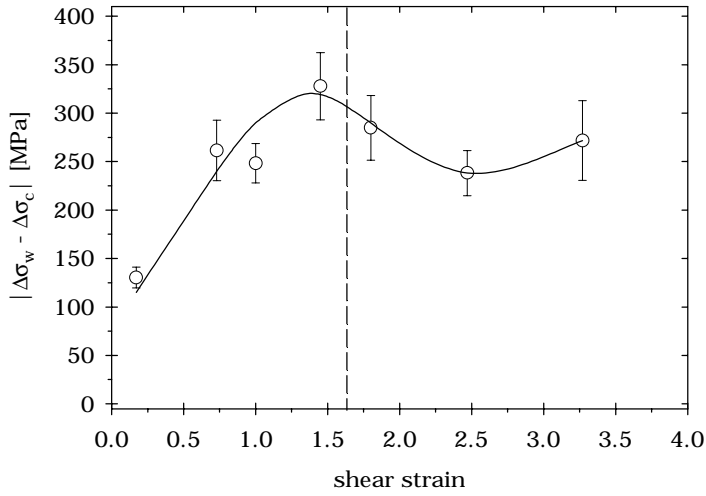


Fig. 1.

Evolution of long range internal stresses  $|\Delta(\Delta\sigma_i)|$  with increasing plastic deformation. The vertical dashed line indicates the transition from deformation stage III to deformation stage IV.

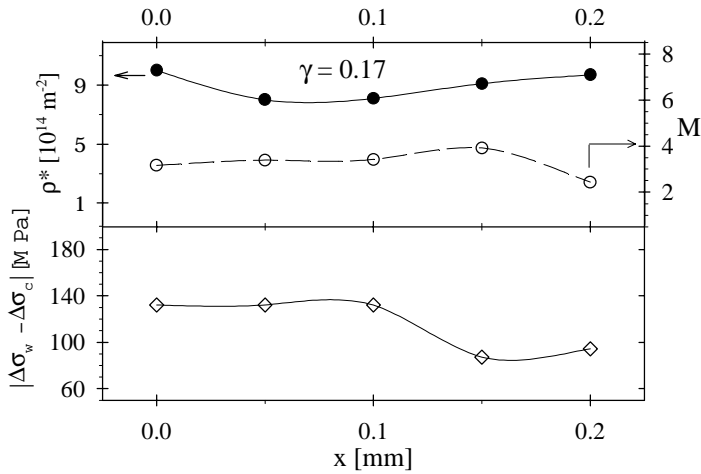


Fig. 2.

Variation of dislocation density  $\rho^*$ , and long range internal stresses  $|\Delta(\Delta\sigma_i)|$  within one grain, at small plastic deformation. The quantity  $M$  describes the extent of local strains connected with dislocation density considered [1].

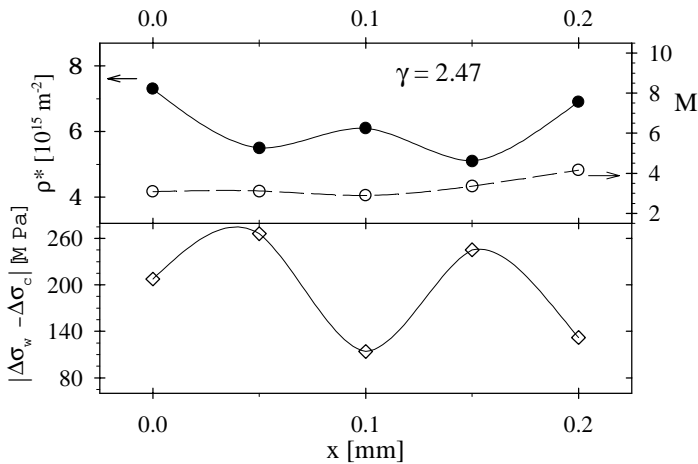


Fig. 3.

Same as in Fig. 1, but for samples being plastically deformed far into stage IV.

## 2. Life Sciences

## 16 $\mu$ S TIME RESOLUTION X-RAY DIFFRACTION MEASUREMENTS IN LIVING SKELETAL MUSCLE CELLS OF THE FROG

H. Amenitsch, C.C. Ashley\*, M.A. Bagni<sup>+</sup>, S. Bernstorff<sup>#</sup>, G. Cecchi<sup>+</sup>, B. Colombini<sup>+</sup> and P.J. Griffiths\*.

<sup>#</sup>SAXS, Elettra, Sincrotrone Trieste, Trieste, Italy.

<sup>+</sup> Dipartimento di Scienze Fisiologiche, University of Florence, Florence, Italy

\*University Laboratory of Physiology, Oxford, U.K.

Institute for Biophysics and X-ray Structure Research, Graz, Austria

Striated muscle cells possess perhaps the most highly ordered intracellular structure to be found in nature. The calcium-dependent interaction of two overlapping, hexagonal arrays of protein filaments (one composed of aggregated actin molecules, the other of aggregated myosin molecules) causes a sliding motion powered by ATP consumption. In addition to the highly ordered hexagonal lattice which is arranged radially relative to the fibre axis, the filaments are also highly ordered axially along the cell, having a uniform length, and forming a regular repeat of actin, then myosin regions, in which the filaments are radially aligned. This gives rise to sarcomeres, the fundamental contractile units, which are aligned in series along the whole length of a muscle fibre. The myosin filaments themselves are also highly structured axially, bearing 400 kD projections of part of the myosin molecules along their length, at intervals of 14.3 nm. These projections (crossbridges) carry both actin and ATP binding sites, and are the molecular motors of muscle contraction, thought to act by performing a power stroke in which they rotate about a point of attachment to the actin filament. In vertebrates, sarcomeres are typically of ca. 2 micrometres in length, so the length of the fundamental structure of muscle contraction can be determined by diffraction of electromagnetic radiation in the visible range of the spectrum. The crossbridges are too small for examination by visible radiation and electron microscopy can only give a static view on fixed specimens. However crossbridges structure changes which accompany the performance of work by the muscle can be detected by diffraction of X-ray even in living intact preparation.

The strongest X-ray diffraction reflection arising from the axial crossbridge periodicity is that at  $14.3 \text{ nm}^{-1}$ , termed the M3 reflection. Its intensity ( $I_{M3}$ ) is sensitive to the structural events of the power stroke. However, these structural changes result from the formation of chemical intermediates in the hydrolysis of ATP whose reactions are governed by rate constants of the order of thousands of reciprocal seconds, therefore  $I_{M3}$  must be sampled at submillisecond time resolution to detect accompanying structural events. In addition, in order to increase the homogeneity of the preparation and to perform fast mechanical measurements and to correlate structural changes, measured by X-ray diffraction, with accompanying sarcomere length and force changes it is essential to work with a small number of isolated cells. Therefore the X-ray source must be very intense to provide the required time resolution from such a small diffracting body. These requirements are met by synchrotron sources, and consequently the time resolution of X-ray diffraction measurements has fallen from several hours, using whole muscle, to submillisecond for a single fibre, over the space of 20 years.

We have examined  $I_{M3}$  from skeletal muscle from the frog, *Rana temporaria*, during sinusoidal length oscillations (about 3 nm per half sarcomere) applied at the plateau of isometric tetanic tension, using the SAXS beamline at Elettra. The beam dimensions at the preparation were 4 by 0.3 mm, which gave a photon flux of  $10^{12} \text{ photons.s}^{-1}$  at a wavelength of 0.15 nm. The meridional X-ray diffraction spectrum was collected using an one dimensional delay line detector, driven by a PC-based data collection system by which force, sarcomere length and fibre length could be simultaneously sampled. In order to maximise  $I_{M3}$  while avoiding space charge saturation of the detector at high flux density in the region of a reflection peak, preparations were chosen to have a diameter of not more than 250  $\mu\text{m}$ , comprising between 1 and 3 muscle fibres. The end compliance of the preparations was reduced by use of aluminium clips attached to the tendons close to the point of insertion of the cell, and the preparation was mounted between a capacitance force transducer and a moving coil motor by means of these clips. The force transducers had a sensitivity of ca. 0.5 -1 mV/mg and a resonance frequency of 31-55 kHz. The motor was capable of performing 50  $\mu\text{m}$  length steps in 100  $\mu\text{s}$ . The mean

sarcomere length of a fibre region of about 200  $\mu\text{m}$  located in the segment illuminated by the X-ray beam, was measured by means of laser light diffractometer. To avoid fibre fatigue and the harmful effects of prolonged exposure to X-ray radiation, oscillations were imposed for a period of 1s during a sequence of up to 40 tetani given at 3 minute intervals. Spectra were then summed over the sequence of tetani and within an individual tetanus, to obtain 40 averaged spectra covering two periods of the imposed length oscillations. The frequency of the applied oscillations ranged from 1 to 3.12 kHz, with a time resolution for the data of 50 – 16  $\mu\text{s}$ . This very fast sampling was close to the limit of the X-ray detector used at ELETTRA.

At all frequencies of length oscillation examined,  $I_{M3}$  showed a periodic fluctuation almost in phase with the oscillations in force, with peak intensity corresponding to minimum tension (figure 1 and 2). The mean force level during the oscillations was shifted slightly above isometric tension ( $P_0$ ) although the length oscillations were symmetrical about the resting length of the cell. The peak to peak amplitude of the force oscillations was in the range 0.35 to 0.60  $P_0$ . The corresponding peak to peak changes in  $I_{M3}$  were in the range 0.19-0.21, normalised to isometric intensity.

The response of  $I_{M3}$  to a step length change is a fall, irrespective of whether the change is a stretch or a release. The intensity signal lasts much longer than the period during which length is changing, and resembles the time course of the recovery of tension after the step, during which the instantaneous elastic change in tension during the step is reversed, and force recovers towards its isometric level over a period of 1 ms. During high frequency sinusoidal length oscillations such as those used here, the time available for the force recovery processes is much reduced, and changes in force arise largely from the elastic properties of the contractile system. Therefore the presence of intensity changes in phase with the force signal supports the view that M3 intensity must also be sensitive to an elastic structural change in the crossbridge, in addition to that associated with the recovery of force after a length step which is believed to arise from the redistribution of crossbridge intermediates about the power stroke step in the ATPase cycle.

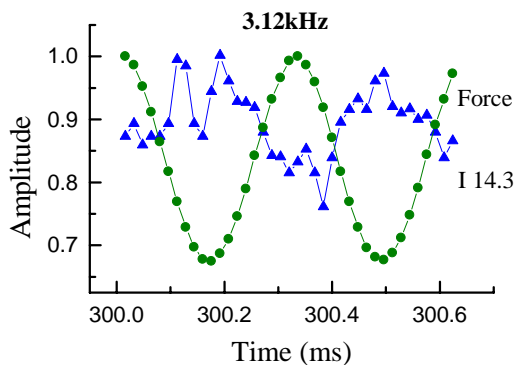


Figure 1.  $I_{M3}$  (filled triangles) and force (filled circles) for a two fibre bundle undergoing 3.12 kHz sinusoidal length oscillations. Force and  $I_{M3}$  have been normalised to their maximum value attained during the response. Time is measured from the start off the data collection cycle, at which stimulation begins. Sampling time 16  $\mu\text{s}$ .

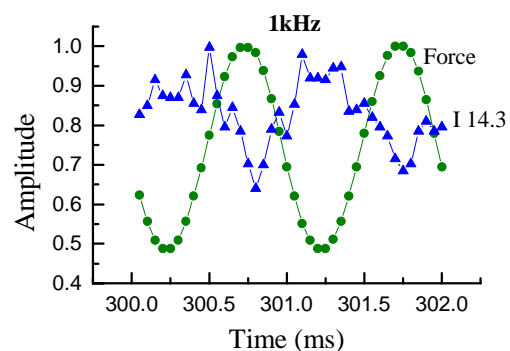
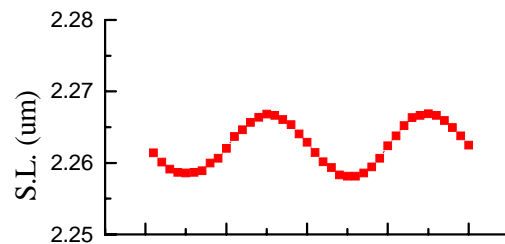


Figure 2. Sarcomere length (S.L., filled squares), force (filled circles) and  $I_{M3}$  (I14.3, filled triangles) for a single fibre undergoing 1 kHz sinusoidal length oscillations. Amplitudes and time as in figure 1.



## PERTURBATION OF PHOSPHOLIPID PHASE TRANSITIONS BY VIRAL FUSION PEPTIDES

Jeremy Bradshaw & Malcolm Darkes

Department of Preclinical Veterinary Sciences, University of Edinburgh, R(D)SVS, Summerhall, Edinburgh EH9 1QH, Scotland, UK

Karl Lohner & Erich Staudegger

Institute of Biophysics and X-ray Structure Research, Austrian Academy of Sciences, Steyrergasse 17/VI, A-8010 Graz, Austria

Membrane fusion plays a vital role in a large and diverse number of essential biological processes. Despite this fact, the precise molecular events that occur during fusion are still not known. Modelling studies have suggested that fusion peptides insert obliquely into target lipid membranes, and thus destabilise lipid packing (Brasseur *et al.*, 1990). Longitudinal precession of the obliquely oriented peptide would lead to greater disruption of the bilayer centre than of its surface. This, in turn, would increase the negative curvature strain on the bilayer, and thereby promote the formation of the highly-curved inverted lipid phases necessary for the fusion of two distinct membranes (Epand *et al.*, 1992; Epand *et al.*, 1994). However, more recent studies (Davies *et al.*, 1998a) have shown that fusion peptides are structurally promiscuous, leading to the suggestion that conformational rearrangement of the peptide is central to the fusion process.

We are currently engaged on a study of membrane fusion as mediated by viral fusion peptides. One of our model peptides is that from feline leukaemia virus (FeLV). Sometimes called p15e, this peptide is 27 amino acids long. We are using a number of biophysical techniques in order to address questions such as: What is the molecular mechanism by which the peptide induces membrane-fusion? Is the fusion process influenced by the phospholipid composition of the membrane? What is the conformation of the peptide within phospholipid membranes?

In an attempt to complement our  $^{31}\text{P}$ -NMR data, differential scanning calorimetry data and preliminary X-ray measurements carried out at Daresbury (Davies *et al.*, 1998b), we have used the SAXS instrument at Elettra for time-resolved X-ray experiments. Much of the uncertainty about membrane fusion stems from the fact that fusion events are extremely difficult to observe mechanistically. Indeed, time-resolved X-ray diffraction experiments are possibly the only way of obtaining structural data on these transitory phases.

In the experiments described here, time-resolved X-ray diffraction was used to study the effect of the peptide on lipid polymorphism. Dispersions of monomethyl-dioleoylphosphatidylethanolamine (Me-DOPE), some of which contained the fusion peptide were prepared. X-ray diffraction experiments were performed on the SAXS instrument. The temperature of the sample cell was linearly increased from 30°C to 80°C, at a heating rate of 30°C/hour. This temperature range covers the  $L_{\alpha}$  –  $H_{II}$  phase transition of Me-DOPE. All samples were at pH 7.4.

Although detailed analysis of the data has not yet been completed, it is possible to make a number of observations. The X-ray diffraction patterns confirm that the phase transitions recorded in previous  $^{31}\text{P}$ -NMR and DSC measurements were from  $L_{\alpha}$  to  $H_{II}$ , through an inverted cubic ( $Q_{II}$ ) intermediate.  $Q_{II}$  phase was observed at temperatures close to the transition. In samples containing the fusion peptide, the  $Q_{II}$  phase was extensive and persisted over a wide temperature range. Presence of the peptide reduced the onset temperature of  $Q_{II}$  and raised the temperature of the  $Q_{II}$  –  $H_{II}$  transition, in a concentration-dependant manner.

These findings are consistent with a mode of action of the fusion peptide that involves increasing the negative curvature strain of phospholipid membranes (Yeagle, 1994).

In a second series of experiments, carried out during the same beamtime allocation, the effect of lyso-phosphatidylcholine (LPC) on Me-DOPE systems, and the combined effect of LPC and FeLV peptide on Me-DOPE, were studied. The rationale behind these measurements was that LPC is known to decrease negative curvature strain in phospholipid systems. We were interested, therefore, to see if LPC counteracted the effect of FeLV peptide and reduced its effect on the phase transitions of Me-DOPE. This was, in fact, the case. The presence of LPC increased the  $L\alpha - H_{II}$  transition temperature of Me-DOPE, even in the presence of FeLV peptide, thereby further supporting the hypothesis that FeLV peptide promotes fusion by a mechanism involving increased intrinsic negative curvature strain.

### References:

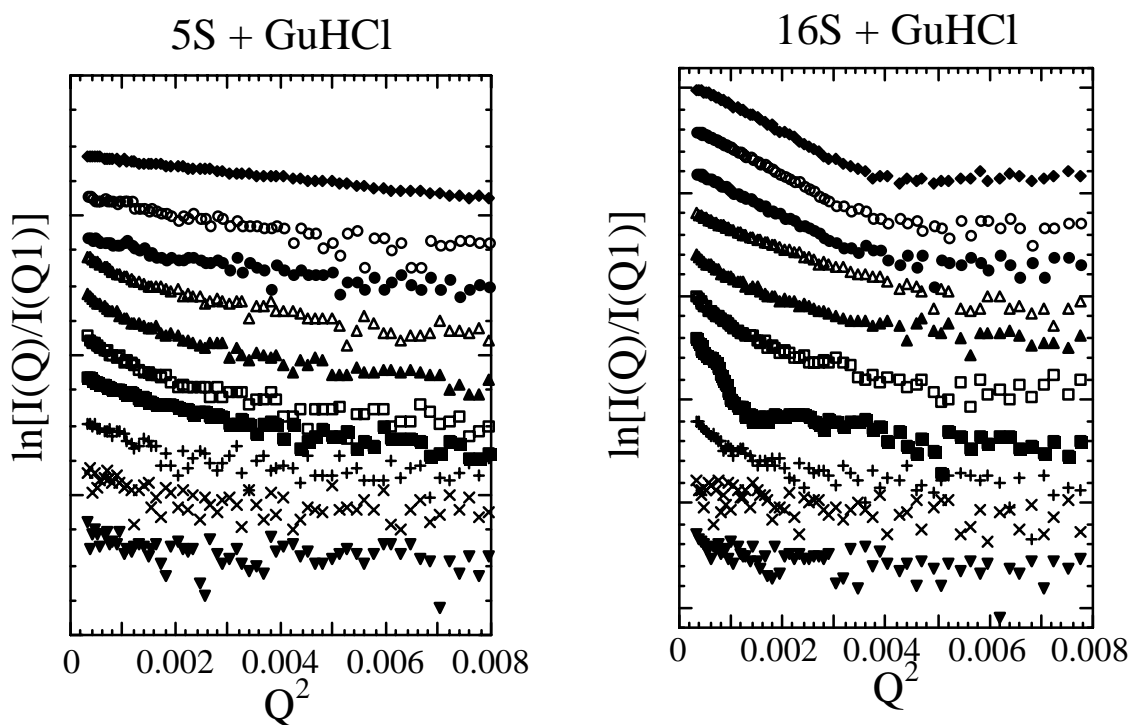
- Brasseur, R., Vandenbranden, M., Cornet, B., Burny, A., & Ruyschaert, J-M. (1990)  
*BBA* 1029, 267.
- Davies, S.M.A., Bradshaw, J.P., Price, N. & Kelly, S.M. (1998a)  
*FEBS Letters* 425 415-418
- Davies, S.M.A., Bradshaw, J.P. & Epand, R.M. (1998b)  
*Biochemistry* 37 5720-5729
- Epand, R.F., Martin, I., Ruyschaert, J.M. & Epand, R.M. (1994)  
*B. B. R. C.* 205, 1938.
- Epand, R.M., Cheetham, J.J., Epand, R.F., Yeagle, P.L., Richardson, C.D., Rockwell, A. & DeGrado, W.F. (1992) *Biopolymers* 32, 309.
- Yeagle, P.L. (1994) *Current Topics In Membranes* 40, 197.

## SAXS STUDIES OF THE STRUCTURAL PROPERTIES OF CARCINUS AESTUARIUM HEMOCYANIN PROTEINS IN SOLUTION

F. Del Signore<sup>1</sup>, R. Favilla<sup>1</sup>, B. Salvato<sup>2</sup>, P. Mariani<sup>3</sup>, F. Spinuzzi<sup>3</sup>, E. Maccioni<sup>3</sup>

1. Unità INFM, Dipartimento di Fisica, Parma (I); 2. Dipartimento di Biologia, Padova; (3) INFM - Istituto di Scienze Fisiche, Università, Via Ranieri, 65 - 60131 Ancona (I)

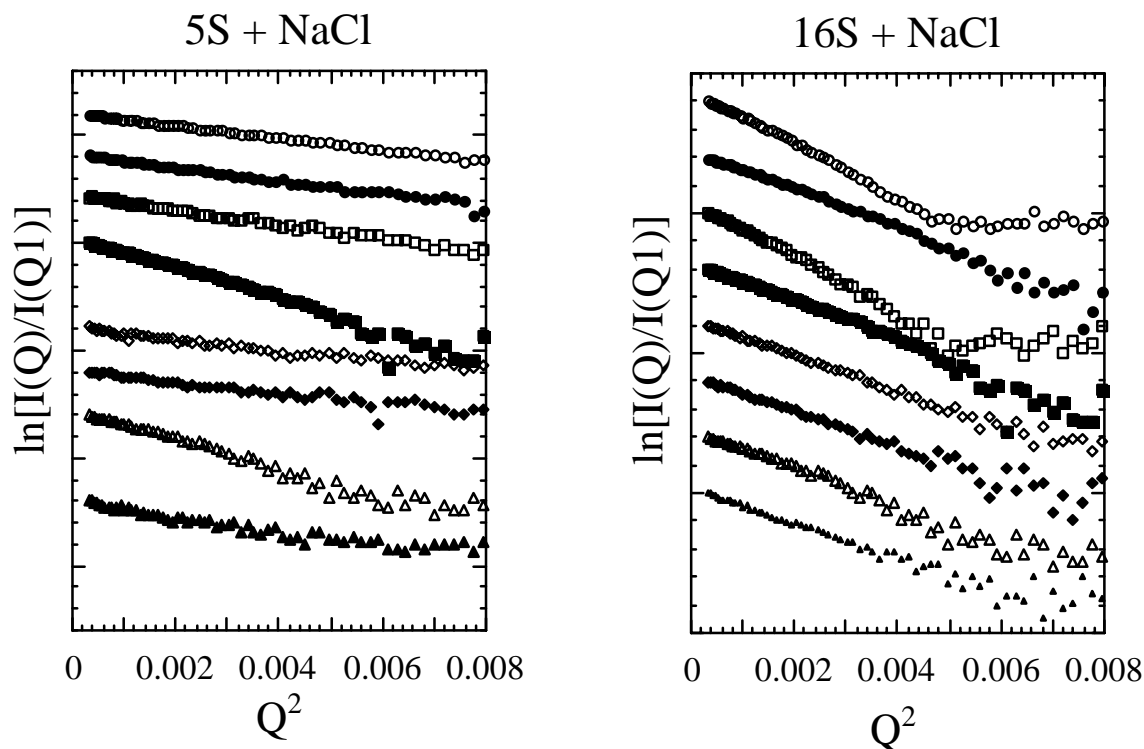
Hemocyanins are the oxygen transport proteins in some molluscs and arthropods, which bind the substrate in a binuclear copper containing active site. Hemocyanins are extracellular proteins containing 2 copper atoms, directly bonded to the polypeptidic chain, which constitute the bond site for the oxygen. In arthropod hemocyanins, 5S, 16S, 25S, 37S, 48S and 64S sedimentation coefficients have been found and have been associated to the presence of well established aggregates. The 5S unit, which corresponds to the minimum functional subunit, has a molecular weight of 75 kD. The 16S specie is considered the basic functional unit, and shows a hexagonal shape, attributed to the presence of 6 subunits 5S, arranged as two trimers superposed each on the top of the other, staggered of 60°. The other species seem to correspond to dimers, tetramers, hexamers, and octamers of the 16S structure.



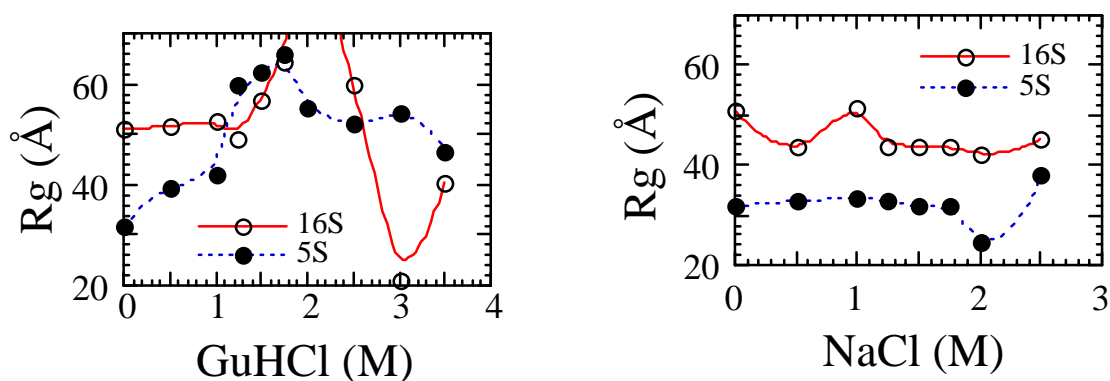
We have studied by small angle scattering techniques the structural properties of the hemocyanins, considering in particular the unfolding process induced by the guanidinium chloride (GuHCl) on the olo (copper ions containing) preparations of 5S and 16S subunits. These forms, obtained from the native oligomeric protein of the crab *Carcinus aestuarii*, have been studied by SAXS at the Elettra Synchrotron facility (SAS camera on the beamline 5.2 L). Hemocyanins were dissolved in a phosphate buffer (pH 7.5) at concentration of 10 mg/ml and measured in 1 mm quartz capillaries. The scattering from a buffer capillary was subtracted from the data after correction. The scattering curves, in the form of Guinier plots, are reported in the above figure. The molarity of

the GuHCl in the protein analyzed samples is (from the top curve in the figure): 0, 0.5, 1, 1.25, 1.5, 1.75, 2, 2.5, 3, 3.5.

To obtain information on the nature of the interactions between the subunits, SAXS experiments have been also performed as a function of the ionic strength of the solution, i.e. by changing the concentration of NaCl in the protein solution. The scattering curves are reported below. The molarity of the NaCl is (from the top curve): 0, 0.5, 1, 1.25, 1.5, 1.75, 2, 2.5.



Modifications of the structure of the scattering particles have been detected (see the variations of the radii of gyration as a function of GuHCl and NaCl concentrations reported below) and have been associated to the aggregation properties of the different species and to unfolding process. The data analysis is in progress.



# KINETICS AND MECHANISM OF APO AI ADSORPTION AND INSERTIONS INTO PHOSPHOLIPID BILAYERS

R. Farkas<sup>1</sup>, M. Kriechbaum<sup>1</sup>, R. Prassl<sup>1</sup>, M. Steinhart<sup>2</sup> and P. Laggner<sup>1</sup>

<sup>1</sup> Institute of Biophysics and X-Ray Structure Research  
Austrian Academy of Science, Steyrergasse 17, A-8010 Graz

<sup>2</sup> Institute of Macromolecular Chemistry  
Academy of Science of the Czech Republic, Heyrovsky Sq. 2, CZ-162 06 Prague 6

## BASICS

Apolipoprotein AI (apo AI), an amphiphilic 28 kDa protein, is the major protein constituent of the antiatherogenic human high density lipoprotein (HDL). The HDL plays a key role in reverse cholesterol transport (RCT) from peripheral tissues including the arterial wall to the liver. Therefore apo AI appears as the primary candidate for the development of apolipoprotein-like pharmaceuticals to be employed in the treatment of cardiovascular diseases.

So far, the kinetics and the structural mechanisms of protein refolding, adsorption and insertion into lipid bilayers are only poorly understood. The high flux of the SAXS-beamline at ELETTRA in combination with the high pressure x-ray cell (HPXC) allows the investigation of the folding conditions and denaturation of this protein.

Apo AIMilano is a less active mutant which differs from the wild-type for an Arg173 Cys substitution, leading to the formation of disulfide-linked dimers. The apo AIMilano mutation thus results in low plasma HDL but no increased risk for cardiovascular diseases. Reconstituted HDL particles consisting of palmitoyl-oleoyl-phosphatidylcholine (POPC) and apo AI as well as apo AIMilano with or without cholesterol have been synthesized by the sodium cholate dispersion and dialysis method.

Using the HPXC these particles were pressurized up to 1.5 kbar at two different temperatures. The change in the folding conditions of the protein and also the structural changes in the lipid phase were measured.

## EXPERIMENTAL EQUIPMENT

The HPXC is made of Cr-Ni-Mo-Ti steel, the irradiated sample volume is approximately 0.3 L. Two disc-shaped x-ray windows, one for the incoming beam, one for the scattered outgoing beam, are made of beryllium characterized by a theoretical transmittance of 55 % for Cu K radiation and high pressure resistance. These windows are coated with a polyimide film at the inner surface to protect it from contact with the pressure transmitting medium.

The HPXC allows principally measurements with pressures up to 2 kbar. The cell is sandwiched between two copper blocks passed by water to hold a desired temperature adjusted by a thermostat within a range between - 20 and + 80 °C.

## CONCLUSION

A high background radiation of the beryllium windows of the HPXC and the pressure dependency of the cell transmission influenced the quality of the collected data. A transition from unilamellar to multilamellar bilayer stacking did not occur in the investigated pressure range.

To improve the transmission of the HPXC windows modifications are planned to simplify the elaboration of data.

A further investigation of apo AI, including experiments to obtain real-time information about the kinetics should be performed to make another step in developing cholesterol-lowering drugs.

## LITERATURE

Sirtori CR, Calabresi L, Franceschini G. *Atherosclerosis*. 1999; 142: 29-40.

Pressl K, Kriechbaum M, Steinhart M, Laggner P. *Rev. Sci. Instrum.* 1997; 68(12): 4588-4592

## SAXS STUDY ON THERMO-REVERSIBLE $\kappa$ -CARRAGEENAN GELS BY SYNCHROTRON RADIATION

Amelia Gamini<sup>1</sup>, Sergio Paoletti<sup>1</sup>, Karin Bongaerts<sup>2</sup>, Elizabeth Theunissen<sup>2</sup>, Guennady Evmenenko<sup>2</sup>, Harry Rheynaers<sup>2</sup>, Heinz Amenitsch<sup>3</sup>, Sigrid Bernstorff<sup>4</sup>

1.) Department of Biochemistry, Biophysics and Macromolecular Chemistry, University of Trieste, Via L. Giorgieri 1, I-34127, Trieste, Italy

2.) Laboratory of Macromolecular Structural Chemistry, University of Leuven, Celestijnenlaan 200F, B-3030, Heverlee, Belgium

3.) Institute of Biophysics and X-ray Structure Research, Austrian Academy of Science, Steyrerg. 17, A-8010 Graz, Austria

4.) Sincrotrone Trieste, Strada Statale 14, km 163.5, I-34012, Basovizza, Trieste, Italy

$\kappa$ -carrageenan is a sulfated poly-galactose extracted from red algae. It is known to undergo thermoreversible conformational transition generally described as disorder-to-order transition on increasing ionic strength, eventually leading to gel formation the extent of which depending on type and concentration of the added salt. In NaI 0.1M it has been shown that the ordered polysaccharide conformation is fairly described by a single polymer chain of relatively high stiffness which „melts“ at around 30°C. To the contrary KCl aqueous solutions are known to be a typical gelling solvents. The gel-sol transition of  $\kappa$ -carrageenan KCl 0.1M occurring at around 40°C.

Being the secondary  $\kappa$ -carrageenan ordered structure still a debated matter in as much as single, double or multiple chains may represent the fundamental ordered state from which gel formation takes place, we performed SAXS study in order to have a better insight of conformational changes during the „melting“ processes. The intensity of the scattered light as function of temperature was measured in a static as well as in a dynamic mode. In the former case the intensity of light scattered by the polysaccharide-electrolyte solution was measured at constant T after a suitable equilibration time (i.e.30 min). In the latter case, after a heat shock, the structural relaxation of the polymer system towards the equilibrium was followed by the change of the scattered intensity light with time.

The scattering profiles obtained as function of temperature from equilibrium measurements for comparable ( $\approx$ 1% w/w) polymer concentration in KCl and NaI are reported in Fig. 1 a and b, respectively. The different temperature dependence of the intensity for the gelling and non-gelling system is clearly shown by the high scattering power and the anomalous intensity increase above the melting temperature observed for aqueous KCl with respect to NaI (inserts of Fig.1). At the melting temperature the intensity scattered by the  $\kappa$ -carrageenan super-structure in KCl reduces to one half, whereas only a  $\approx$ 15% decrease (if any) is observed for the corresponding NaI salt solution. As deduced from Fig. 1 and contrary to what can be observed by using other techniques (e.g. optical activity and enthalpy changes) the „melting“ processes of the ordered associated chains does not end at a temperature as high as 70°C. As a matter of fact the anomalous intensity increase can only be understood if it is ascribed to the dissociation of chain clusters which average dimensions are outside the experimentally accessible minimum value of the scattering vector.

Due to the relatively high stiffness of the polysaccharide backbone and to the relatively high polymer concentration, Guinier analysis of the scattered intensity might be performed in order to obtain only the average dimension of the cross-sectional area  $R_c$ :

$$qI(q) \approx \exp(-R_c^2 q^2/2) \quad (1)$$

If eq.1 is applied a slightly higher  $R_c$  value is obtained ( $\approx$ 7nm) for  $\kappa$ -carrageenan/KCl than for  $\kappa$ -carrageenan/NaI system ( $\approx$ 5nm). Despite the same order of magnitude the interesting feature is the temperature increase of  $R_c$  observed in presence of KCl (i.e. 9 nm at T= 70°) whereas a constant value throughout the temperature range is obtained for the corresponding dimension in NaI aqueous solution.

Additional informations on the melting processes of the ordered conformations of  $\kappa$ -carrageenan salt solution are given by following with time the scattering intensity changes upon sudden temperature

variation. Although a truly kinetic analysis of the data has not yet been performed the results are rather interesting.

In Figs. 2a and 2b the saxs and waxd total intensity as a function of time are reported for  $\kappa$ -carrageenan/NaI system after the temperature was quickly dropped from 65°C to 25°C. Figs. 3a and 3b show the corresponding T-jump for the for  $\kappa$ -carrageenan/KCl system. The fast (likely one-step) formation of the  $\kappa$ -carrageenan ordered conformation in NaI has as a counter part the slower adjustment of the conformational state of the polysaccharide chains in KCl. The slow decreases of the intensity by time accounts for the disappearance from the active q range of big clusters (Fig.1). Moreover the increasing intensity in the waxd region soon after the temperature chock suggests, in agreement with the previous equilibrium measurements, that the supra-molecular structure is only partially melted.

The preliminary, mainly qualitative, analysis of the SAXS data collected for  $\kappa$ -carrageenan in gelling and non gelling condition strongly support the different molecularity of the ordered conformational state which characterize the polysaccharide chains in the two different media.

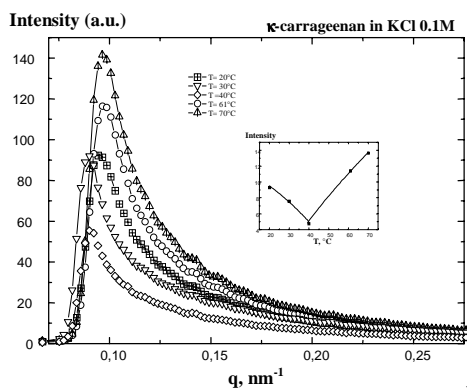


Fig. 1a

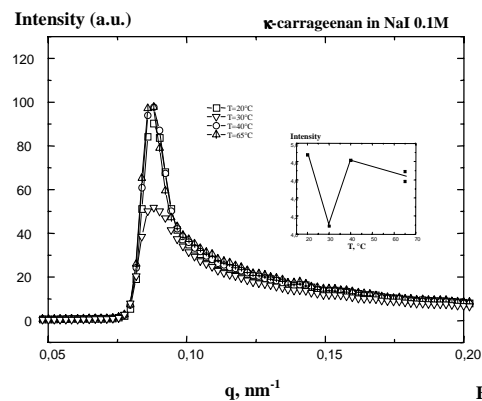


Fig. 1b

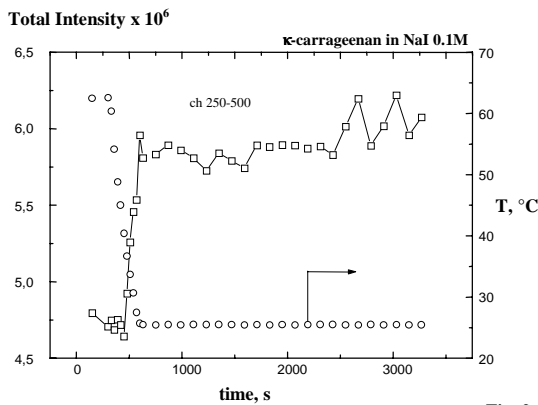


Fig. 2a

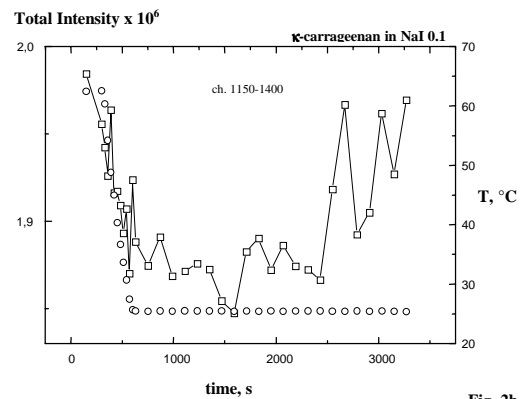


Fig. 2b

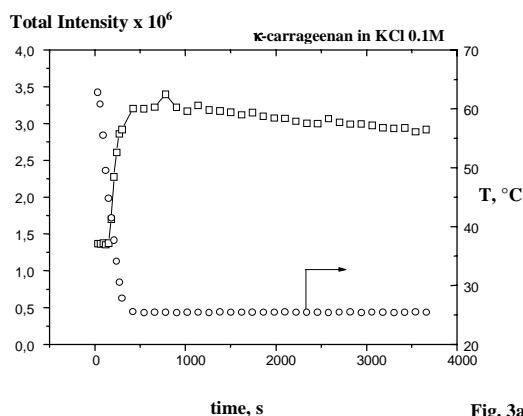


Fig. 3a

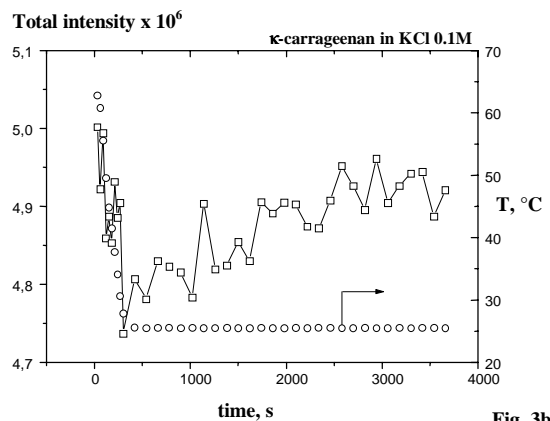


Fig. 3b

# STRUCTURE AND DYNAMICS OF THYLAKOID MEMBRANES AND LAMELLAR AGGREGATES OF LHCII.

## I. IRREVERSIBLE STRUCTURAL CHANGES IN THYLAKOIDS

G. Garab<sup>1</sup>, Z. Cseh<sup>1</sup>, T. Javorfi<sup>1</sup>, H. Amenitsch<sup>2</sup> and S. Bernstorff<sup>3</sup>

1.) Hungarian Academy of Sciences, Biological Research Center, Institute of Plant Biology

2.) Institute for Biophysics and X-ray Structure Research

3.) Sincrotrone Trieste

**Main goal:** to elucidate the nature of the irreversible light-induced structural changes in chloroplast thylakoid membranes, most specifically, to establish the effect of irreversible structural changes on the membrane thickness.

### Main results:

We have shown that, in contrast to the expectations, the light induced irreversible structural changes in chloroplasts *do not* involve changes in the membrane thickness. Earlier, some electron microscopic data suggested that the thickness of thylakoid membranes was likely to change upon prolonged illumination of thylakoid membranes with intense light. However, because of the possible staining artifacts in EM, no firm conclusion could be reached. Our investigations rule out variations in the thickness at a precision of 0.01-0.02 nm. (Fig. 1 and Table I). Modulation of the amplitudes of the main bands of the magnetically aligned membranes due to preillumination strongly suggest that the irreversible structural changes affect the lateral organization of the complexes in the membranes.

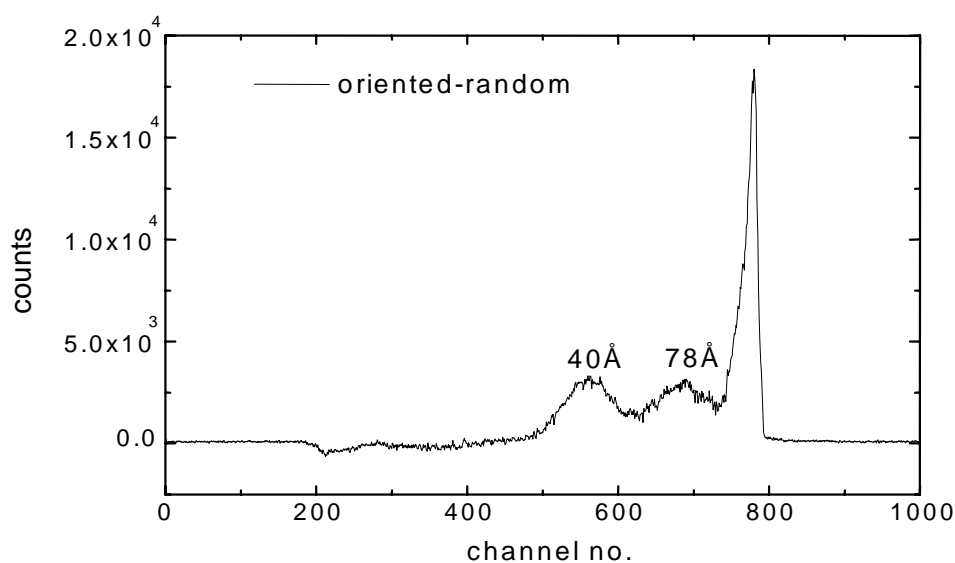


**Figure 1.** X-ray scattering profile of magnetically aligned minus randomly oriented chloroplasts.



**Table 1.**

Sample #	Before illumination	After illumination
1	40.60 Å	40.33 Å
2	40.33 Å	40.32 Å
3	40.32 Å	40.32 Å
4	40.34 Å	40.38 Å

**Publication:**

Jávorfi T., Amenitsch H., Laggner P., Cseh Z., Mustárty L., Borbély S., Rosta L., Garab G. (1998) Nature of irreversible structural changes induced by intense light in thylakoids. Small angle X-ray and neutron scattering of magnetically aligned chloroplasts. In *Photosynthesis: Mechanisms and Effects* (ed.: G. Garab) Kluwer Acad. Publ., Dordrecht, pp. 349-352.

# STRUCTURE AND DYNAMICS OF THYLAKOID MEMBRANES AND LAMELLAR AGGREGATES OF LHCII.

## II. LHCII-CONTAINING ARTIFICIAL MEMBRANES

G. Garab<sup>1</sup>, Z. Cseh<sup>1</sup>, T. Javorfi<sup>1</sup>, H. Amenitsch<sup>2</sup> and S. Bernstorff<sup>3</sup>

1.) Hungarian Academy of Sciences, Biological Research Center, Institute of Plant Biology

2.) Institute for Biophysics and X-ray Structure Research

3.) Sincrotrone Trieste

**Main goal:** to elucidate the nature of the irreversible light-induced structural changes in chloroplast thylakoid membranes, most specifically, to establish the effect of irreversible structural changes on the membrane thickness.

### Main results:

Experiments performed on different artificial membranes revealed that two bilayer forming lipids species, DGDG and SQDG (not shown), formed micelles, as expected, when vortexed in water. Upon the addition of isolated, purified LHCII, micelles disappeared, evidently due to the formation of vesicles upon the association of the lipids and the proteins (Fig. 1).

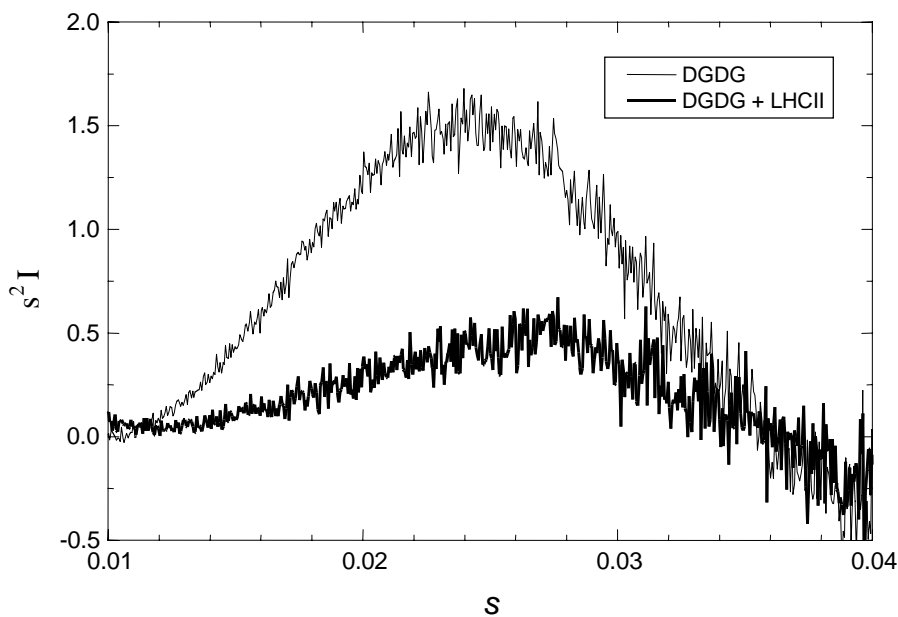


Figure 1.

MGDG, a non-bilayer forming lipid, in water led to the formation of  $H_{II}$  phase. These structures were gradually ‘dissolved’ upon the admixture of LHCII, and the formation of the artificial membranes (Fig. 2). To our knowledge, this is the first direct demonstration that these lipids are capable of forming membranes, evidently due to the presence of integral proteins of the native membranes. Independent experimental evidence concerning the formation of the membranes, and the role of these lipids in arranging the complexes in an array with long range order have been given by negative staining electron microscopy and circular dichroism spectroscopy, respectively.

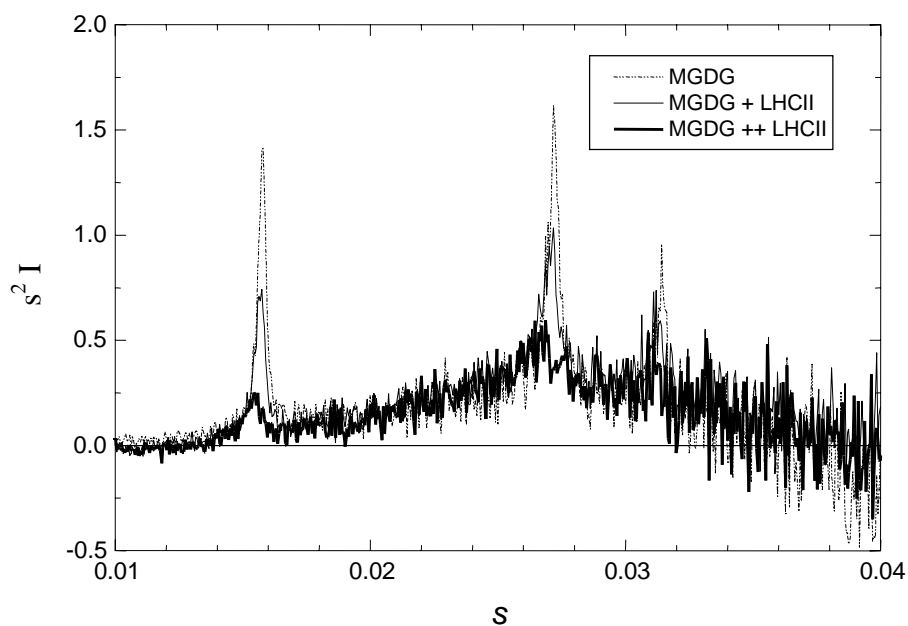


Figure 2.

**Publication:**

Simidjiev I., Stoylova S., Holzenburg A., Amenitsch H., Laggner P., Jávorfí T., Mustárdy L., Garab G. (1998) Reconstitution of membranes using non-bilayer forming lipids and plant LHCII. In *Photosynthesis: Mechanisms and Effects* (ed.: G. Garab) Kluwer Acad. Publ., Dordrecht, pp. 1799-1802.

# KINETICS OF MEMBRANE PERTURBATION AND DISRUPTION BY ANTIMICROBIAL PEPTIDES

K. Lohner, H. Amenitsch & E. Staudegger

Institute of Biophysics and X-ray Structure Research, Austrian Academy of Sciences,  
Steyrergasse 17, A-8010 Graz, Austria.

A totally new approach to kill antibiotic-resistant bacterial strains is based on host defense peptides which evolved in nature. Such amphiphilic peptides (around 20 amino acids) act by perturbing the barrier function of bacterial cell membranes. Thereby these antimicrobial peptides exhibit a high specificity towards distinct target membranes. The molecular mechanism of their action is still a matter of debate. While many conventional antibiotics disable or kill bacteria over a period of days antimicrobial peptides kill almost instantaneously, i.e. within minutes.

Our results obtained so far on the frog skin peptide, PGLa, and on human defensin using thermodynamic and structural techniques gave only information on the equilibrium situation. However, in order to understand the mechanism it is important to study the interaction between the peptides and model membranes in real time. Therefore we studied the kinetics of membrane perturbation by the bacterial peptide  $\delta$ -lysin (see Fig. 1), which can even lead to gross morphological changes of the supramolecular membrane structure. An understanding of how these peptides lyse cell membranes would contribute to the design of novel peptide antibiotics.

The Synchrotron X-ray scattering experiments revealed that the mechanism of membrane perturbation seems to be separated into two kinetical processes. The lipid and peptide samples were filled into two separate syringes, automatically injected into a stopped-flow cell and triggered with the beam shutter. Upon mixing of suspensions of multilamellar vesicles of dimyristoylphosphatidylcholine (DMPC) or palmitoyloleoylphosphatidylcholine (POPC) with a phosphate buffer solution of  $\delta$ -lysin, the Bragg intensity of the small-angle X-ray diffractograms decreased within the time range of 5 minutes (see Fig. 2). This was interpreted as the disruption of multilamellar vesicles into smaller lipid aggregates by the peptide. This time scale would correlate with the suggested time course of the disruption of biological cell membranes by lytic peptides. In all mixing experiments an initially very rapid and unexpected process ( $\sim 4$  sec) occurred (see Fig. 3), again characterized by a strong decrease of the Bragg peak intensity as compared to the control sample without peptide.

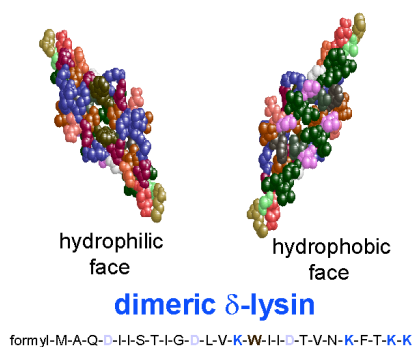


**Fig. 1:** Space filling model of the dimeric  $\delta$ -lysin molecule, a membranolytic toxin of *Staphylococcus aureus*, adopting a lateral amphipathic  $\alpha$ -helix with a pronounced hydrophobic and hydrophilic face. It has a cationic, lysine (Lys) rich C-terminus and a tryptophane (Trp) at the polar/apolar interface surrounded by three negatively charged aspartate residues (Asp); amino acid sequence of  $\delta$ -lysin (bottom).

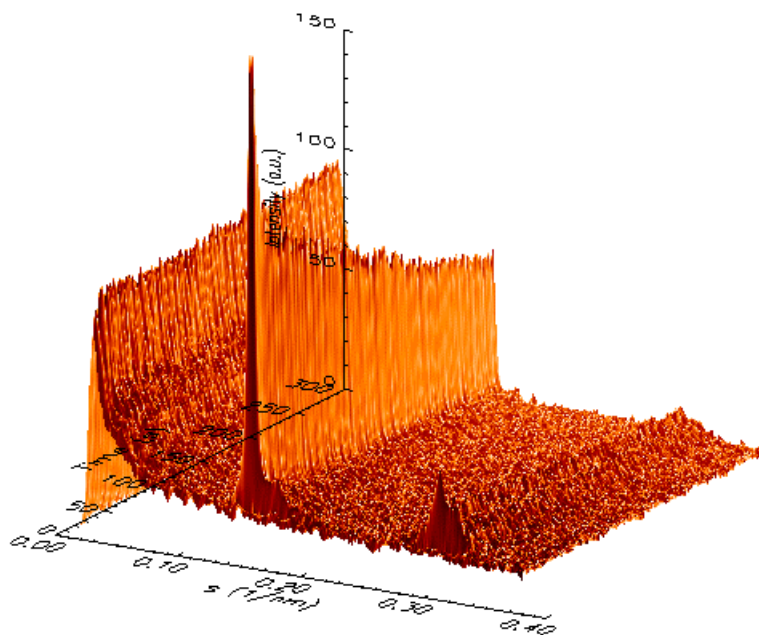


**Fig. 2:** Time resolved diffraction pattern (time resolution 0.5 s/frame) after admixing of  $\delta$ -lysin (10 mg/ml) to DMPC (71 mg/ml) (1:1 by vol.). The decrease of the first and second order Bragg peaks, characteristic for multilamellar DMPC vesicles, are clearly visible.

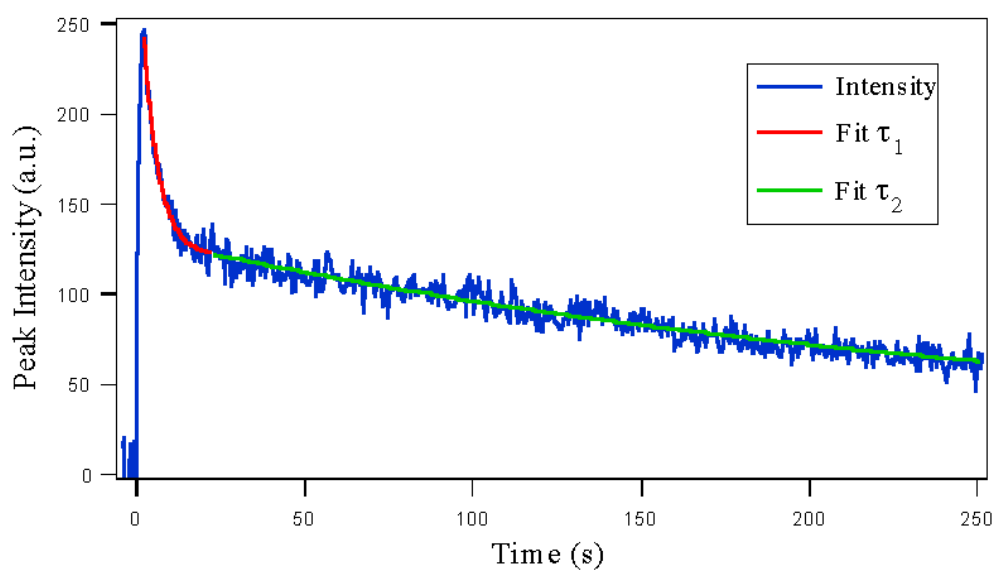


**Fig 3:** Change of the relative intensity of the first order Bragg peak with time after admixing of  $\delta$ -lysin (10 mg/ml) to multilamellar vesicles of DMPC (71 mg/ml) (1:1 by vol.) suggesting that the kinetics of membrane perturbation and disruption contains two time constants ( $\tau_1 = 4.0$  s and  $\tau_2 = 260$  s).

## STRUCTURAL ASPECTS OF AFTER-STRETCH POTENTIATION STUDIED BY COMBINED MECHANICAL AND TIME-RESOLVED X-RAY DIFFRACTION EXPERIMENTS IN SINGLE FIBRES FROM FROG SKELETAL MUSCLE

L. Lucii, M.E. Vannicelli, M. Linari, G. Piazzesi, V. Lombardi

Dipartimento di Scienze Fisiologiche, Università degli Studi di Firenze, 50134 Firenze, Italy

The force enhancement following a stretch imposed on an active muscle fibre is accompanied by a potentiation also in the shortening capability as shown by the ability to shorten against a load equal to the maximum isometric force before the stretch ( $T_0$ ). This has been attributed either to a stretch-dependent rise in mechanical energy of the elementary force generators in the half-sarcomere (hs) the myosin cross-bridges (Cavagna et al., *J. Physiol.* **481**, 689-708, 1994), or to strain of the elastic structures in parallel with weak sarcomeres (Edman and Tsuchiya, *J. Physiol.* **490**, 191-205, 1996).

In the experiments reported here the question was reinvestigated by comparing the intensity of the third order myosin-based meridional reflection at 14.5 nm (M3, sensitive to the axial movements of the myosin cross-bridges) during after-stretch potentiation with those in the isometric contraction and during steady lengthening. Single muscle fibres, freshly dissected from the tibialis anterior muscle of *Rana temporaria*, were mounted in the experimental trough between the lever arms of a force transducer and a servocontrolled loudspeaker motor (Lombardi and Piazzesi, *J. Physiol.* **431**, 141-171, 1990 and references therein). To avoid leakage of the physiological solution a perspex cover was sealed with silicone grease on the top of the trough. The linear gas-filled detector was placed parallel to the fibre axis in order to collect reflections along the meridian at a distance 2.2 m from the sample. In some experiments the detector was rotated by 90° and shifted vertically to the level of the third myosin-based layer line, in order to collect the changes in the dispersion of the M3 reflection across the meridian ( $W$ ) and correct for the change in lattice sampled by the reflection due to change of filament coherence in different physiological conditions. Tetanic contraction was induced at 4°C and 2.2  $\mu$ m sarcomere length by electrical stimulation at the frequency of 15-30 Hz. The intensity of the M3 reflection was recorded with 250 ms frames at rest, during the isometric tetanus when force had attained a plateau value ( $T_0$ ), during the steady state force response ( $1.6 T_0$ ) to lengthening of 60 nm per hs, at the velocity of 200 nm per hs and during the force enhancement after stretch (starting 50 ms after the end of the stretch, when force declined from 1.3 to 1.2  $T_0$ ). Control frames were collected also during a second isometric plateau ( $T_{0,R}$ ) attained after abolishing the after stretch potentiation with a fast shortening of the same amplitude as the lengthening imposed just at the end of the ramp stretch (Fig. 1). Data obtained from a total of 11 fibres were analysed by means of Sigmaplot (Jandel Scientific) software.

Spacing of M3 reflection,  $S(M3)$ , increased by  $1.46 \pm 0.05$  % during the transition from rest to isometric tetanus plateau. During force response to steady lengthening there was a further increase of  $S(M3)$  of  $0.18 \pm 0.06$  %, not fully explained by the filament compliance (Wakabayashi et al. *Biophys. J.* **67**, 2422-2435, 1994; Huxley et al. *Biophys. J.* **67**, 2411-2421, 1994). During force enhancement after stretch  $S(M3)$  recovered towards the isometric plateau value and was practically the same as during the second isometric plateau (Table 1). The intensity of M3 reflection,  $I(M3)$ , decreased to  $0.53 \pm 0.04 I(M3)_0$  (the isometric plateau value) during steady lengthening and partially recovered during the after stretch potentiation ( $0.74 \pm 0.06 I(M3)_0$ ) or during the second isometric plateau ( $0.80 \pm 0.06 I(M3)_0$ ). After the correction for the change in lattice sampled by the reflection (estimated from the change in  $W$  and for the influence of the beam size,  $I(M3)$  reduced to  $0.82 \pm 0.09 I(M3)_0$ ) during steady

lengthening and recovered the original value either during force enhancement after stretch or during the second isometric plateau (Table 1).

By assuming that steady lengthening induces in the cross-bridge the conformation characteristic of the beginning of the force generating process (Piazzesi et al. *J. Physiol.* **445**, 659-711, 1992) and that the orientation of the head in the isometric tetanus is close to the perpendicular to the filament axis (Dobbie et al., *Nature* **396**, 383-387, 1998), the drop in  $I(M3)$  during lengthening can be simulated by using the crystal structure of the myosin head (Rayment et al., *Science* **261**, 58-65, 1993).

The recovery of the M3 intensity at the end of the ramp stretch indicates that the extension of the myosin heads attached to actin during lengthening disappears at the end of lengthening because of the rapid detachment/attachment process which involves specifically the more strained cross-bridges (Colomo et al. *J. Physiol.* **415**, 130P). These results solve the question of the nature of the contribution of the cross-bridges to after-stretch potentiation, that cannot consist in potential energy stored in a long-lived state of cross-bridges, but rather in the increase in number of attached cross-bridges, recruited during the previous lengthening.

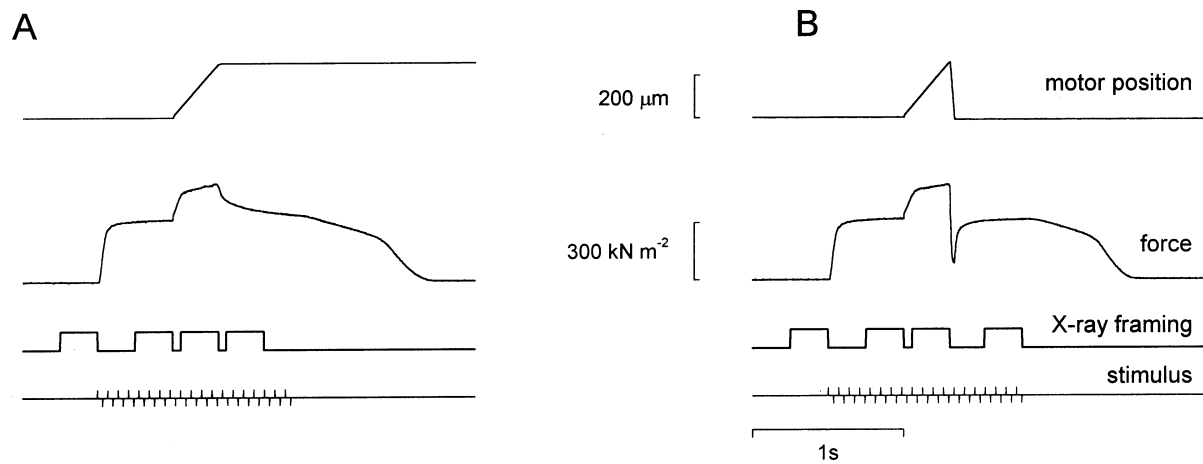


Fig. 1. Protocols for X-ray experiments. 250 ms time frames were collected from the fibre at rest, at the plateau of the isometric tetanus ( $T_0$ ), during steady force response to lengthening and during either force enhancement after stretch (A) or a second isometric plateau ( $T_{0,R}$ ) attained after a fast ramp shortening applied just at the end of the stretch (B).

Table 1. Mean values  $\pm$  SD of spacing and intensity of M3 reflection in the different physiological conditions. The intensity ( $I$ ) is normalised by the value at the isometric tetanus plateau ( $I_0$ ).

	rest	plateau	stretch	after stretch	second plateau
spacing (nm)	14.339 $\pm$ 0.005	14.549 $\pm$ 0.005	14.575 $\pm$ 0.007	14.559 $\pm$ 0.007	14.562 $\pm$ 0.006
$I(M3)/I(M3)_0$	1.53 $\pm$ 0.08	1.00	0.53 $\pm$ 0.04	0.74 $\pm$ 0.06	0.80 $\pm$ 0.06
corrected $I(M3)/I(M3)_0$	0.71 $\pm$ 0.05	1.00	0.82 $\pm$ 0.09	1.14 $\pm$ 0.13	1.06 $\pm$ 0.11

# STRUCTURE DYNAMICS OF F<sub>1</sub>ATPASE DURING AZIDE-INHIBITION OBSERVED BY TIME RESOLVED X-RAY SMALL ANGLE SCATTERING (TR-SAXS)

Thomas Nawroth<sup>1</sup>, Iris Lauer<sup>1</sup>, Manfred Rößle<sup>2</sup>, Hermann Heumann<sup>2</sup>, Sigrid Bernstorff<sup>3</sup>,  
Heinz Amenitsch<sup>4</sup>

1. Institute of Biochemistry, Gutenberg-Universität, Becherweg 30, D-55099 Mainz, Germany
  2. Max-Planck Institute of Biochemistry, Membrane-Biophysics, D-82152 Martinsried, Germany
  3. ELETTRA Synchrotron Trieste, Strada Statale, I-34012 Basovizza/Trieste, Italy
  4. IBR, Austrian Academy of Sciences, Steyregg. 17, A-8010, Graz, Austria
- WEB : <http://www.uni-mainz.de/FB/Chemie/Biochemie/MPSD/TNa.html>

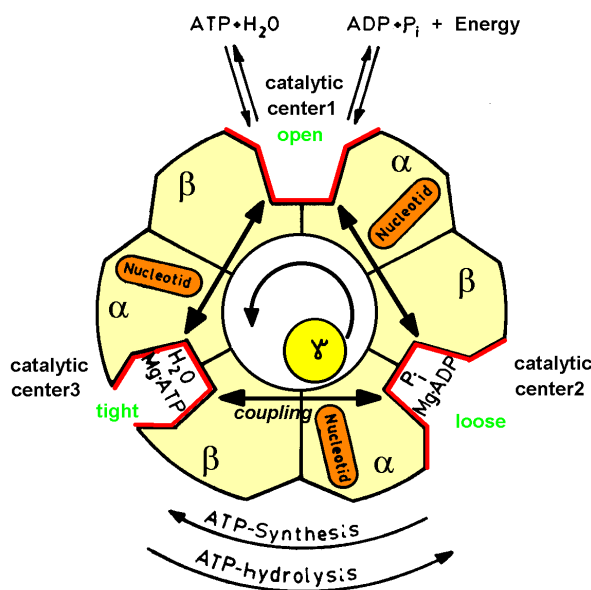


**Fig.1:** ATP-synthase and its catalytic fragment F<sub>1</sub>ATPase contain a hollow assembly of six coupled large subunits ( $\alpha,\beta$ )<sub>3</sub> which bear the three catalytic and three non-catalytic sites. The coupling can be switched off by the artificial inhibitor azide.

The biological function and the regulation on the molecular level of many large proteins depends on structure dynamics of flexible domains. Those intramolecular movements are suggested indirectly by enzyme kinetics, thermodynamic studies and time resolved spectroscopic studies of enzymes, e.g. bacteriorhodopsin, photosynthetic proteins, motor proteins and ATP-synthase or its catalytic F<sub>1</sub>-fragment (F<sub>1</sub>ATPase) [1]. In some cases structures have been estimated before and after the enzymatic catalysis by 2D-NMR or X-ray crystallography, e.g. with the proteins ras and

EF-T<sub>u</sub> using the photolysis of caged-ATP as trigger. Nevertheless the online analysis of structural dynamics during protein activity requires the unrestricted flexibility and accessibility of the protein to diffusion of substrate and products. This is in most cases only possible with protein solutions, which can be structurally investigated by time resolved small angle scattering (TR-SAXS) with high flux synchrotron radiation [2].

ATP-synthase is the major energy converter in cells of higher organisms, e.g. man [1]. It transforms energy, which is locally and transiently available at membranes of respiration or photosynthesis, to the stable transport molecule ATP. This circles in the cell and drives energy dependent processes, e.g. in muscles and enzymes.

The static structure of ATP-synthase is known from crystallography. Nevertheless the molecular mechanisms of energy conversion, the interaction in and between the three catalytic and three non-catalytic nucleotide centers, and the regulation pathways are unknown. Obviously the molecule is a mechanical system, which can act reversibly as motor or generator driving proton transport or migration during the ATP/ADP conversion.

At the SAXS beamline of ELETTRA we have studied the structure dynamics of ATP-synthase and its catalytic headpiece F<sub>1</sub>ATPase using the novel experimental setup for the investigation of transient structural changes of working protein solutions, which was described in the yearly SAXS-ELETTRA report 1997. In the experiments the coupling of the ATPase subunits was switched off by the inhibitor sodium azide (NaN<sub>3</sub>). The effect and kinetics of the inhibition was studied.



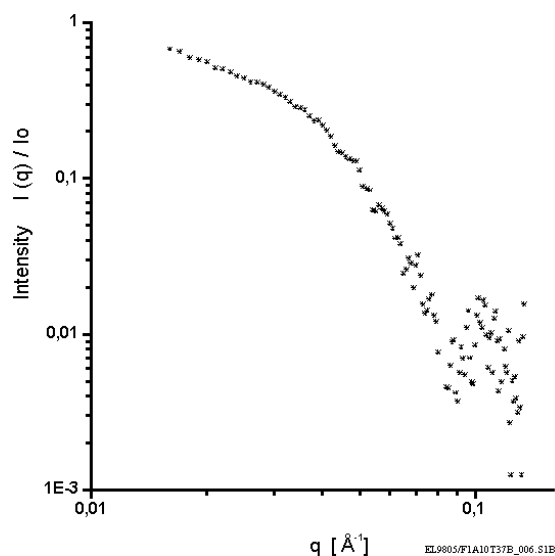


**Fig.2:** X-ray small angle scattering of F<sub>1</sub>ATPase during azide inhibition obtained during a 10 s exposure. The spectrum is a frame of a structural film of 128 pictures after rapid mixing of native enzyme and azide by a stopped flow device (5g/l protein 10mM N<sub>3</sub>).

The samples were formed during 100 ms mixing time from enzyme solution (10g/l) and either azide stock solution or buffer in control experiments. Radiation damage was avoided by degassing and addition of 10% glycerol as radical scavenger. The temperature was held constant by a helium-jet and a remote control thermostat connected to our sample box with the quartz capillary (1 mm dia.). Under that conditions and a flux of 10<sup>12</sup> ph/s at 8 keV in 0.6 x 1.5 mm spot no damage was observed during 2 h

irradiation in control experiments (F<sub>1</sub>ATPase + buffer mixture): the radius of gyration  $R_g = 45,12 \pm 0,27 \text{ \AA}$  (in 1 min. time-frames) was constant within the error limit.

The spectra were taken by a 1D-Gas detector, which showed no reading gaps and related problems on const of reduced yield at higher angles. During the evaluation from each picture a time dependent noise signal was subtracted from each component (see report 1997); additionally the beam monitor B was scaled by a beam-fading signal F(t), which was obtained from the Porod-plot of the water and quartz scattering (inner standard of each time-frame; >99% in the range 0.1-0.136Å<sup>-1</sup>). One frame of a TR-SAXS film of F<sub>1</sub>ATPase during azide inhibition at 37°C is shown in Fig.2. By exposure during 10 s it yielded a radius of gyration of  $R_g = 46.25 \pm 0.45 \text{ \AA}$ . The initial frames of 128 during 2h were taken logarithmically in short time ( $\geq 1$ s) for the detection of fast events. This single shot spectrum shows that protein structure kinetics can be observed at ELETTRA-SAXS with a time resolution down to 10 s in single shots and below 1s, if repetition is applied.

The experiments showed that the expansion of F<sub>1</sub>ATPase and ATP-synthase found by static SAXS experiments at DESY, Hamburg [3] occurs very fast: The size increase of F<sub>1</sub>ATPase from  $R_g = 45.12 \pm 0.27 \text{ \AA}$  to  $46.09 \pm 0.26 \text{ \AA}$  (+2,15 %) by inhibition with 10 mM azide is mainly finished after <15 s (values correspond to  $t_i = 3 \text{ min}$ ).

During the further slow reaction with the inhibitor within 2 h, the expansion of the protein varies after 30 min (further small expansion of 1%). After >60 min a larger molecular species occurs, which is indicated by the leftmost linear range in the USAX range in Fig.3 ( $R_g = 71.24 \pm 1.05 \text{ \AA}$ ).

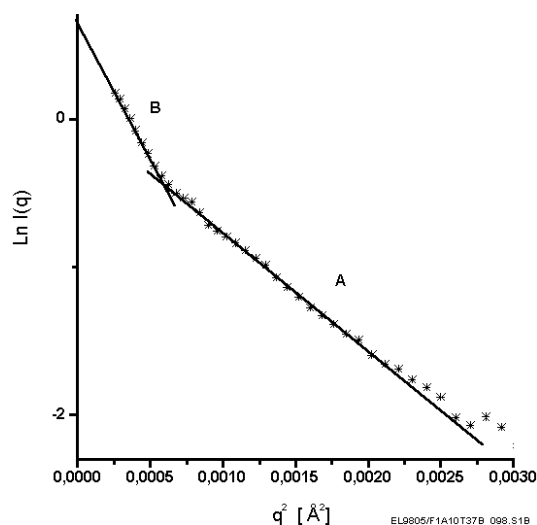


**Fig.3:** The Guinier representation of F<sub>1</sub>ATPase after 90 min azide inhibition indicates the formation of a larger species ( $R_g = 71.24 \pm 1.05 \text{ \AA}$ ,  $\Delta t = 1 \text{ min}$ ) by the linear range B in the USAX region ( $q = 0.016\text{-}0.025 \text{ \AA}^{-1}$ )

1. Junge, W. et al (1997) Trends Biol. Sci, 22, 420-423 and (1999) FEBS Lett. 449, 1 - 6
2. Neidhardt, A.; Nawroth, T.; Hütsch, M.; Dose, K. (1991) FEBS Lett. 280, 179 - 182
3. Nawroth, T. et al. (1997) DESY-HASYLAB report 1997, vol .I, 655 - 656

# NON-EQUILIBRIUM RESPONSE-KINETICS OF PHOSPHOLIPID BILAYERS IN THE BIOLOGICALLY RELEVANT $L_{\alpha}$ -PHASE

G. Pabst<sup>1</sup>, M. Rappolt<sup>1</sup>, H. Amenitsch<sup>1</sup>, S. Bernstorff<sup>2</sup> and P. Laggner<sup>1</sup>

<sup>1</sup>Institute of Biophysics and X-ray Structure Research, Austrian Academy of Sciences, Steyrergasse 17, 8010 Graz, Austria

<sup>2</sup>ELETTRA, Sincrotrone Trieste, SS14, Km 163.5, 34012 Basovizza (TS), Italy

Phospholipids, the main constituents of the biological membrane-matrix, display a distinct polymorphism depending on thermodynamic parameters (T, p, c). One-dimensional bilayers, two-dimensional tubular or three dimensional networks are only a few examples for the structural variety of the supra-molecular associates, wherein the lamellar liquid crystalline phase ( $L_{\alpha}$ ) is the biologically most relevant phase.

Although much is known about the structures and properties of phospholipid phases under equilibrium conditions, little is understood about the kinetics and mechanisms of response processes in lipid bilayers under non-equilibrium circumstances, e.g. upon rapid changes one of the thermodynamic parameters. The high x-ray flux offered by third-generation synchrotron sources has generally enhanced the potential for carrying out real-time jump-relaxation studies [1-4]. Rapid temperature-jump (T-jump) experiments can be carried out using an infra-red laser. The IR-laser apparatus successfully installed at the SAXS beamline [5] induces T-jumps in the order of 10 °C/ms. The structural changes of the phospholipid sample are recorded by time-resolved small-angle X-ray diffraction (time resolution: 5 ms).

The lipid/water systems responds to the T-jump with a very fast discrete thinning of the parent membrane into a structural ordered liquid crystalline phase ( $L_{\alpha}^*$ ), within the first few milliseconds. The intermediate repeat distance then relaxes back into the equilibrium state lattice within a time-scale of seconds (Fig 1).

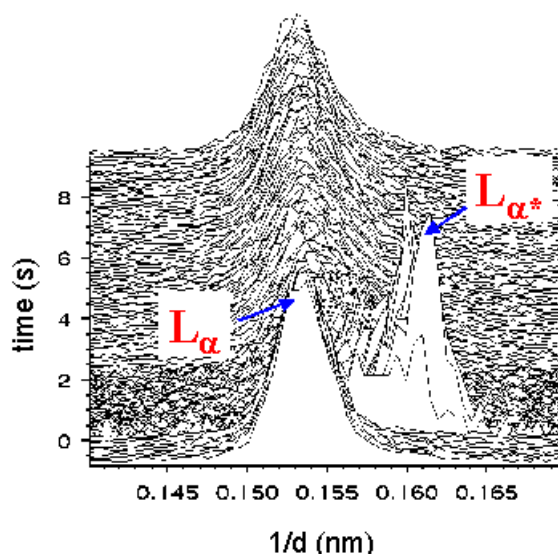


Fig. 1: The first order diffraction peaks of a phospholipid sample during a T-jump experiment (time resolution = 5 ms). The IR-laser was triggered at time zero.

This type of response kinetics is well known and has been studied in detail before [3-8], but since no more than two orders of diffraction peaks were recorded the structure of the liquid crystalline intermediate remained unknown. For the reliable calculation of an electron density distribution one needs at least four diffraction orders; the problem of missing higher orders is usually attributed to packing disorder. In a recent experimental session we made the effort to record four orders of Bragg peaks for a whole T-jump experiment for the system 1-stearoyl-2-oleoyl-*sn*-glycero-3-phosphoethanolamine (SOPE) / water. After determining the form-factors and the phases, the Fourier transform – yielding the electron density distribution – was calculated for the unit cell for each single time frame (Fig. 2 and [6]).

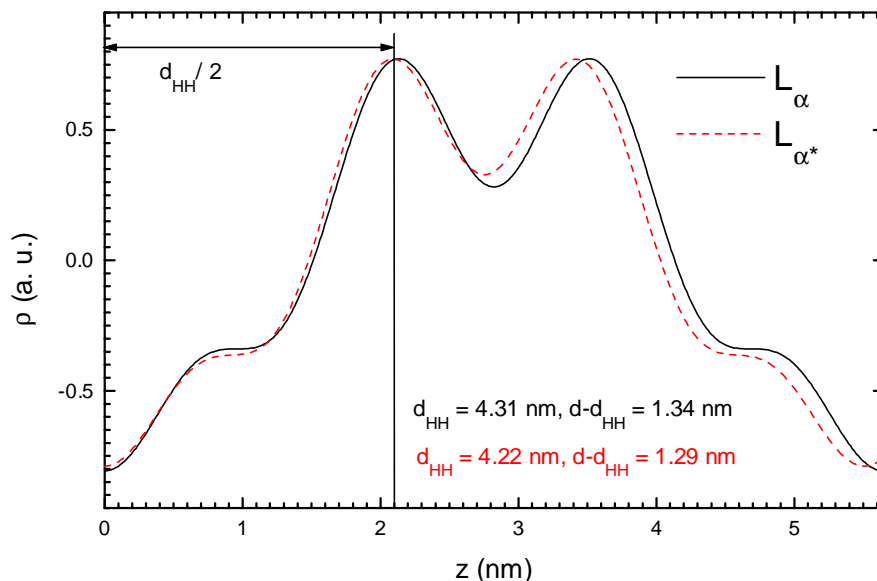


Fig. 2: Superimposed electron density distributions of the original  $L_{\alpha}$ -phase (straight line) and of the intermediate phase  $L_{\alpha^*}$  (dashed line) immediately after the laser flash.

The results show that the T-jump enforces a thinning of both the water layer as well as the bilayer itself, while the qualitative features of the electron density distribution remain the same. This suggests that the phospholipid membrane behaves like a spring that is pushed together and relaxes again to the equilibrium position after it is released ("mattress model"). This reveals on the other hand a highly cooperative interaction of the phospholipid molecules in the supra-molecular compound of a membrane. For cell biology – where all processes like pore formation, self organization, switching processes, etc. are definitely non-equilibrium phenomena – the conservation of the membrane structure even under these extreme conditions is of high importance, since this is the only way of keeping up the vital function of the biological membrane in cell compartmentation and communication.

- [1] M. Caffrey, G. Fanger, R.L. Magin and J. Zhang, Kinetics of the premelting ( $L_{\beta}$ - $P_{\beta}$ ) and main transition ( $P_{\beta}$ - $L_{\alpha}$ ) in hydrated dipalmitoylphosphatidylcholine, *Biophys. J.*, **58**: 667-686, 1990.
- [2] S. M. Gruner, Time-Resolved X-ray Diffraction of Biological Materials, *Science* **238**: 305-312, 1987.
- [3] G. Rapp and R. Goody, Light as a Trigger for Time-Resolved Structural Experiments on Muscle, Lipids, p12 and Bacteriorhodopsin, *J. Appl. Cryst.* **24**: 857-865, 1991.
- [4] M. Kriechbaum and P. Laggner, States of Phase Transitions in Biological Structures. In: "Progress in Surface Science" (ed. S. G. Davidson), **51(3)**: 233-261, 1996.
- [5] G. Pabst, H. Amenitsch, S. Bernstorff, C. Krenn, M. Rappolt and P. Laggner, Infrared-Laser T-jumps with  $10^4$  K/sec at the SAXS beamline, ELETTRA Highlights, 1997 and ELETTRA News Number 21, 1998.
- [6] G. Pabst, M. Rappolt, H. Amenitsch, S. Bernstorff and P. Laggner, Non-Equilibrium Response-Kinetics of Phospholipid Bilayers in the Biologically Relevant  $L_{\alpha}$ -Phase: A REAL-TIME, REAL-SPACE MOVIE. ELETTRA News Number 29, 1998.
- [7] M. Rappolt. Zeitaufgelöste Röntgenbeugung zur Untersuchung von Phasenübergängen an Modellmembranen. PhD thesis, University of Hamburg, 1995.
- [8] P. Laggner, H. Amensitsch, M. Kriechbaum, G. Pabst and M. Rappolt, Trapping of Short-Lived Intermediates in Phospholipid Phase Transitions: The  $L_{\alpha^*}$ -Phase, *Faraday Discussion* **111**, 1999 (in press).

## X-RAY STRUCTURE ANALYSIS OF THE LiCl INDUCED $L_{\alpha}$ -PHASE SEPARATION IN PHOSPHATIDYLCHOLINE-WATER SYSTEMS

G. Pabst, M. Rappolt, H. Amenitsch and P. Laggner

Institute of Biophysics and X-ray Structure Research, Austrian Academy of Sciences, Steyrergasse 17, 8010 Graz, Austria

The effects of alkali chlorides on phosphatidylcholine-water bilayer systems in the  $L_{\alpha}$ -phase have been investigated by means of small angle X-ray diffraction. The ternary system LiCl-POPC- $H_2O$  under isothermal conditions has shown that above  $Li^+$  / POPC molar ratios of 0.1 and a lipid concentration above 5 % (w/w), a splitting of the lamellar Bragg diffraction peaks into discrete components indicates a phase separation of up to three different lamellar liquid crystalline (smectic A) phases [1].

In the following we report on the most important results of a detailed X-ray analysis on a 40% w/w 1-palmitoyl-2-oleoyl-*sn*-glycero-3-phosphocholine (POPC)/water dispersion upon the addition of 0.88 M LiCl (corresponds to a molar ratio of 1  $Li^+$ /POPC). The X-ray patterns have been analyzed in terms of the modified Caillé theory [2]. The structural parameters have been calculated following the formalism introduced by McIntosh and Simon [3] and Nagle et al. [4].

Table 1: Structural parameters for the POPC dispersions at 2°C. The phase separation results are compared with POPC 20% w/w in pure water.

	POPC 20% w/w pure water	POPC 40% w/w 0.88 M LiCl	
		phase A	phase B
A ( $\text{\AA}^2$ )	56.5	57.0	55.5
d ( $\text{\AA}$ )	66.2	64.7	58.8
d <sub>C</sub> ( $\text{\AA}$ )	16.1	15.9	16.3
d <sub>B'</sub> ( $\text{\AA}$ )	50.1	49.8	50.6
d <sub>w'</sub> ( $\text{\AA}$ )	16.1	14.9	8.2
n <sub>w</sub>	21.5	20.7	13.5
n <sub>w'</sub>	6.3	6.5	5.9

A...area per phospholipid molecule

d...d-spacing

d<sub>C</sub>...hydrocarbon chain length

d<sub>B'</sub>...bilayer thickness (steric definition [3])

$d_w$ ...interbilayer water (solution) thickness  $n_w$ ...number of waters per lipid molecule  
 $n_w$ ...number of bound waters per lipid headgroup

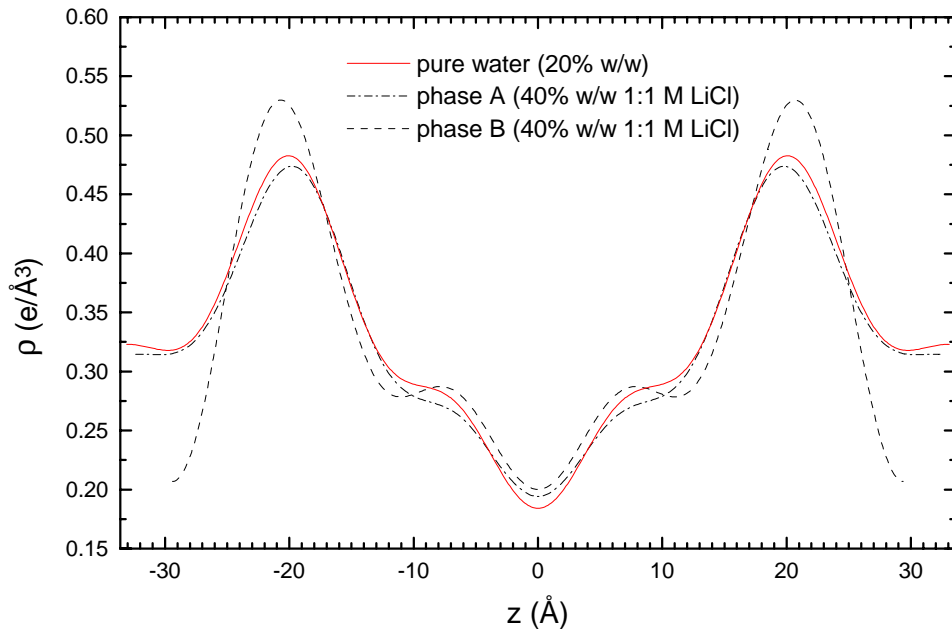


Fig. 1: Absolute electron densities for the POPC dispersions at 2°C.

The POPC/water dispersion reacts upon the addition of LiCl (molar ratio  $\geq 0.1$ ) by a separation into two major phases. Phase A (see Tab. 1 and Fig. 1) corresponds to a fully hydrated phase; the structural differences to the pure water phase are marginal and within the error of the measurement. Phase B on the other hand exhibits a loss of the interbilayer water (dehydration), whereas the phospholipid bilayer itself remains quasi unaffected. The effect can be explained in terms of a conglomeration of liposomes (paper in progress).

- [1] M. Rappolt, K. Pressl, G. Pabst and P. Laggner (1998), *BBA* **1372**: 389-393.
- [2] R. Zhang, R.M. Suter and J.F. Nagle (1994), *Phys. Rev. E* **50**: 5047-5060.
- [3] T.J. McIntosh and S.A. Simon (1986), *Biochemistry* **25**: 4948-4952.
- [4] J.F. Nagle, R. Zhang, S. Tristram-Nagle, W.-J. Sun, H.I. Petrache and R.M. Suter (1996), *Biophys. J.* **70**: 1419-1431.

## TIME-RESOLVED X-RAY DIFFRACTION OF THE CORE LIPID TRANSITION OF HUMAN LOW DENSITY LIPOPROTEINS

M.Pregetter, R.Prassl, H.Amenitsch and P.Laggner

Institute of Biophysics and X-Ray Structure Research

Austrian Academy of Sciences, Steyrergasse 17, 8020 Graz, Austria

Low Density Lipoproteins (LDL) present an important part of the human blood. They are responsible for the transport of lipids, i.e. cholesterol or triglycerides in blood circulation. Failure to function can result in atherosclerosis, followed by myocardial infarct or stroke.

The structure of LDL can be described by a quasispherical core-shell model, in which the apolar constituents (esterified cholesterol and triglycerides) form a core of about 150 Å diameter, which is surrounded by amphiphilic lipids (phospholipids, unesterified cholesterol) and the protein. LDL undergoes a major structural transition of the apolar core closely below physiological body temperature, at about 25 to 32°C, depending on the blood donor. In the outer extremities (finger tips, toes) the blood temperature allows for a transition of the LDL core towards its more rigid and radially ordered state.

Time-resolved measurements provide evidence whether the kinetics of the structural transition permit the transition during the time LDL spends in cooler parts of the human body. High precision SAXS curves in the range of  $1.5 \cdot 10^{-2} < h < 0.2 \text{ \AA}^{-1}$  were measured on well defined subfractions of native LDL. An experimental set-up using an erbium-laser allowed temperature jumps from temperatures below to temperatures well above the core lipid transition in extremely short time. Following the temperature jump a series of measurements elucidated the kinetics of the core-transition. It can be stated that the transition from the rigid towards the fluid core of LDL takes place in less than the 10 ms time-resolution. The rearrangement of the lipid core proceeded with a half-time of 13 s.

1. M.J. Chapman, P.M. Laplaud, G. Luc, P. Forgez, E. Bruckert, S. Goulinet and D. Lagrange (1988). *J. Lipid Res.* 29, 442-458.
2. P. Laggner (1995) in *Modern Aspects of Small-Angle Scattering* (Brumberger H., ed) pp. 371-386, Kluwer Academic Publishers, Leiden, Netherlands.
3. R. Prassl, B. Schuster, P. Laggner, C. Flamant, F. Nigon and J.M. Chapman (1998). *Biochemistry* 37, 938-944.
4. M. Kriechbaum, G. Rapp, J. Hendrix, P. Laggner (1989). *Rev. Sci. Instrum.* 60(7), 2541-2544.
5. M.Pregetter, R.Prassl, B. Schuster, M. Kriechbaum, F. Nigon, J. Chapman, P. Laggner (1999). *JBC* 274(3)1334-1341.

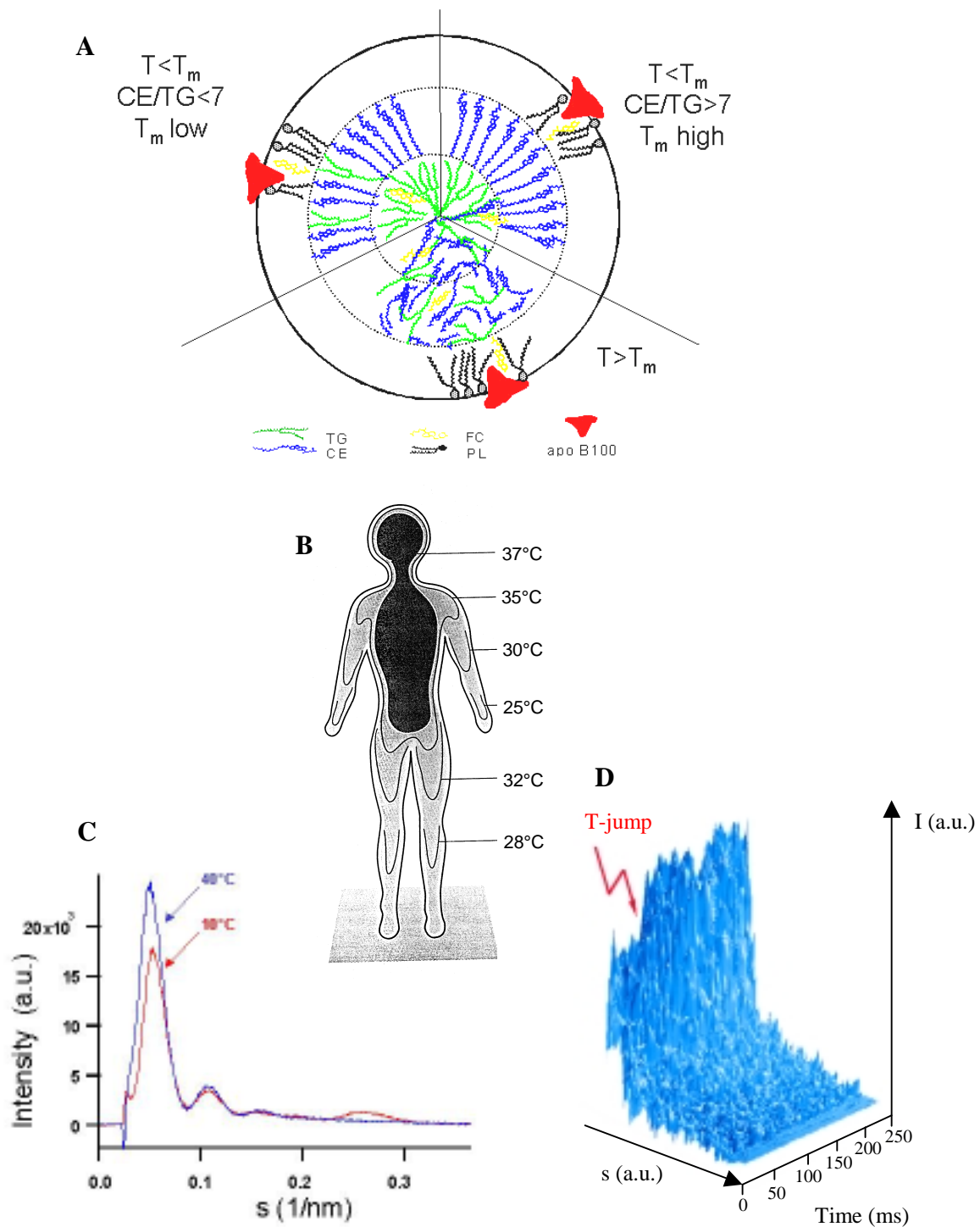


Fig. 1 (A) Sketch of the LDL lipoprotein in the 3 different states: Temperature  $T < T_m$  for ratio  $CE/TG < 7$  and for ratio  $CE/TG > 7$  (core liquid crystalline state), as well as for the  $T > T_m$  (core isotropic state). TG, CE, FC, PL denotes triglycerides, esterified cholesterol, unesterified cholesterol, phospholipids. (B) Temperature distribution in a human body. (C) Static diffraction pattern of LDL at above and below  $T_m$ . (D) Time resolved diffraction pattern of LDL. A sudden increase of the first side-maximum related to the core-melting is observed at the temperature jump.

## TIME RESOLVED SMALL ANGLE SCATTERING STUDIES ON PROTEINS IN SOLUTION USING THE CCD CAMERA AT THE SAXS BEAMLINE

Manfred Rössle<sup>+</sup>, Iris Lauer<sup>\*</sup>, Ronald Gebhardt<sup>\*</sup>, Thomas Nawroth<sup>\*</sup>, Sigrid Bernstorff<sup>§</sup>, Heinz Amenitsch<sup>#</sup> and Hermann Heumann<sup>+</sup>

<sup>+</sup> Max-Planck-Institut für Biochemie, Martinsried (Germany)

<sup>\*</sup> Biochemisches Institut der Universität Mainz, Mainz (Germany)

<sup>#</sup> Austrian Academy of Sciences, Graz (Austria)

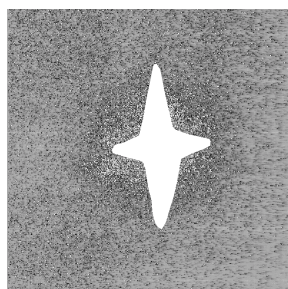
<sup>§</sup> Sincrotrone ELETTRA, Trieste (Italy)

Since third generation synchrotron sources like ELETTRA provide sufficient flux of photons, so that time dependent small angle scattering studies on proteins in solution can be carried out. In order to investigate the structural and conformational changes of proteins upon their reaction the time resolved scattering technique requires a high brilliance and high quality of the x-ray beam and due to this a highly developed detector system designed to detect this high flux of scattered photons. Recently CCD-cameras are the instrument of choice to obtain scattering patterns in the time range of 100ms. Such a CCD device was installed in autumn 1998 at ELETTRA's SAXS beamline.

In former experiments we have investigated the binding behavior of the chaperonin system GroEL-GroES in the presence of different nucleotides. Using a 1-dim gas detector we were able to obtain scattering patterns in the time range of 1s with sufficient good statistic. The CCD detector allowed us now to follow the cycle of the chaperonin reaction in the time range of about 100 ms and therefore to study the conformational changes during the reaction.

**Fig. 1.:**

Small angle scattering pattern (100 ms exposure time, incident flux,  $10^{12}$  ph/s)



The readout time of the CCD chip was reduced to 100 ms and the data acquisition was started by a trigger signal. In figure 1 an image of a 100 ms exposure is shown. The „star“ in the middle is a special adapted beamstop in order to avoid blooming of the CCD. The counting rates are about 100 counts/pixel in the outer range of the image (background and water scattering) and 400 counts/pixel in the inner area (=protein scattering).

Currently software is under development in order to analyze the sequence files (containing 256 frames images and covering about 73 Mb of memory) transforming them from the raw data to the scattering curve for further data treatment.



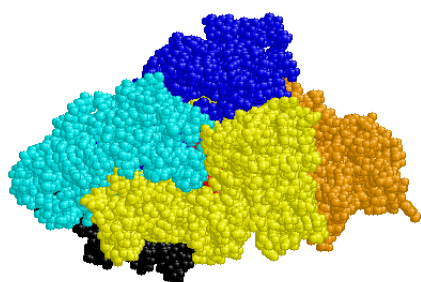
# LIGAND EFFECTS AND STRUCTURAL PROPERTIES OF TISSUE TRANSGLUTAMINASE BY SMALL ANGLE X-RAY SCATTERING

(July, 15-18, 1998)

Franco RUSTICHELLI, Flavio CARSUGHI, Sandro ROMANZETTI, Francesco SPINOZZI and Paolo MARIANI

INFN - Istituto di Scienze Fisiche, Università di Ancona,  
Via Ranieri, 65 - 60131 Ancona (I)

Transglutaminases (TG-ase) comprise a wide group of enzymes which catalyze the post-translational modification of proteins at glutamine residues, with formation of isopeptide bonds (Greenberg et al., 1991). The predominant intracellular isoenzyme is the so-called type-2 tissular TG-ase, a monomeric protein with molecular mass of 80 kDa, which is involved in the programmed cell death (Fesus et al., 1992). The combined actions of  $\text{Ca}^{2+}$  (an activator) and GTP (an inhibitor) control the activity of the intracellular isoenzyme. The crystallographic structure of TG-ase is not known, but much has been learned about possible structural changes in the protein secondary and tertiary structures under the influence of the ligands.  $\text{Ca}^{2+}$  binds to relatively high-affinity binding sites (up to six), activating the enzyme, through conformational changes which allow exposure of the active sites to the incoming protein substrate (Bergamini, 1988). In contrast, GTP binds to a single site, hampering  $\text{Ca}^{2+}$  binding and related structural modifications. Hence, the full understanding of the structural changes are extremely important. A computer-designed model for the structure of TG-ase, based on the sequence homology with human Factor XIIIa and confirmed by SANS experiments, has been recently proposed (Bergamini et al., 1998).



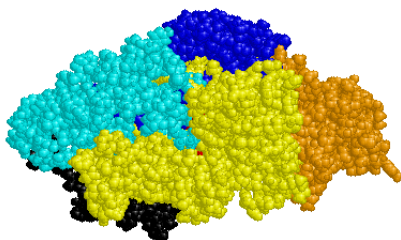
The model is shown in the figure: the protein has a prolate ellipsoidal shape with axis lengths of 62, 42 and 110 Å ( $Rg_{80\text{kDa}} = 30.1$  Å) and is composed of four domains, assembled in two pairs which can be separated into N- and C-terminal regions (56 kDa and 31 kDa, and  $Rg_{56\text{kDa}} = 19.1$  Å and  $Rg_{31\text{kDa}} = 15.6$  Å, respectively) by limited proteolysis. The active site is buried in a cleft between the two regions, hidden from the contact with the solvent or with the macromolecular substrates.

In the present experiment, SAXS measurements were performed on TG-ase in solution in the presence of  $\text{Ca}^{2+}$  and/or GTP to detail the conformational changes. In particular, the enzyme was analysed both in native (from erythrocyte) and in proteolysed (by incubation with chymotrypsin) forms. TG-ase samples were dissolved in 20 mM Tris, 50 mM NaCl, 0.5 mM mercaptohetanol, 0.1 mM EDTA buffer (pH 7.5). The final samples were at the the protein concentrations of  $5 \text{ gL}^{-1}$ . Three sample series were investigated: in the first, native TG-ase was analyzed pure and after addition of  $\text{CaCl}_2$  2.5 mM, of GTP 0.5 mM and of  $\text{CaCl}_2$  2.5 mM and GTP 0.5 mM, respectively. Measurements were repeated in the same conditions for the proteolysed enzyme. In the last series,

guanidine-HCl (Gdn-HCl) 0.5, 0.8, 1.0, 2.0, 2.6 and 4 M were respectively added to the proteolyzed enzyme. The scattering curves were analysed following the usual procedure, i.e., gyration radii  $R_g$  were determined by Guinier approximation from scattering curves. The measured radii of gyration are reported in the Table. Note that for last samples, the hyphen refers to the absence of any SAXS signal in the investigated region.

Sample	$R_g$ (Å)	Sample	$R_g$ (Å)
nTG-ase	$31.4 \pm 1.2$	pTG-ase/Gdn-HCl 0.5 M	$30.5 \pm 3.3$
nTG-ase/calcium	$38.6 \pm 1.4$	pTG-ase/Gdn-HCl 0.8 M	$31.2 \pm 3.0$
nTG-ase/GTP	$29.6 \pm 0.5$	pTG-ase/Gdn-HCl 1.0 M	$19.0 \pm 5.6$
nTGase/GTP/calcium	$38.0 \pm 0.7$	pTG-ase/Gdn-HCl 2.0 M	-
pTG-ase	$31.8 \pm 1.2$	pTG-ase/Gdn-HCl 2.6 M	-
pTG-ase/calcium	$30.7 \pm 0.6$	pTG-ase/Gdn-HCl 1.0 M	-
pTG-ase/GTP	$30.1 \pm 1.2$		

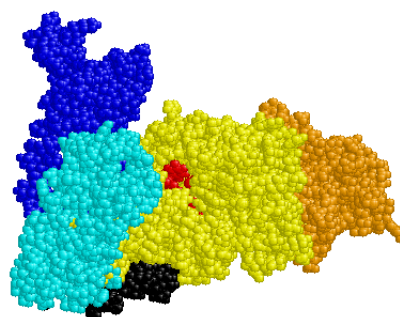
Scattering data demonstrate that large conformational changes follow activation. In the presence of  $\text{Ca}^{2+}$  or both calcium and GTP, the radius of gyration increases up 38 Å; by contrast, the presence of GTP only slightly reduces the radius of gyration of the protein. It is also evident that the cleavage by proteinases of the flexible peptide loop connecting the two domain pairs prevents the occurrence of the calcium dependent protein widening. Concerning the proteolysed another aspect is noticeable: the radius of gyration of the proteolyzed enzyme is equal (inside the experimental error) to that observed for the native TG-ase, indicating that after proteolysis the two N- and the C-terminal protein peptides are still joined. Guanidine is expected to interfere with hydrogen and electrostatic bonds, taking place at the interface between the two domains: up to 0.0 M guanidine does not break interdomains bonds, while, at the higher concentration, the whole protein appears denatured. At intermediate guanidine concentrations, data were consistent with the presence of particles with a gyration radius of about 19 Å, which corresponds to the one expected for the N-terminal peptide.



A method for calculating small-angle scattering profile using Monte Carlo simulation of the scattering volume was used to deduce the shape of transglutaminase in the native and in the calcium activated and GTP inhibited forms (Hansen, 1990). For the native TG-ase, a good fit of the experimental scattering profile was obtained using the computer-designed protein model (see the figure in the left side) and adjusting the width of the gaussian used to describe the hydration shell at the particle border. To fit the experimental scattering data observed in the presence of GTP and calcium, we simulate the scattering volume moving different regions of the protein from the

position occupied in the computer-designed model. However, to restrict the number of possibility, we assumed that the observed conformational changes only concern the arrangement of the C-terminal domain pair, which is

considered free to move in any directions, rotating around the flexible peptide loop. The best model for the protein conformation in the presence of the ligands are reported in the two last figures. In the presence of GTP (see the figure in the left side) the reconstructed model shows that the contact between the two domain pairs is closer, so that the catalytic site appears even shielded. By contrast, the large conformational changes which follows  $\text{Ca}^{2+}$  activation (see the figure in the right side) appear realised moving



away from the second domain the C-terminal pair. In the reconstructed protein, the C-terminal pair is rotated around the solvent-exposed peptide loop of  $55^\circ$ : in this condition, the active site becomes available to the substrates.

## References

- Bergamini, C.M. (1988). GTP modulates calcium binding and cation-induced conformational changes in erythrocyte transglutaminase. *FEBS Lett.*, 239, 255-258.
- Bergamini, C.M., Casadio, R., Polverini, E., Matteucci, G., Mariani, P., Spinozzi, F., Carsughi, F. & Fontana, A. (1998). The structural basis for regulation of tissue Transglutaminase by ligand. *European Biochemical Journal*, in print.
- Fesus, L., Davies, P.J.A. & Piacentini, M. (1992). Apoptosis: molecular mechanisms in programmed cell death. *Eur. J. Cell. Biol.*, 56, 170-177
- Greenberg, C.S., Birckbichler, P.J. & Rice, R.H. (1991). Transglutaminases: multifunctional crosslinking enzymes that stabilize tissues. *FASEB J.*, 5, 3071-3077
- Hansen, S. (1990). Calculation of small-angle scattering profiles using Monte Carlo simulation. *J. Appl. Cryst.*, 23, 344-346.

## Time-resolved structural transformations of trehalose polymorphs

Fabiana Sussich<sup>1</sup>, Heinz Amenitsch<sup>2</sup>, Francesco Princivalle<sup>3</sup>, Attilio Cesaro<sup>1</sup>

<sup>1</sup>Dip. Bioch., Biofis. Chim. delle Macromolecole, Università di Trieste, I-34127 Trieste

<sup>2</sup>Institute of Biophysics and X-ray Structure Research, Austrian Academy of Sciences, Steyrerg. 17, A-8010 Graz, Austria

<sup>3</sup>Dep. of Earth Sciences, Università di Trieste, I-34127 Trieste

Trehalose ( $\alpha$ -D-glucopyranosyl-(1 $\rightarrow$ 1)- $\alpha$ -D-glucopyranoside, also called *Mycose*) is a non reducing disaccharide that certain living organisms (plants, seeds, invertebrates) synthesize in significant amounts as a natural protection against water stress. Among the many sugar molecules that have attracted the scientists' and technologists' attention, trehalose seems to be unique in Nature, being involved in the still cryptic process of protecting cellular biomolecules during severe dehydration.<sup>1</sup>

Trehalose can be produced under low humidity conditions and it permits these organism to be dried at high temperatures and confers to plant and animal cells the ability to survive under extreme conditions of dehydration, a process also called "cryptobiosis" or "anhydrobiosis", to underline that the organisms do not freeze-dry but dry at high temperatures.<sup>2</sup>

An enormous interest is put on the possibility of using trehalose or other semi-synthetic sugars, as a means of preserving valuable delicate biologically active proteins or living cells at ambient temperature without the need of lyophilization.<sup>3,4</sup> However, the action mechanism of trehalose is not understood completely.

Trehalose can be found either in its crystalline dihydrate form ( $T_h$ ) or as anhydrous forms,  $T_\beta$  and  $T_\alpha$ . Furthermore a new form has been discovered by Sussich *et al.*,<sup>5</sup> called  $T_\gamma$ . If trehalose is involved in the preservation of organisms under thermal stresses, it seems obvious that a global vision of the structural features and of all the transformations induced by the temperature is needed. Therefore, during heating, time resolved powder diffraction patterns are used to explore the phase transitions occurring in the systems  $T_h$ ,  $T_\alpha$  and  $T_\gamma$ .

At the Austrain SAXS beamline the SAXS/WAXS set-up has been used to record powder diffraction patterns in the angular range between 2.6° and 24.5°. The sample has been placed in a capillary, which was rotated slowly in the thermostat unit. The pattern were recorded with 10 s/frame, and in the temperature range between 30 and up to 250 °C with a heating rate of 20 °C/min, following the scanning parameters of the calorimeter measurements<sup>5</sup>. As an example Fig. 1 shows the diffraction pattern of the new form  $T_\gamma$  heated from 30 to 230 °C.

The solid-solid phase transition at 110 °C between  $T_\gamma$  and  $T_\beta$  is important because it has given a new insight in the interpretation of the corresponding calorimetric measurements.

Several phase transitions have been identified during the heating of the various forms. The results are listed in table 1.

Sample	Phase	Temp. Regime/°C	Phase	Temp. Regime/°C	Phase	Temp. Regime/°C
Crystalline dihydrate $T_h$	$T_h$	30 - 120	$T_\beta$	120 - 240	amorphous	>240
Anhydrous form $T_\alpha$	$T_\alpha$	30 - 100	amorph.	100 - 145	$T_\beta$	> 145
Form $T_\gamma$	$T_h + T_\beta$	30 - 105	$T_\beta$	> 105		

**Table 1** Phase and temperatures regimes of the various forms of trehalose crystalline dihydrate ( $T_h$ ), anhydrous form ( $T_\alpha$ ), and the form  $T_\gamma$ , as measured at the SAXS beamline.

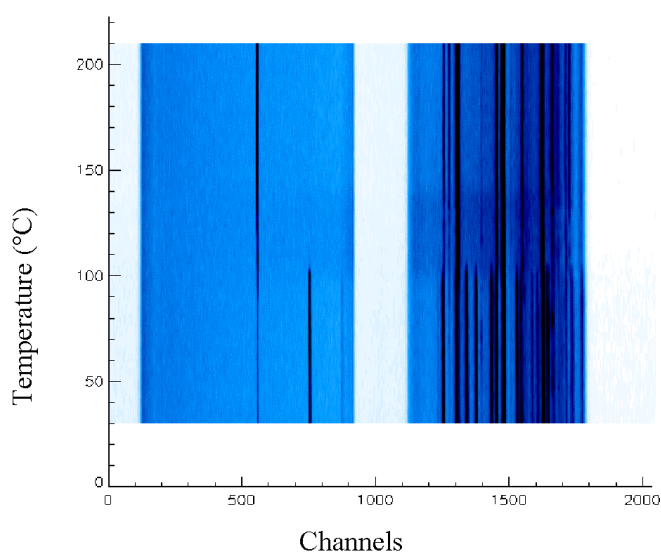


**Fig. 1** Typical diffraction pattern of the form  $T_\gamma$  heated from 30 to 230 °C with a heating rate of 20°/min. Left SAXS range between 2.6 and 10.6°, right WAXS range between 10.2 and 24.5°. The transition from  $T_\gamma$  to  $T_\alpha$  at 110 °C is clearly resolved by this experiment

- Young S. *New Scientist*, **1985**, 10, 40-44.
  - Fox, K.C.; *Science*, **1995**, 267, 1922-1923.
  - Colaco, C.; Kampinga, J.; Roser, B. *Science*, **1995**, 268, 788.
- Crowe, J.H.; Crowe, L.M.; Carpenter, J.F. and Aurell Wistrom, C. *Biochem. J.* **1987**, 242, 1-10.
- Lee, C.W.B.; Waugh, J.S.; Griffin, R.G.; *Biochemistry*, **1986**, 25, 3737-3742.
- Lee, C.W.B.; Das Gupta, S.K.; Mattai, J.; Shipley, G.G.; Abdel-Maged, O.H.; Makriyannis, A.; Griffin, R.G.; *Biochemistry*, **1989**, 28, 5000-5009.
- F. Sussich, R. Urbani, F. Princivalle and A. Cesàro, *J. Am. Chem. Soc.*, **1998**, 120, 7893.

## THE INFLUENCE OF DOMAIN SIZE ON THE STABILITY OF PHOSPHOLIPID MULTILAYERS: A TIME-RESOLVED X-RAY DIFFRACTION STUDY

D. Woo<sup>\*</sup>; S. S. Funari<sup>#</sup>; F. Richter<sup>°</sup>; M. Rappolt<sup>§</sup>; H. Amenitsch<sup>§</sup>; S. Bernstorff<sup>§</sup>; G. Rapp<sup>\*</sup>

<sup>\*</sup>European Molecular Biology Laboratory (EMBL) Outstation Hamburg, Notkestr. 85, D-22603 Hamburg (Germany),

<sup>#</sup>Universitätskrankenhaus Eppendorf c/o EMBL-Outstation Hamburg,

<sup>°</sup>Department of Physics, E22 Biophysics, TU München, D-85748 Garching (Germany),

<sup>§</sup>Sincrotrone Trieste, Basovizza, I-34012 Trieste

Model membranes on solid support are of interest for both scientific and technical reasons. They provide a geometrically well-defined system to study some of the basic properties of amphiphilic molecules, which are the main structural components of biological membranes. Also they are a natural environment for many proteins, thus bearing the potential to design very specific biosensors. In this work we took advantage of the fact that a supported system does not need an aqueous environment. In situ studies of diffusion processes are thus greatly simplified, since the substance to be diffused can be delivered through the gaseous phase. The use of synchrotron radiation from the SAXS beamline at ELETTRA provided the necessary X-ray intensity for time-resolved measurements on thin multilayered films with simultaneous recording of the SAXS- and WAXS-region. Due to the orientation of the samples the WAXS-detector had to be set up at an angle of 90° relative to the SAXS-detector. Ordered multilayers of 1,2-dimyristoyl-*sn*-glycero(3)phosphocholine (DMPC) were mounted in a closed sample holder fit for control of temperature and atmospheric conditions at a relative humidity of 60 %. The glass substrate was bent, allowing for simultaneous detection of multiple reflections<sup>1</sup>. Unlike reported earlier<sup>2</sup>, these samples appeared to be stable even when exposed to an atmosphere of hexane. To further investigate the difference between these and previously used samples, the temperature was slowly altered from 26 °C to 36 °C and back.

At the beginning two peaks (at 4.33 Å and 4.16 Å) in the WAXS-region could clearly be resolved. With the onset of a phase transition at around 33 °C they disappear without reappearing when cooling down again, although the d-spacing of the initial phase is restored (Fig. 1).

After this temperature treatment the sample became sensitive to the exposure to hexane vapour. This behaviour supports the view of enhanced diffusion of hexane into the bilayers along defects, since the initial observation of the WAXS-signal is indicative of a much larger lateral domain size compared to the status after the temperature-cycle.

### References:

- 1) G. Rapp, M. H. J. Koch, U. Höhne, Y. Lvov, and H. Möhwald, *Langmuir* (1995) **11**, 2348
- 2) D. Woo, R. Kläring, and G. Rapp, HASYLAB Annual Report II (1997), 205

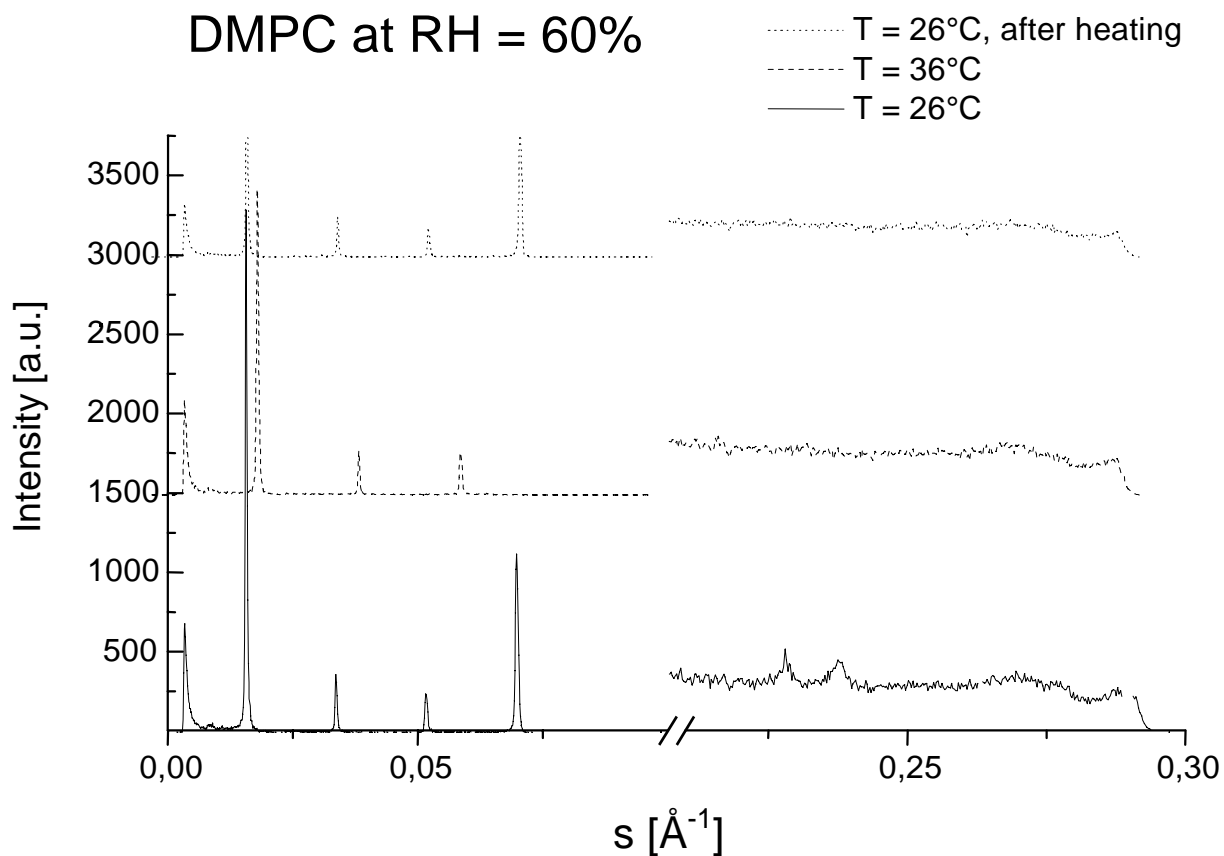


Fig. 1:  
 DMPC at RH = 60% (saturated NaBr-solution inside sample holder) at three different stages:  
 before T-cycle (bottom), d-spacing 54.7 Å;  
 after phase transition (middle), d-spacing 48.6 Å;  
 after cooling back (top), d-spacing 54.4 Å. The small difference of 0.3 Å before and after the  
 T-cycle most likely reflects a small difference in water content, since the sample was initially  
 equilibrated at RH = 75%.  
 The exposure time was 30s for each pattern shown, but the WAXS-reflections are also clearly  
 visible in the scan-data at an exposure time of 5s taken every 30s.

# INVESTIGATION OF MESOPHASE OF CETYLTRIMETHYLAMMONIUM BROMIDE IN H<sub>2</sub>O AND D<sub>2</sub>O BY X-RAY DIFFRACTION

B. Yang and J.W. White

Research School of Chemistry, The Australian National University, 0200  
ACT, Australia

F. Ciuchi and F. Rustichelli

Istituto di Scienze Fisiche, Universita degli studi di Ancona, 60131  
Ancona, Italy

The liquid-crystalline phase behavior of C<sub>16</sub>TAB/H<sub>2</sub>O and C<sub>16</sub>TAB/D<sub>2</sub>O lyotropic systems, in higher concentration of the surfactant 60-90 wt%, are investigated by small angle X-ray diffraction with synchrotron radiation [1-3]. Phase transition temperatures and lattice parameters of hexagonal, 2D monoclinic (deformed hexagonal), cubic and lamella phases were determined between 30 °C and 120 °C. Accordingly, phase diagrams of the systems have been constructed, in which the region of 2D monoclinic are clearly reported. Some interesting isotope effects have been observed by comparing the two systems at same volume fractions of the surfactant.

Replacement of H<sub>2</sub>O with D<sub>2</sub>O in the system, leads to (at about 2 °C) a higher phase transition temperature and larger lattice size of hexagonal phase. However, the mismatch of lattice size between them decreases with increasing concentration of surfactant as well as temperature. Such isotope effects, similar to previous observations in other lyotropic systems, may be related to a stronger hydrogen bond in D<sub>2</sub>O.

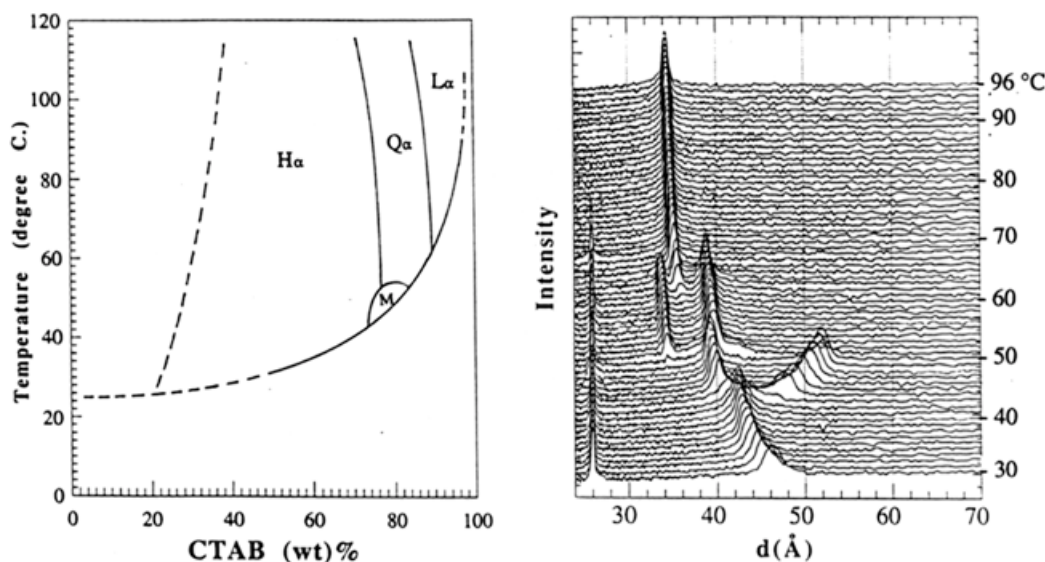


Figure 1. The phase diagram of CTAB/H<sub>2</sub>O system.

Figure 2. The diffraction profiles of the sample which consists of 90% of CTAB and 10% of H<sub>2</sub>O at different temperatures.

## References:

- 1) F. Husson, H. Mustacchi, V. Luzzati (1960) *Acta Cryst* 13, 668.
- 2) V. Luzzati, A. Tardieu, T. Gulik-Krzywicki, E. Rivas, F. Reis-Husson (1968) *Nature* 220, 485.
- 3) X. Auvray, C. Petipas, R. Anthore, I. Rico, A. Lattes (1989) *J Phys Chem* 93, 7458.



## HIGH RESOLUTION SCANNING SAXS/WAXD OF CONNECTIVE TISSUE

I. Zizak<sup>1</sup>, O. Paris<sup>1</sup>, P. Roschger<sup>2</sup>, H. Amenitsch<sup>3</sup>, S. Bernstorff<sup>4</sup>, K. Klaushofer<sup>2</sup>, P. Fratzl<sup>1</sup>

- 1.) Erich Schmit Institut für Materialwissenschaft der ÖAW, Leoben & Institut für Materialphysik der Montanuniversität Leoben
- 2.) Ludwig Boltzmann Institut für Osteologie
- 3.) Institut für Biophysik und Röntgenstrukturforschung der ÖAW
- 4.) Sincrotrone Trieste, ELETTRA

The mechanical properties of connective tissue like bone or cartilage are determined by their structure at different hierarchical levels. At the nanometer scale, bone and mineralised cartilage consist of small mineral particles embedded in an organic matrix (collagen). For bone, these particles are known to be needle- or plate-shaped with an average thickness of about 3 nm and a length of a few hundred nanometers [1]. The size, shape and orientation of these mineral crystals within the collagen matrix can be determined experimentally by the method of Small-Angle X-ray Scattering (SAXS). Moreover, the mineral type and crystallographic orientation of the crystals may be investigated with Wide-Angle X-ray Diffraction (WAXD). The main intention of the present experiment was to study the structural changes of the mineral particles at the interface between bone and mineralised cartilage in human femoral head. It is therefore necessary to scan the interface using a small X-ray beam of only a few micrometer width. Using the scanning equipment described in the previous contribution, information at an atomistic (WAXD) and a nanometer scale (SAXS) can be derived with a spatial resolution of 20  $\mu\text{m}$  and hence, structural changes at the bone-cartilage interface may be detected.

The first step of the experiment consisted in acquiring a radiography of the whole sample by measuring the transmitted intensity with the X-ray sensitive diode (Fig. 1b). This radiography provides an exact mapping of the mineral density-distribution in the sample which can be compared with e.g. light micrographs (Fig. 1a) or scanning electron micrographs. In the second step, the SAXS-signal was recorded with the 2D-detector along lines normal to the bone-cartilage interface. Finally, WAXD patterns were taken (at the same positions) with the 2D-detector. The 2D-patterns were evaluated with methods described elsewhere [2] and the results (shown in Fig. 1c-e for one of the linear scans) can be summarised as follows:

1. In bone, the orientation of the mineral crystals follows exactly the direction of the trabeculae (Fig. 1c)
2. The mineral crystals are thicker in cartilage than in bone (Fig 1e).
3. The size and/or shape distribution of the mineral particles (as measured by the  $\eta$ -parameter [2]) in cartilage differs from that in bone (Fig 1d).
4. The orientation of the mineral particles changes at the bone-cartilage interface (Fig 1c). The degree of alignment of mineral crystals in bone is larger than in cartilage (Fig 1c).
5. The crystallographic orientation (measured using WAXD) correlates strongly with the orientation of the particles, the type of the mineral is however the same in both tissues.

These interesting results are a first step towards a more detailed understanding of the complex processes leading to the biochemically optimized structure of bone.

### References

- [1] P. Fratzl et al. *J. Bone Miner. Res.* **7** (1992) 329-334.
- [2] P. Fratzl, S. Schreiber, K. Klaushofer, *Connective Tissue Research* **34** (1996) p247.

The project is supported by the "Fonds zur Förderung der wissenschaftlichen Forschung" FWF (project P11762-PHY)

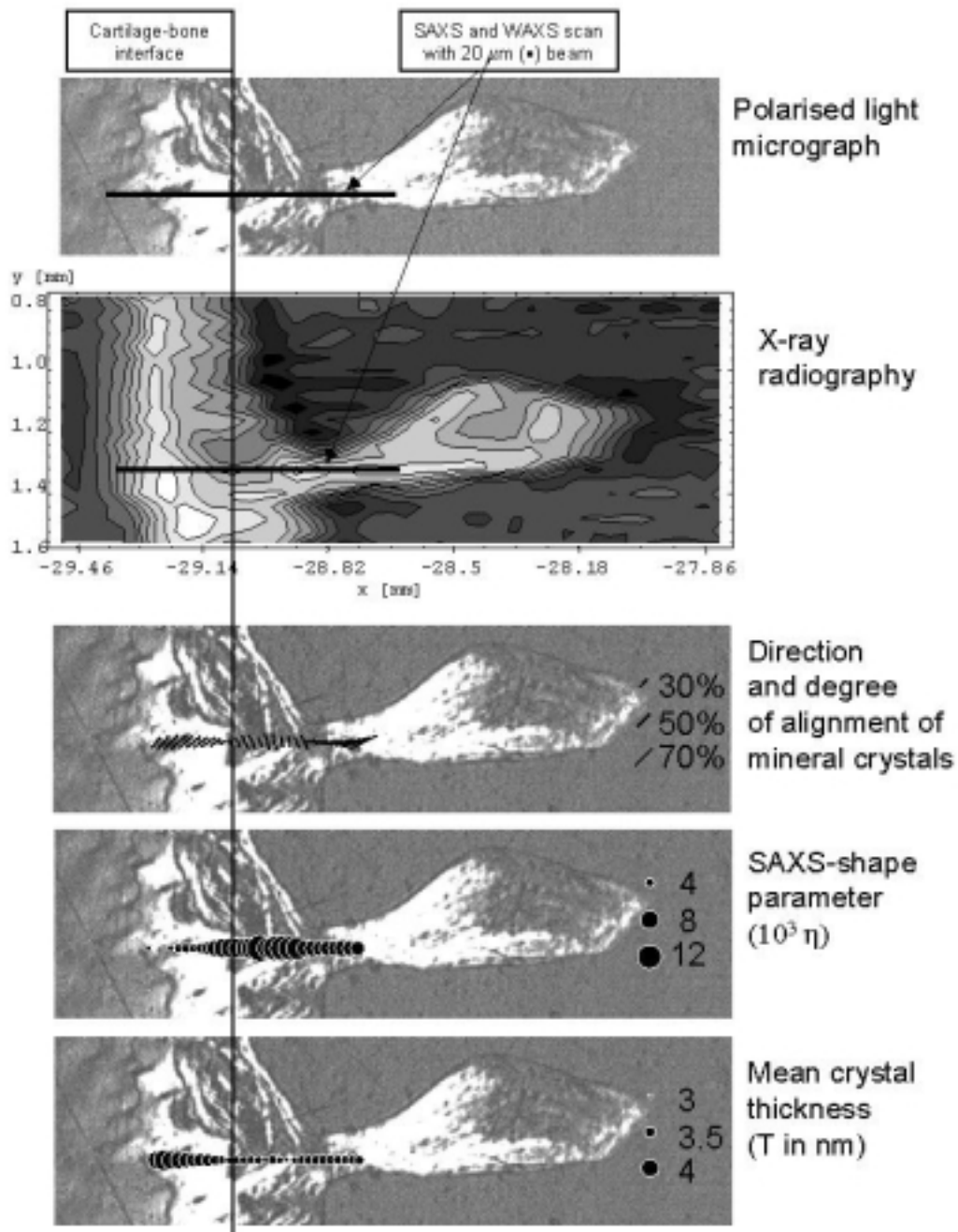


Fig. 1: Comparison of different parameters derived from a scanning-SAXS measurement. Fig. 1b shows the x-ray radiography as compared to a polarised light micrograph (1a). One-dimensional SAXS and WAXD scans were performed along the horizontal line across the cartilage (left) and bone (right) interface. Fig. 1c shows the average direction of the mineral crystals (direction of the lines and the degree of the alignment (length of the lines)). The shape parameter  $\eta$  and the mean crystal thickness  $T$  are visualised in 1d and 1e.

## IN SITU MEASUREMENTS OF VISCO-ELASTIC PROCESSES IN COLLAGEN

I. Zizak, O. Paris, B. Grabner, P. Fratzl

Erich Schmid Institut für Materialwissenschaft der Österreichischen Akademie der Wissenschaften , und  
Institut für Metallphysik der Montanuniversität Leoben  
Jahnstraße 12, A-8700 Leoben, Austria

S. Bernstorff

Sincrotrone Trieste, Area Science Park, I-34012 Trieste, Italy

H. Amenitsch

Institute of Biophysics and X-Ray Structure Research, Austrian Academy of Sciences, Steyrerg. 17, A-8010  
Graz, Austria.

Collagen type I is among the most important stress carrying structures in mammals. The outstanding mechanical properties of collagen, in particular the specific shape of the stress-strain curve, are still not understood in full detail. Recent dynamic synchrotron x-ray scattering studies have shown that in the linear region of the stress-strain curve the macroscopic strain is considerably larger than the strain within the collagen fibrils [1,2]. In this region, stretching of the collagen triple helices as well as a side by side gliding of neighbouring molecules or fibrils are possible mechanisms determining the mechanical properties of the tissue. While the first contribution should be purely elastic due to the strong binding forces within the molecules, the second one could include plastic or visco-elastic contributions due to the binding of the molecules through cross-links or the weaker binding of the fibrils. Visco-elastic contributions are expected to show a strain rate dependence (i.e. dependence on stretching velocity) of the d-spacing change in the intermolecular scattering, that is, the 67 nm period of collagen. Moreover, the elongation of the molecules for a given strain-rate can be determined by measuring the 0.28 nm molecular reflection from the collagen triple helix (intra-molecular scattering).

The aim of the present experiment was to clarify the role of visco-elastic processes at the different hierarchical levels by measuring the microscopic strains as a function of the macroscopic strain and strain rate in rat tail tendon. The investigations were performed with a specially constructed device for in situ synchrotron x-ray scattering experiments under mechanical tension [3]. The strain rate was varied by almost two orders of magnitude by changing the stretching-velocity of the tendon. For each strain rate the whole macroscopic stress-strain curve was measured dynamically together with the scattering patterns at small (intermolecular scattering) and large angles (intra-molecular scattering). The detailed data evaluation is not yet completed, but first results show already interesting features:

For every macroscopic strain  $\delta$  within the linear part of the stress-strain curve, the microscopic strain  $\epsilon$  within the collagen fibrils (change in the 67 nm period) was determined from the scattering data. In this region, the relation between  $\epsilon$  and  $\delta$  was found linear for all strain rates (see also [1]). Fig.1 shows the ratio  $d\epsilon/d\delta$  (the slope of the  $\epsilon$ - $\delta$  curve) versus the macroscopic strain rate. There is a rather large scatter in the data but a clear trend is visible. For fast stretching velocities, the macroscopic strain is not much larger than the strain within the collagen fibrils. For very slow strain-rates, however, only about 10-20% of the macroscopic strain can be attributed to a stretching of the fibrils, indicating a viscous side by side gliding of the fibrils. Not all measured data are included in this plot yet, but we are confident that this experiment is the key for a more detailed understanding of the visco-elastic processes in collagen.

By measuring the change in the 0.28 nm helix reflection and in the 67nm reflection, the intramolecular versus intermolecular strain contributions can be separated, allowing to study the influence of cross-linking between the molecules. Here, the data evaluation is still under

progress, and no definitive statement can be made at present. Surprisingly the trends indicate a much stronger helix contribution to the strain within the fibrils than it was expected.

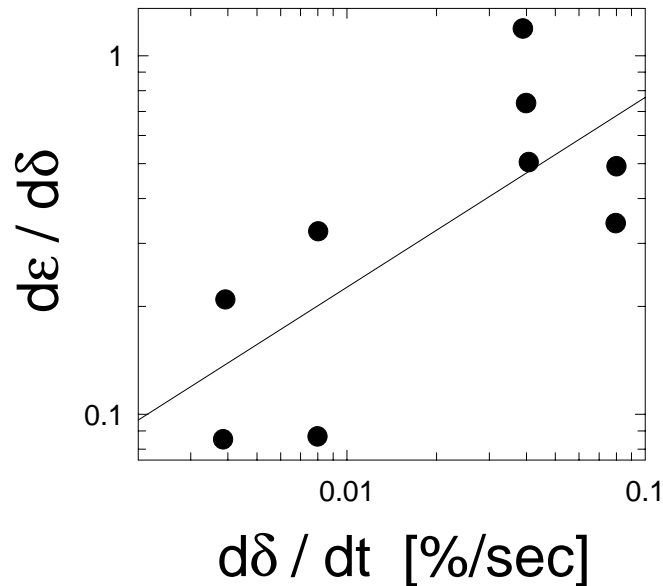


Fig. 1: Change of the microscopic strain  $\varepsilon$  ( $\varepsilon = (d-d_0)/d_0$  with  $d_0 = d$ -spacing of the unstretched tendon,  $d = d$ -spacing of the stretched tendon of the 67 nm meridional reflection of collagen) and the change of the macroscopic strain  $\delta$  ( $\delta = D-D_0/D_0$ ,  $D_0 =$  length of the unstretched tendon,  $D =$  length of the stretched tendon) versus the macroscopic strain rate.

## References

- [1] P. Fratzl, K. Misof, I. Zizak, G. Rapp, H. Amenitsch and S. Bernstorff, *J. Struct. Biol.* **122** (1997) 119-122.
- [2] P.Fratzl, K.Misof, I.Zizak, G.Rapp, H.Amenitsch, S.Bernstorff, *ELLETRA News and ELETTRA Highlights*, (July 1998)  
(hyperlink: [http://www.elettra.trieste.it/Documents/News/Newsletter/Volume\\_025/#4](http://www.elettra.trieste.it/Documents/News/Newsletter/Volume_025/#4) )
- [3] K. Misof, G. Rapp, P. Fratzl, *Biophys. J.* **72** (1996) 1367-1381.

The work was supported by the "Fonds zur Förderung der wissenschaftlichen Forschung" FWF (project P11762-PHY)

# 3. Physics

# GRAZING INCIDENCE SMALL ANGLE X-RAY SCATTERING STUDY OF IRRADIATION INDUCED DEFECTS IN MONOCRYSTALLINE SILICON

P. Dubcek<sup>1,2</sup>, B. Pivac<sup>2</sup>, S. Bernstorff<sup>1</sup>, H. Amenitsch<sup>3</sup>, R.Tonini,<sup>4</sup> F. Corni<sup>4</sup> and G. Ottaviani<sup>4</sup>

<sup>1</sup>Sincrotrone Trieste, SS 14 km 163,5, 34012 Basovizza (TS), Italy

<sup>2</sup>Ruder Boskovic Institute, Bijenicka 54, 10000 Zagreb, Croatia

<sup>3</sup>Institute for Biophysics and X-ray Structure Research, Austrian Academy of Sciences, Steyrerg. 17, 8010 Graz, Austria

<sup>4</sup>University of Modena, Physics Department, Via Campi 213a, 41100 Modena, Italy

Structural defects in monocrystalline silicon samples, irradiated with a dose of  $2E16$  He ions per square centimetre at 77K and annealed at temperatures in 100 - 800 °C temperature range, were investigated using small angle X-ray scattering. Because the induced defects were expected to be present in a thin layer close to surface, grazing angle incidence was chosen due to its surface sensitivity.

The aim of the experiment was to determine the conditions for bubbles formation within the solid film, which can have great importance either for fundamental<sup>1</sup> or for applied research<sup>2</sup>.

Apart from the scattering intensity shape typical for this surface roughness,<sup>3</sup> all the samples showed wave-like scattering intensity, as a result of interference of the scattering from highly correlated upper and lower film surface (see fig 1.).

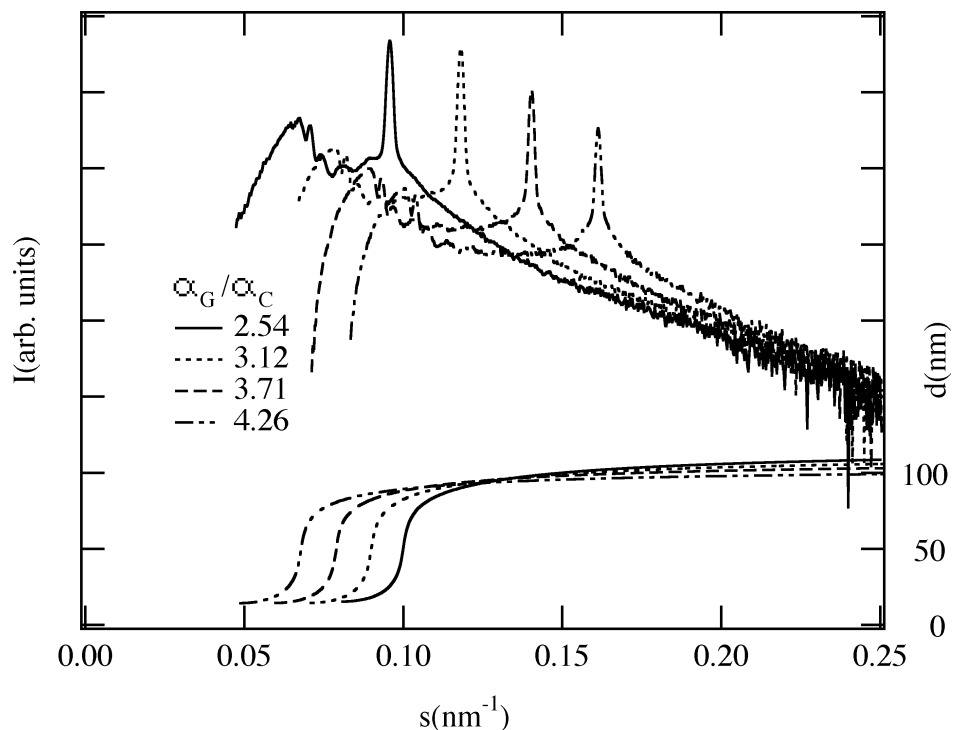


Fig.1. SAXS intensities and calculated penetration depths for silicon vs. scattered angle for four different grazing angles ( $\alpha_C$ ) for as implanted sample

Additionally, by measuring the position of the Yoneda peak<sup>4</sup>, critical angle variation with the annealing temperature was determined. Apart from the step-down from nonimplanted to implanted sample, the critical angle is slowly decreasing with the annealing temperature increasing up to 600°C, when it starts to rise again. This results from redistribution of defects, and is indicating bubbles formation onset. Some of the induced defects are lost due to the diffusion towards the surface. This increases surface roughness, and causes the sample density to rise slowly and is detected as lowering of intensity of the reflected primary beam and the change of the shape of reflection. It is believed that the bubbles start to form at 600°C, and this is the temperature at which film thickness and the change in critical angle reverse their dependence on temperature of annealing.

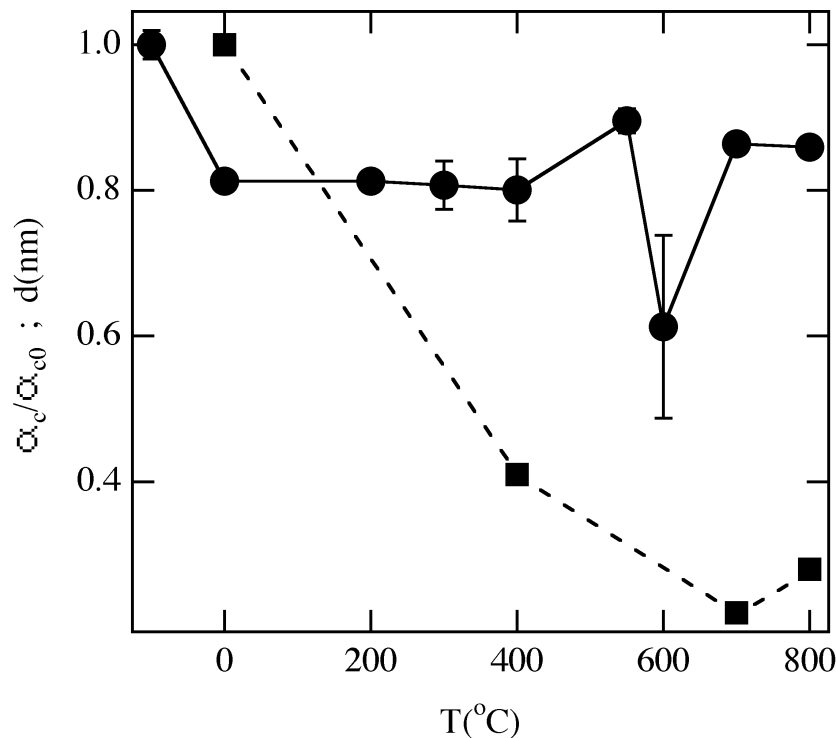


Fig.2. Relative critical angle (circles) and film thickness (squares) vs. annealing temperature.

Due to the variation of the surface quality with the annealing temperature, and the short time available, not all the above mentioned parameters are measured precisely enough for the complete temperature range. Therefore, further investigation is necessary to confirm the bubbles formation.

1. D.J. Eaglesham, A.E. White, L.C. Feldman, N. Moriya, and D.C. Jacobson, Phys. Rev. Lett. **70**, 1643 (1993).
2. V. Raineri and S.U. Campisano, Appl. Phys. Lett. **66**, 3654 (1995)
3. S. K. Sinha, E. B. Sirota and S. Garoff, Phys. Rev. B **38**, 2297 (1988)
4. Y. Yoneda, Phys. Rev. **131**, 2010 (1963)

## SMALL-ANGLE X-RAY SYNCHROTRON STUDY OF PHTHALOCYANINE CONTAINING LANGMUIR-BLODGETT SUPERLATTICES

V. Erokhin<sup>1</sup>, S. Carrara<sup>2</sup>, S. Paddeu<sup>1</sup>, C. Paternolli<sup>2</sup>, S. Bernstorff<sup>3</sup>, P. Dubcek<sup>3</sup>, L. Valkova<sup>4</sup>, and C. Nicolini<sup>2</sup>

1.) Fondazione El.B.A., Corso Europa 30, Genova 16132, Italy

2.) Institute of Biophysics, University of Genova, Corso Europa 30, Genova 16132, Italy

3.) SAXS beamline, Elettra Synchrotron, Trieste, Italy

4.) Ivanovo State University, Ivanovo, Russia

Phthalocyanines are considered as perspective materials for the molecular electronics. It was shown the possibility to construct electro/optic devices and gas sensors based on these molecules. Langmuir-Blodgett (LB) technique is suitable for the formation of thin films of Phthalocyanines. The technique is also considered as one of the most perspective for realization of molecular architecture structures. X-ray patterns of LB films of Phthalocyanines are not very informative. Usually, it is impossible to register more than one Bragg reflection. However, it is possible to improve strongly the ordering of the film by realization of superlattices, where phthalocyanine layers are alternated with fatty acid layers. This work presents preliminary results of the study of such superlattices by small-angle X-ray scattering. Different superlattices containing Phthalocyanines and cadmium arachidate were deposited by Langmuir-Blodgett technique. Structure was studied on SAXS station of Elettra. X-ray pattern of superlattice containing 40 repetitions of one monolayer of cadmium arachidate and one monolayer of phthalocyanine is presented in Fig. 1.

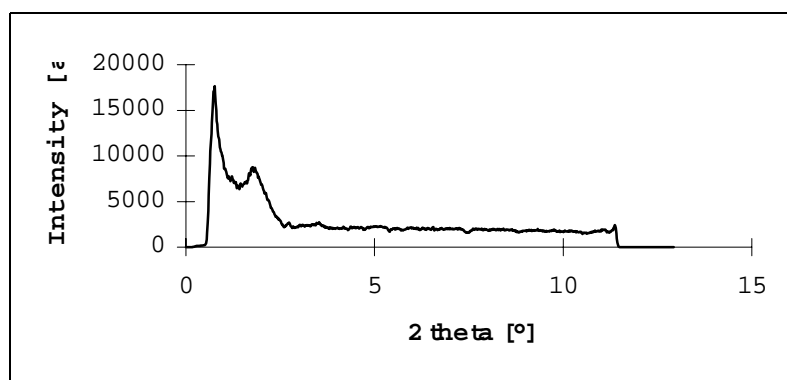


Fig. 1. X-ray pattern of LB superlattice containing 40 periods of (1 monolayer of cadmium arachidate+1 monolayer of phthalocyanine).

The pattern contains 2 reflections corresponding to the spacing of 5.06 nm. The thickness of the cadmium arachidate monolayer is about 2.7 nm, therefore, the thickness of the phthalocyanine monolayer is about 2.3 nm. X-ray pattern of 60 periods of (4 monolayers of cadmium arachidate + 2 monolayers of phthalocyanine) is presented in Fig. 2.



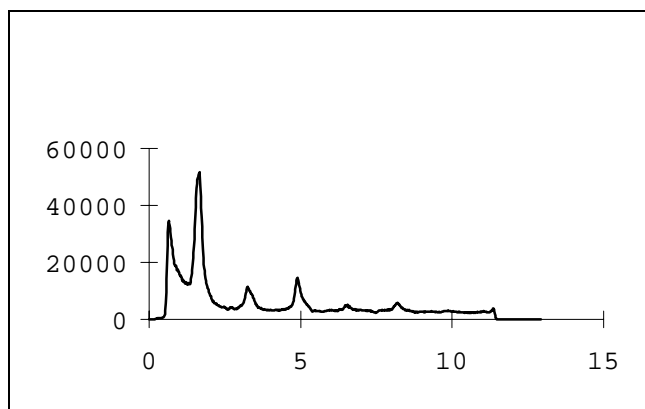


Fig. 2. X-ray pattern of 60 periods of (4 monolayers of cadmium arachidate + 2 monolayers of phthalocyanine).

The pattern contains the system of reflections, corresponding to the spacing of 5.39 nm. This spacing corresponds to the bilayer of cadmium arachidate. This result allows to suggest that phthalocyanine in the film is distributed in rather amorphous way and all the structure is determined by the cadmium arachidate layer packing. X-ray pattern of the same sample after heating it to 80°C is shown in Fig. 3.

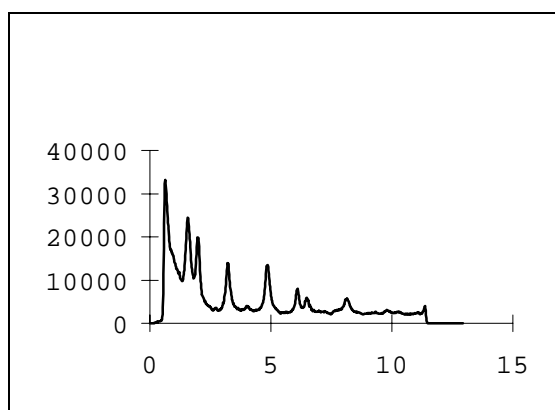


Fig. 3. X-ray pattern of 60 periods of (4 monolayer of cadmium arachidate + 2 monolayers of phthalocyanine) after heating to 80°C.

Heating temperature was intermediate between melting points of cadmium arachidate and phthalocyanine. The pattern contains two systems of reflections, one of which gives the spacing of 5.43 nm, what can be attributed to the cadmium arachidate packing, and the other of 4.32 nm. Such result allows to suggest, that after the melting of cadmium arachidate sublayers, the system was splitted into two phases, corresponding to the zones of cadmium arachidate and that of Phthalocyanines. Phthalocyanine rings are oriented perpendicular to the substrate plate and their bilayer is repeating unit.

When the sample was heated to the temperature more than melting point of phthalocyanine (120°C) the X-ray pattern was once more changed (Fig. 4).

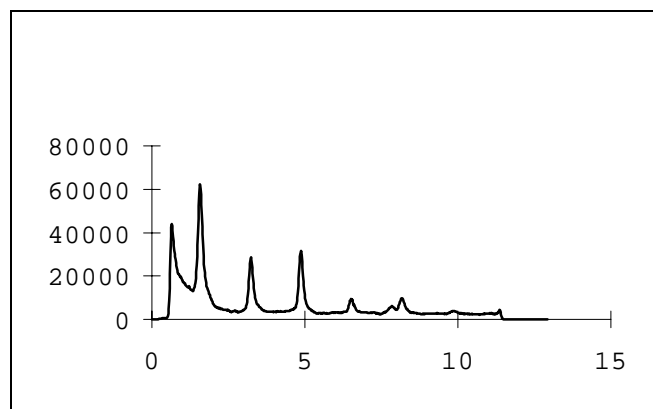


Fig. 4. X-ray pattern of 60 periods of (4 monolayers of cadmium arachidate + 2 monolayers of phthalocyanine) after heating to 120°C.

The pattern contains again the system of reflections corresponding to cadmium arachidate packing (spacing is 5.39 nm). However, the pattern contains also a small peak at 7.835°, corresponding to the 1.13 nm spacing. This peak can be attributed to the packing of phthalocyanine molecules with rings oriented parallel to the support plane.

These preliminary results allowed to determine the orientation of phthalocyanine molecules in LB superlattices. Interesting structural reorganisation of the film were observed after the sample heating when one or both components were melt.

## X-RAY DIFFRACTRION STUDY OF THE STRUCTURE OF DNA-LIPOSOME-METAL COMPLEXES

O. Francescangeli\*, P. Bruni^, R. Caciuffo\*, M. Iacussi^, E. Maurelli^

\* Dipartimento di Scienze dei Materiali e della Terra e Istituto Nazionale per la Fisica della Materia, Università di Ancona, Via Breccie Bianche I-60131, Ancona, Italy

^ Dipartimento di Scienze dei Materiali e della Terra, Sezione Chimica, Università di Ancona, Via Breccie Bianche I-60131, Ancona, Italy

Extremely rapid developments in molecular biology are making gene therapy a promising new therapeutical modality. Somatic gene therapy depends on the successful transfer and expression of extracellular DNA to the nucleus, with the aim of replacing a defective or adding a missing gene. While appropriate plasmids (genes) can be prepared in large quantities, their efficient and safe delivery into appropriate cells *in vivo* seems to be the main obstacle in successful medical applications. Cationic liposomes (CL) were shown to be a promising gene delivery system. Despite numerous studies and commercially available liposomes kits, however, the structure of DNA-cationic liposomes complexes is still not well understood, and only few papers have been published in this subject up to now [1,2]. The solution structure of CL-DNA complexes was probed on length scale from subnanometer to micrometer by synchrotron x-ray diffraction which revealed a novel multilamellar structure with alternating lipid bilayers and DNA monolayers [2].

Within the general scope of providing new biological materials for gene delivery systems we have undertaken a study of the interactions among DNA, liposomes (L) and bivalent metal cations (M) in triple DNA-L-M complexes. The introduction of a metal cation leads to the formation of complexes that, in principle, are more stable and less toxic as compared with those with CL. The formation of the triple complex has been proved by different techniques [3] such as turbidimetry and FT-IR. The stoichiometry and the stability constants have been determined by elemental analysis and ESR, respectively. The structural characterization of these complexes is an essential feature to be investigated in order to understand the role played by the metal cations in stabilizing the DNA-liposome interactions and then in the formation of supramolecular aggregates. We have performed X-ray diffraction (XRD) studies on complexes of DNA, DOPC (dioleilphosphatidilcholine) and  $Mn^{++}$ , at different concentrations of the metal and at different dilution of the complex. The results show the presence of two sharp diffraction peaks of very low intensity in the small (scattering) angle region of the spectrum, corresponding to spacings 61.0 Å and 72.7 Å, respectively (Fig. 1). The former periodicity, which is also present in the XRD spectrum of the DOPC solutions in buffer (HEPES) at pH=7.2, should correspond to the 1D periodic lamellar structure of the liposomes, whereas the latter one indicates the presence of a 1D periodic superstructure where the DNA and/or the metal cations are intercalated between the liposome layers. However, the periodicity of 61 Å is much larger than the values of 40 Å reported in the literature for the same liposomes in water solution but without buffer

[1,2]. This higher value seems to indicate the occurrence of a somewhat different arrangement of the liposomes in our samples, which has never been observed up to now. On the other hand, the periodicity measured at 72.7 Å is in agreement with a high ordered multilamellar structure where both DNA and metal cations are “sandwiched” between liposome layers (similar to the model proposed in refs [1,2] for DNA-CL complexes), in case the periodicity associated to the liposome layered structure is actually 40 Å as reported in the literature. If this were not the case, one should imagine different structural arrangement and/or conformations of the molecular components in order to explain the experimental data. In addition, the preliminary XRD experiments indicate that: (i) the peak at 72.7 Å is completely absent when the molar ratio of the three components DNA-L-M is 2-3-1; (ii) on increasing the concentration of  $Mn^{++}$ , it becomes apparent and its intensity increases consequently. These experimental evidences, in connection also with EPR measurements performed by the authors, seem to suggest that the ordered superstructure is present only at high  $Mn^{++}$  molar ratios. Finally, an interesting kinetic effect has been evidenced in the performed experiments, consisting in a different time-evolution of the integrated intensities  $I_1$ ,  $I_2$  of the two diffraction peaks. In particular a continuous reduction of the intensity of the peak at 72.7 Å is observed with increasing the measuring time, thus suggesting the possibility that the ordered superstructure is kinetically favored even if thermodynamically unstable. This interpretation is in agreement with the experimental data taken at higher temperatures (up to 45 °C) which show a continuous increase of the intensity of the peak at 72.7 Å, thus indicating the existence of an endothermic equilibrium. This point deserves further experimental investigation.

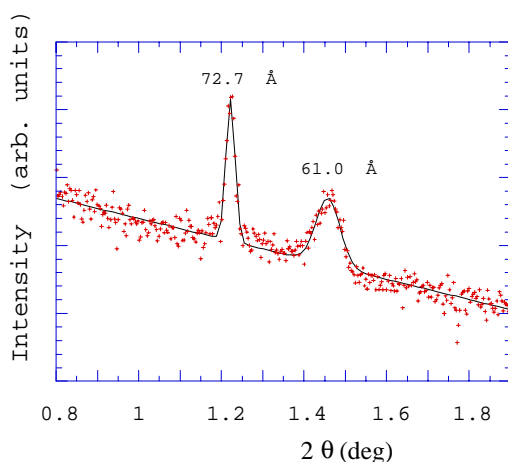


Figure 1

## References

- [1] D. Lasic et al., *J. Am. Chem. Soc.*, **119**, 832 (1997).
- [2] O. Joachim et al., *Science*, **275**, 810 (1997).
- [3] P. Bruni et al., *Gazzetta Chimica Italiana*, **127**, 513 (1997).

## KINETICS OF STRUCTURAL CHANGES IN POLYMER MEMBRANES

H. Grigoriew<sup>1</sup>, A. G. Chmielewski<sup>1</sup>, H. Amenitsch<sup>2</sup>, S. Bernstorff<sup>3</sup>, J. Domagała<sup>4</sup>

<sup>1</sup> *Institute of Nuclear Chemistry and Technology, Warsaw, Poland*

<sup>2</sup> *Institute of Biophysics and X-Ray Structure Research AAS, Graz, Austria*

<sup>3</sup> *Sincrotrone Trieste, Basovizza, Italy,* <sup>4</sup> *Institute of Physics PAS, Warsaw, Poland*

As it was found in our lab, in the process of water sorption by cellulose membrane, the volume of absorbed water becomes equal to 1.5 volume of cellulose. It is kind of sol-gel transition. Also previous SAXS experiment showed creation of heterogeneity after soaking cellulose with water [1,2].

At ELETTRA SAXS beamline, the structure of the system cellulose-water has been studied in kinetic and thermal way. SAXS and WAX measurements were performed simultaneously, in time-resolved mode using linear detectors. The samples were placed in a chamber built in INCT. The chamber makes possible continuous supply of wet saturated penetrant vapor to the sample, as well as rising its temperature, during synchrotron experiment.

The samples were made by regenerated cellulose Tomophan I and light or heavy water, because a difference in permeation rate for each kind of water exists.

First, the time interval of the sol-gel type structural transition was estimated. After starting measurements with dry cellulose the wet vapor was supplied to the sample. We found that the all structural change takes place in very short time about 1 sec, for both kinds of water. As it was found earlier, gyration radius of particles generated during the change is about 7nm, and there is simultaneous decrease of chains order in WAX [1,2].

Next, time-resolved measurements made during increasing temperature of the system cellulose-water from room to 85°C showed emerging peak with broad shoulder on the side of greater angles in SAXS, and simultaneously a slight increase of chains order in WAX is observed, greater for D<sub>2</sub>O (Fig. 1) [3].

The peak emergence in SAXS suggests that particles formed in the first structural change (sol-gel) are gradually ordered during increase of temperature and they are probably micelles. Only slight increase in chains ordering observed in WAX suggests that the micelle structure remains almost unchanged during heating. The difference between H<sub>2</sub>O and D<sub>2</sub>O action in WAX is probably caused by weaker influence of heavy water on cellulose structure. This kind of water also permeates through cellulose with smaller rate.

For better display of the temperature depending changes in structure we subtracted the SAXS curve for room temperature from the curves for higher temperatures. On Fig. 2 (for cellulose-heavy water) two of subtracted curves are fitted by Gauss functions. We needed at least 3 Gauss functions to fit the experimental one, because of great shoulder on the side of larger angles. We found that the position of the first Gauss function is about 30nm. This can be treated as a creation of crystal-type short range order of micelles, but a shape of the shoulder not makes possible to do an univocal fitting.

On the other hand, the generated peak became gradually that of typical butterfly shape which was predicted by the PR (Panyukow-Rabin) theory of gels structure. According to the theory the structure factor consists of a contribution from static density inhomogeneities and from time-dependent fluctuations of density.

H. Grigoriew, A. G. Chmielewski, *J. Mat. Sci. Lett.* 16 (1997) 1945

H.Grigoriew, A.G.Chmielewski, J.Membr.Sci. 142 (1998) 87  
H.Grigoriew, A.G.Chmielewski,H.Amenitsch,S.Bernstorff, J.Domagała, EPDIC-6 Abstracts Book, Budapest, 1998, P09-18.  
S.Panyukow,V.Rabin,Phys.Rep. 269 (1996) 1.

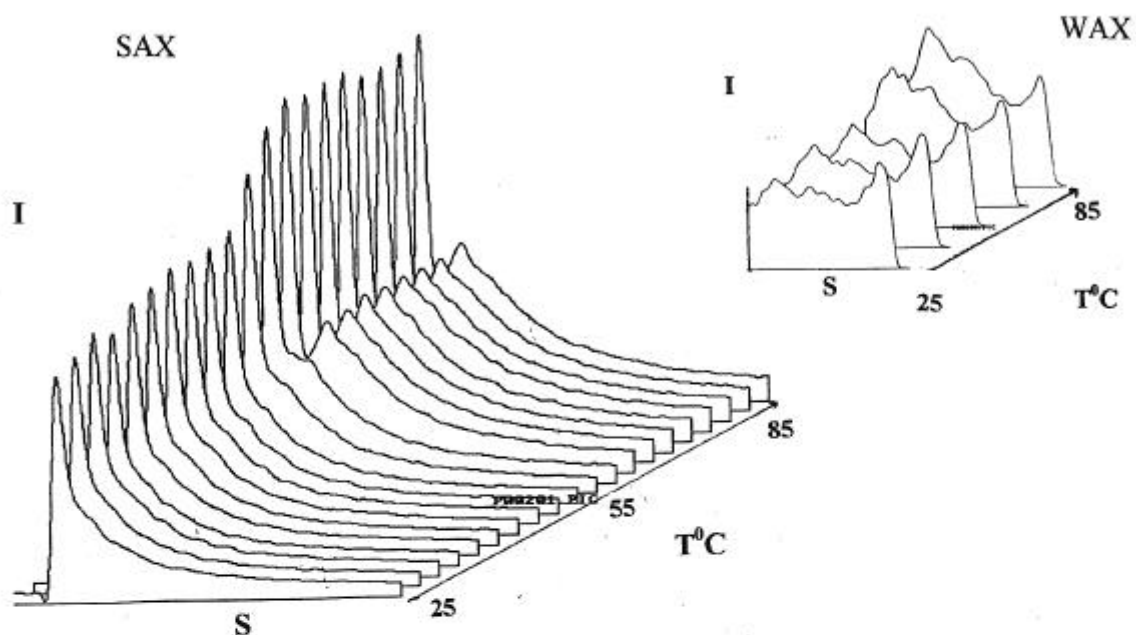


Fig.1 Temperature changes of SAX and WAX for cellulose - D<sub>2</sub>O.

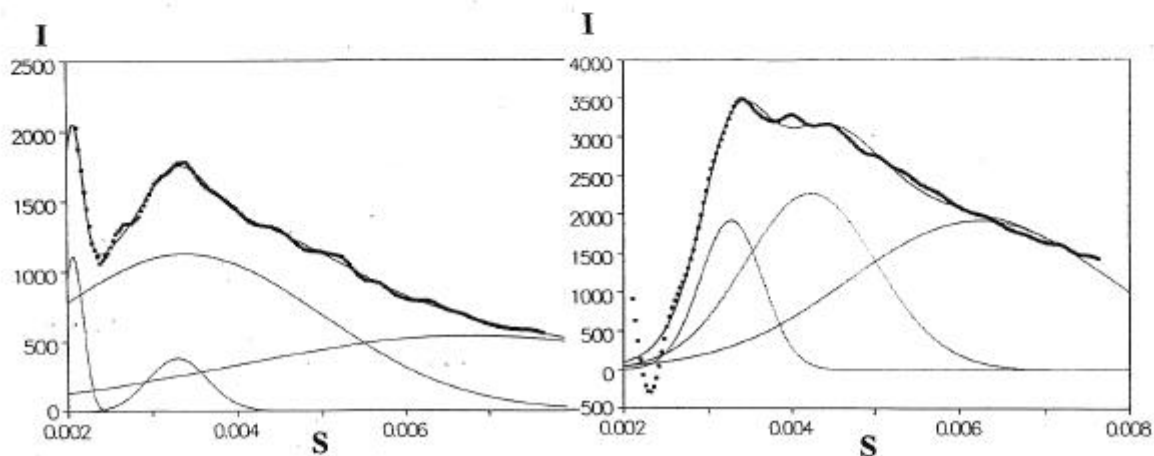


Fig.2 Fitting of subtracted curves cellulose - D<sub>2</sub>O, for 65<sup>0</sup> C (left) and 85<sup>0</sup> C (right) .

## STUDY OF AMORPHOUS TO NANOCRYSTALLINE TRANSFORMATION IN Fe-Cu-Nb-Si-B ALLOYS INDUCED BY FURNACE OR CURRENT ANNEALING

A. Gupta<sup>1</sup>, N. Bhagat<sup>1</sup>, G. Principi<sup>2</sup>, A. Maddalena<sup>2</sup>, N. Malhotra<sup>1</sup>, B.A. Dasannacharya<sup>1</sup>, P.S. Goel<sup>3</sup>, H. Amenitsch<sup>4</sup> and S. Bernstorff<sup>5</sup>

<sup>1</sup>Inter-University Consortium for DAEF, Khandwa Road, Indore – 452 017, India

<sup>2</sup>INFM (Unit<sup>^</sup> di Trento), and Universit<sup>^</sup> di Padova, DIM, Settore Materiali, via Marzolo 9, I-35131 Padova, Italy

<sup>3</sup>Inter-University Consortium for DAEF, R-5 Shed, BARC, Mumbai, India

<sup>4</sup>Institute for Biophysics and X-ray Structure Research, Austrian Academy of Sciences, Steyrergasse 17, A-8010 Graz, Austria

<sup>5</sup>Sincrotrone Trieste, SS 14, Km 163.5, I-34012 Basovizza (Trieste), Italy

Nanocrystalline alloys produced by controlled partial crystallisation of transition metal-metalloid metallic glasses containing small amounts of Cu and Nb are excellent soft magnetic materials, possessing high permeability and saturation magnetisation [1,2]. Partial crystallisation is generally accomplished, starting from the amorphous Fe-metalloid alloy, by annealing at a temperature of 500/600 °C, which results in formation of nanocrystals of a fcc Fe-Si phase dispersed in an amorphous matrix. The nanocrystalline phase formation is related to the presence in the alloy of small amounts of niobium and copper: copper, being virtually immiscible in iron, forms local atomic clusters that enhance the nucleation of nanocrystalline structures; the addition of niobium stabilises the residual amorphous phase and hinders the grain growth. Extreme brittleness of furnace-annealed alloys limits their practical applications in transformer cores etc. However, nanocrystallisation achieved through current annealing of amorphous alloys results in improved ductility of these systems. Small angle x-ray scattering and Mössbauer spectroscopy have been used to elucidate the mechanism of nanocrystallisation and the possible cause of improved ductility through current annealing process.

Ribbons of Fe-Si-B-Cu-Nb amorphous alloy, obtained from Vacuum-Schmelze GmbH, Hanau, were nanocrystallised by *i*) annealing in furnace under protective atmosphere at 590 °C for 20 or 87 min (FA samples) and *ii*) annealing by passing a current of 7.8 A through the samples for periods of 12 or 90 s (CA samples). X-ray scattering measurements were done using the beamline 5.2L at Elettra Synchrotron Source, Trieste. Two one-dimensional detectors were used in order to cover the small-angle (SAXS) as well as the wide-angle (WAXS) regions simultaneously. Static measurements have been done on both FA and CA treated samples and, in order to obtain information on the early stages of nano-crystallisation, also on previously untreated samples heated in situ by passing for a time of 500 s a current of 7.8 A and recording a diffraction pattern every second.

We found that current annealing (CA) of Fe-Si-B-Cu-Nb alloys is as effective as furnace annealing (FA) in producing nanocrystals dispersed in an amorphous matrix. However, for the same amount of nanocrystalline phase, the crystallite size in CA samples is smaller than that in the case of FA samples. The analysis of Mössbauer spectra (taken at room temperature using a <sup>57</sup>Co:Rh source in transmission geometry) shows that in the case of FA and CA samples the nanocrystalline grains consist of non-stoichiometric ordered Fe<sub>3</sub>Si phase, and that there is an indication of the presence of boron atoms in the nanocrystals of CA samples. This

implies a lower segregation of boron atoms or of borides at the boundaries of nanocrystallites of CA samples and can be connected to their lower brittleness.

The small angle scattering from the CA samples is significantly lower as compared to that in the FA samples in the  $q$  range  $0.2$  to  $0.7 \text{ nm}^{-1}$ , suggesting that the contrast between crystallites and the amorphous medium in CA samples is lower than that in the FA samples, in agreement with the Mössbauer data. In particular, CA samples display a lower grain size and retention of boron atoms, which can be related to a lower brittleness.

We found further that appreciable differences occurred in the SAXS and WAXS data of the four amorphous specimens having different Nb and Si concentrations suggesting that the short range order in the amorphous phase itself is effected by the presence of Nb in the system. In the samples furnace annealed for a time period which is just short of inducing nanocrystallisation in the sample as seen by WAXS, significant modifications in the small angle scattering regime have been observed which correspond to particles of size  $\sim 1\text{nm}$ . Mössbauer spectra of this specimen also gives some indication of the beginning of crystallisation. Time resolved WAXS measurements show that the position of the crystalline peak is systematic shifted as a function of time. This shift is being interpreted in terms of i) stress on the nanocrystals due to difference in the mass density of the amorphous and the nano-crystalline phase, ii) composition variation of the nano-crystalline phase due to out diffusion of Nb and B.

#### References

1. Y. Yoshizawa, S. Oguma, K. Yamauchi, J. Appl. Phys. 64(1988) 6044.
2. G. Herzer, IEEE Trans. Magn. 25 (1989) 3327.
3. P. Allia, M. Barico, M. Knoble, P. Tiberto, F. Vinai, J. Magn. Magn. Mater. 133 (1994) 243.

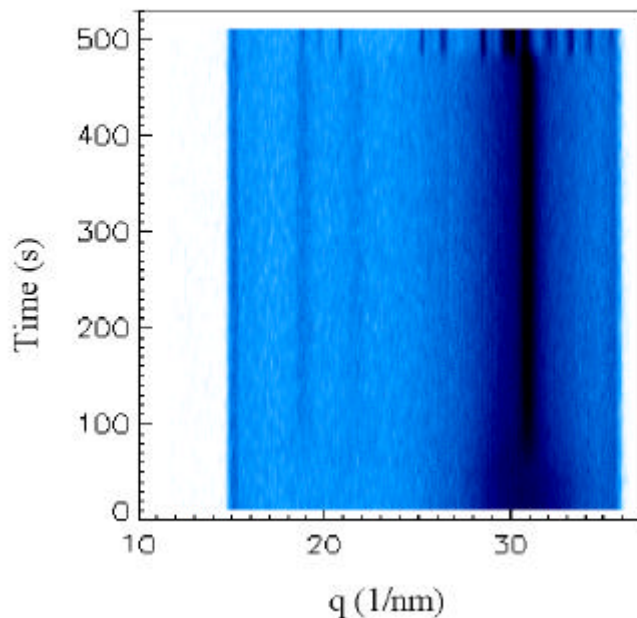


Fig.1: Time-resolved wide angle scattering patterns of  $\text{Fe}_{72}\text{Cu}_1\text{Nb}_{4.5}\text{Si}_{13.5}\text{B}_9$  amorphous alloy submitted to *in situ* 7.8 A current annealing.



## SAXS AND WAXS ON TiO<sub>2</sub>, CeO<sub>2</sub> AND CeO<sub>2</sub>-SnO<sub>2</sub> THIN FILMS AT GRAZING ANGLES

A Turkovic<sup>1</sup>, P Dubcek<sup>1,2</sup>, M Lucic-Lavcevic<sup>3</sup>, O Milat<sup>4</sup> and S Bernstorff<sup>2</sup>

<sup>1</sup>Institute "Ruder Boskovic", P.O.Box 1016, 10000 Zagreb, Croatia

<sup>2</sup>Sincrotrone Trieste S.c.p.A., SS. 14, km 163,5 Basovizza, 34012 Trieste, Italy

<sup>3</sup>Department of Physics, Faculty of Technology, University of Split, Teslina 10/V, 21000 Split, Croatia

<sup>4</sup>Institute of Physics, University of Zagreb, P.O.Box 162, 10000 Zagreb, Croatia

Dye-sensitized CeO<sub>2</sub> and mixed CeO<sub>2</sub>-SnO<sub>2</sub> films electrodes using Ru(by) - complex were used as photo anodes in photoelectrochemical solar and galvanic cells<sup>1,2</sup>. The cells were prepared following the description by Grätzel and co-workers, except using CeO<sub>2</sub> and mixed CeO<sub>2</sub>-SnO<sub>2</sub> films instead of TiO<sub>2</sub> film. The reason that CeO<sub>2</sub> and mixed CeO<sub>2</sub>-SnO<sub>2</sub> were chosen are similar optical and electrical properties of CeO<sub>2</sub> and TiO<sub>2</sub> films and because of suitable and new method of dip-coating preparation which was recently published<sup>3,4</sup>.

We presented our Ag/AgI/TiO<sub>2</sub>,SnO<sub>2</sub> rechargeable, photosensitive, electrochromic galvanic cell at MatTech'90-Finland in 1990<sup>5</sup>. Its performance is based on photon or electrically induced Ag<sup>+</sup> ion diffusion in TiO<sub>2</sub>. Our research was, in fact, a search for rechargeable battery for solar-cells back-up and resulted in a solar-battery. It was a small contribution to the world-wide quest for clean and renewable electrical energy sources. This ecological idea has encouraged large-scale research activities and brought about advancement in the field of photo voltaic solar cells in the last twenty years<sup>6</sup>.

In 1991, Grätzel and co-workers<sup>7</sup> made a breakthrough in preparing an efficient dye-sensitized cell, which was made of relatively non pure material by using a cheap preparation procedure achieving energy conversion efficiencies ranging from 7 to 12 %. It was a great satisfaction for us to learn that TiO<sub>2</sub> semiconductor electrodes were used in this cell, i.e., the same material that we had used in our photo-sensitive galvanic cell<sup>5,8</sup>. Also, the application of AgI<sup>9</sup>, similarly as of dye<sup>7</sup>, to TiO<sub>2</sub> has produced a shift of absorption maximum to the visible region of the solar spectrum. The performance of the cell also depends on the porosity of nanosize grains in the TiO<sub>2</sub> electrode, which produces a 2000-fold increase in surface area.

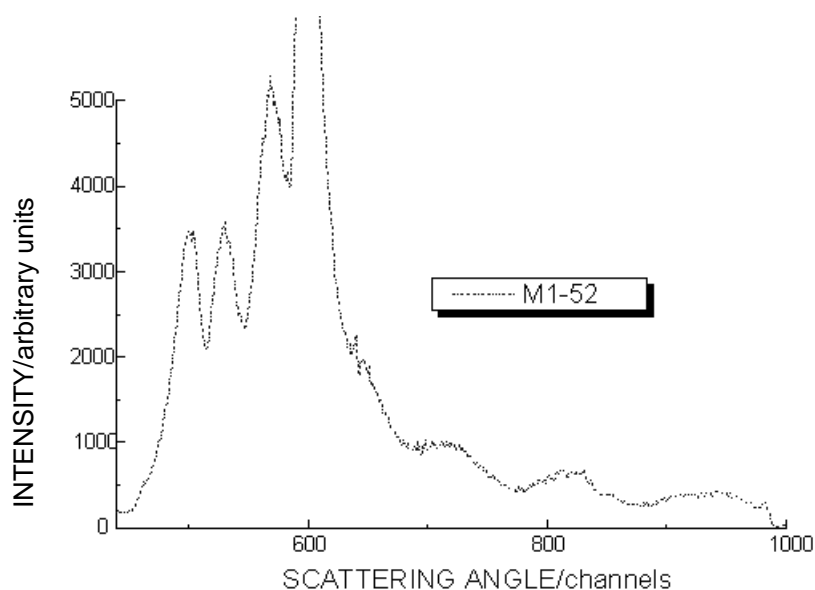


Fig 1. Wave features of GISAXS on CeO<sub>2</sub> sample obtained by inorganic sol-gel method revealing lamellar structure of the film

Dye-sensitized cells differ from the conventional semiconductor devices in that they separate the function of light absorption from charge carrier transport. The device is based on a 10- $\mu$ m-thick optically transparent film of titanium dioxide particles of a few nanometers in size, coated with a monolayer of charge-transfer dye to sensitize the film for light harvesting. The nano-size properties of TiO<sub>2</sub> obtained by the sol-gel method we have studied by Raman spectrometry, X-ray diffraction, high resolution electron microscopy and small angle X-ray scattering<sup>10</sup>. Grain sizes and distributions obtained by these four methods agreed varying from 4 to 12 nm with the temperature of Ti calcination.

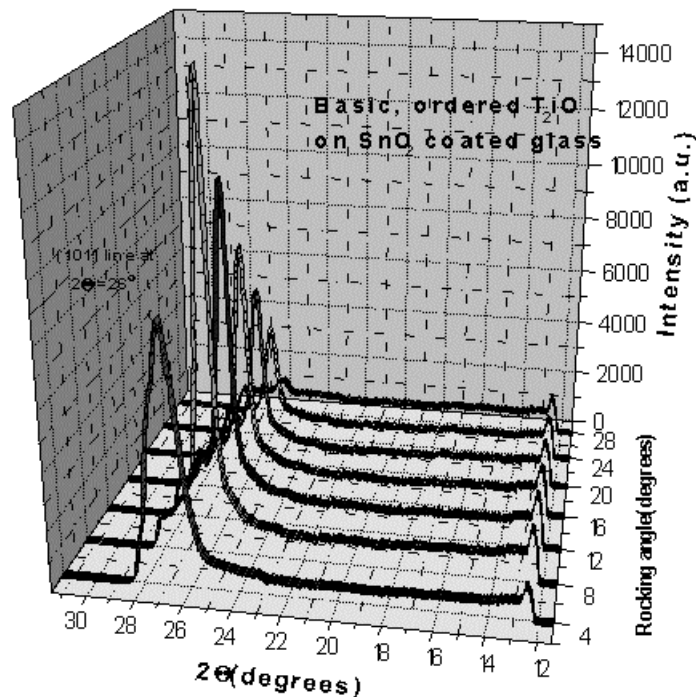


Fig 2. Rocking-angle 3D-diagram of GIWAXS on  $\text{TiO}_2$  sample revealing (101) orientation of the film

In SAXS - beamline on ELETTRA we have measured SAXS and WAXS of thin films  $\text{CeO}_2$ ,  $\text{CeO}_2\text{-SnO}_2$  and  $\text{TiO}_2$  on glass substrate in reflection geometry at grazing angles from 0.18 to 1 degrees.  $\text{TiO}_2$  samples were prepared by five preparation procedures (sol-gel, CVD, spray, ALE and from commercial P25 material) and  $\text{CeO}_2$  and  $\text{CeO}_2\text{-SnO}_2$  by sol-gel dip-coating method. The goal of this work is to determine relevant parameters as grain sizes and porosity of all samples and then make decision which preparation is the most suitable for construction of nanostructured solar cells. The results of the previous measurements, which we have performed on ELETTRA beamline 8 KeV from 13. III to 16. III 1997. (193/96), are published in international journals<sup>11,12,13</sup> and presented at four international conferences<sup>14,15,16,17,18</sup>. Also, the Ph.D. thesis<sup>19</sup> of Magdy Lucic-Lavcevic: "Raspršenje X-zraka pod malim kutom na filmovima nanofaznog  $\text{TiO}_2$ " was defended on December 29<sup>th</sup>, 1998. We have recorded SAXS and WAXS curves on 50 samples in period from 19. III to 22. III 1998. on SAXS-beamline of ELETTRA (173/97). We have applied general Guinier and Porod approximation to the first set of nanosized  $\text{CeO}_2$  and  $\text{CeO}_2\text{-SnO}_2$ , 120-420 nm thick, films on glass substrate prepared using sol-gel dip-coating method procedure. The average grain size  $\langle R \rangle$ , obtained by SAXS, varied with the number of dips for the  $\text{CeO}_2\text{-SnO}_2$  samples. For the  $\text{CeO}_2$  films,  $\langle R \rangle$  increased compared to  $\text{CeO}_2\text{-SnO}_2$  films from 3.15 to 5.12 nm. Specific surface areas of both these films were also determined and varied from  $0.44 \times 10^7$  to  $3.2 \times 10^7 \text{ cm}^{-1}$ . Also, we have recorded equidistant peaks in  $s(\text{nm}^{-1})$  representation, which reveal lamellar structure of films due to dip-coating way of preparation. These results were presented at Sixth Users' Meeting<sup>20</sup> and in paper which is accepted for publication in Nanostructured Materials<sup>21</sup>. Also, we have analyzed data of  $\text{CeO}_2$  prepared by inorganic sol-gel method in order to decide which preparation method is the best in our case (Fig 1.). These results are accepted for publication in Materials and Science Engineering B<sup>22</sup>. But, if we do not achieve required porosity, we will modify preparation and this will require further SAXS measurements. Also, we constructed a model of SAXS at grazing angles, which interprets the signal from surface as coming from "islands like" planar structure<sup>23</sup>. Results of measurements on ordered and acidified  $\text{TiO}_2$  samples (Fig 2.) were presented at Sixth Users' Meeting<sup>24</sup>. At moment we are analyzing the data of  $\text{TiO}_2$  micelles in preparation for publications in some of international scientific journals for materials science and physics.

## REFERENCES

1. A. Turkovic and Z. Crnjak-Orel, Dye-sensitized solar cell with CeO<sub>2</sub> and mixed CeO<sub>2</sub>-SnO<sub>2</sub> photo anodes, *Solar Energy Materials and Solar Cells* 45 (1997) 275-281.
2. A. Turkovic and Z. Crnjak-Orel, Electrical and Optical Properties of Thin Films Zn/(PEO)4ZnCl<sub>2</sub>/CeO<sub>2</sub>, or CeO<sub>2</sub>/SnO<sub>2</sub>(17%),ITO Galvanic Cells, *Solid State Ionics* 89 (3-4), (1996) 255.
3. Z. Crnjak-Orel and B. Orel, Structural and electrochemical properties of CeO<sub>2</sub> and mixed CeO<sub>2</sub>/SnO<sub>2</sub> coatings, *Solar Energy Materials and Solar Cells* 40 (1996) 205.
4. Z. Crnjak-Orel and B. Orel, Ion storage properties of CeO<sub>2</sub> and mixed CeO<sub>2</sub>/SnO<sub>2</sub> coatings *J. Mater. Sci.*, 30, 1995, 001.
5. A. Turkovic and V. Vraneša, *Int. J. of Materials and Product Technology*, 47 (1992) 51.
6. K. Zweibel, *Harnessing Solar Power; The Photovoltaic Challenge*, Plenum Press, New York, 1990.
7. B. O'Regan and M. Grätzel, A low cost, high-efficiency solar cell based on dye-sensitized colloidal TiO<sub>2</sub> films, *Nature*, 353 (1991) 737.
8. A. Turkovic, M. Ivanda, A. Drašner, V. Vraneša and M. Peršin, *Thin Solid Films* 198 (1991) 199.
9. A. Turkovic, N. Radic and D. Šokcevic, *Materials Science & Engineering B23* (1994) 41.
10. A. Turkovic, M. Ivanda, S. Popovic, A.M.Tonejc, M. Gotic, P. Dubcek and S. Music, Comparative Raman, XRD, HREM and SAXS studies of grain sizes in nanophase TiO<sub>2</sub>, *J. of Mol. Structure* 410-411 (1997) 271.
11. M.Lucic-Lavcevic, P.Dubcek, O.Milat, B.Etlinger, A.Turkovic, D.Šokcevic and H.Amenitsch, Nanostructure of sol-gel TiO<sub>2</sub> thin films on glass substrate measured by small angle scattering of synchrotron light, *Materials Letters* 36 (1-4) (1998) 56.
12. A.Turkovic, M.Lucic-Lavcevic, A.Drašner, P.Dubcek, O.Milat, B.Etlinger, H.Amenitsch and M.Rappolt Small angle X-ray scattering studies of nanophase TiO<sub>2</sub> thin films at ELETTRA, *Materials Science & Engineering B54*, 174-181 (1998).
13. M.Lucic-Lavcevic, A.Turkovic, D.Šokcevic, P.Dubcek, O.Milat, B.Etlinger, P.Laggner and H.Amenitsch, Small angle scattering of synchrotron radiation on nanosized TiO<sub>2</sub> thin films obtained by chemical vapour deposition and spray method, *Fizika A* 7 119-132 (1998) 3.
14. P.Dubcek, O.Milat, M.Lucic-Lavcevic, A.Turkovic B.Etlinger and H.Amenitsch, Small Angle X-ray Scattering and X-ray reflection on Thin Films, *Book of Abstracts: Sixth Croatian-Slovenian Crystallographic Meeting*, 57, Umag, Croatia, June 19-21, 1997.
15. M.Lucic-Lavcevic, P.Dubcek, O.Milat, B.Etlinger, A.Turkovic and H.Amenitsch, Small Angle X-ray Scattering on Thin Films at Grazing Angles, *Book of Abstracts: Sixth Croatian-Slovenian Crystallographic Meeting*, 58, Umag, Croatia, June 19-21, 1997.
16. A.Turkovic, M.Lucic-Lavcevic, D.Šokcevic, A.Drašner, P.Dubcek, O.Milat, B.Etlinger and H.Amenitsch, Studij raspršenja X-zraka pod malim kutem na nanofaznim TiO<sub>2</sub> tankim filmovima na ELETTRI, *Zbornik sazetaka s V Susreta vakuumista Hrvatske i Slovenije*, 15-16, Institut "Ruder Boškovic", 20 Svibanj 1998.
17. P.Dubcek, O Milat, M.Lucic-Lavcevic, A.Turkovic, B.Etlinger, and H.Amenitsch, Small Angle X-ray Scattering and X-ray reflection on Thin Films, *Book of Abstracts: Fifth User's Meeting, Sincrotrone Trieste*, Trieste, Italy, December 1-2, 1997.
18. P.Dubcek, A.Turkovic, B.Etlinger, O Milat, M.Lucic-Lavcevic, S.Bernstorff and H.Amenitsch, Small Angle X-ray Scattering Study of TiO<sub>2</sub> Thin Films at Grazing Angles, 18th European Crystallographic Meeting, Praha, Czech Republic, August 15-20, 1998.
19. M.Lucic-Lavcevic, Ph.D.Theses: "Sincrotrone Source X-ray Scattering at Small Angle on Films of Nanophased TiO<sub>2</sub>", defended on December 29<sup>th</sup> 1998.
20. A.Turkovic, P.Dubcek, Z.Crnjak-Orel and S.Bernstorff, Grazing-incidence small-angle scattering of synchrotron radiation on nanosized CeO<sub>2</sub> and CeO<sub>2</sub>-SnO<sub>2</sub> thin films obtained by sol-gel dip-coating method, *Book of Abstracts: Sixth User's Meeting, Sincrotrone Trieste*, 78, Trieste, Italy, Nov. 30- Dec. 1, 1998.
21. A.Turkovic, P.Dubcek, Z.Crnjak-Orel and S.Bernstorff, Small angle scattering of synchrotron radiation on nanosized CeO<sub>2</sub> and CeO<sub>2</sub>-SnO<sub>2</sub> thin films obtained by sol-gel dipcoating method, accepted to *Nanostructure materials* (1998).
22. A.Turkovic, P.Dubcek and S.Bernstorff, Grazing-incidence small-angle and wide-angle scattering of synchrotron radiation on nanosized CeO<sub>2</sub> thin films, accepted to *Materials Science & Engineering B* (1998).
23. P.Dubcek, A.Turkovic, B.Etlinger, O Milat, M.Lucic-Lavcevic, S.Bernstorff and H.Amenitsch, Small Angle X-ray Scattering Study of TiO<sub>2</sub> Thin Films at Grazing Angles, *Book of Abstracts: Sixth User's Meeting*, 80, Sincrotrone Trieste, Trieste, Italy, Nov. 30- Dec. 1, 1998.
24. A.Turkovic, M.Lucic-Lavcevic, O.Milat, P.Dubcek, S.Burnside, M.Grätzel and S.Bernstorff, Rocking- angle scattering od synchrotron radiation on nanosized TiO<sub>2</sub> ordered and acidified thin films, *Book of Abstracts: Sixth User's Meeting, Sincrotrone Trieste*, 79, Trieste, Italy, Nov. 30- Dec. 1, 1998.

# 4. Chemistry

## IN SITU SYNCHROTRON SAXS STUDY OF THE FORMATION OF MCM-41 AND MCM-50

P. Ågren, M. Lindén and J.B. Rosenholm,

Dept. of Physical Chemistry, Åbo Akademi University, Porthaninkatu 3-5, FIN-20500 Turku, Finland

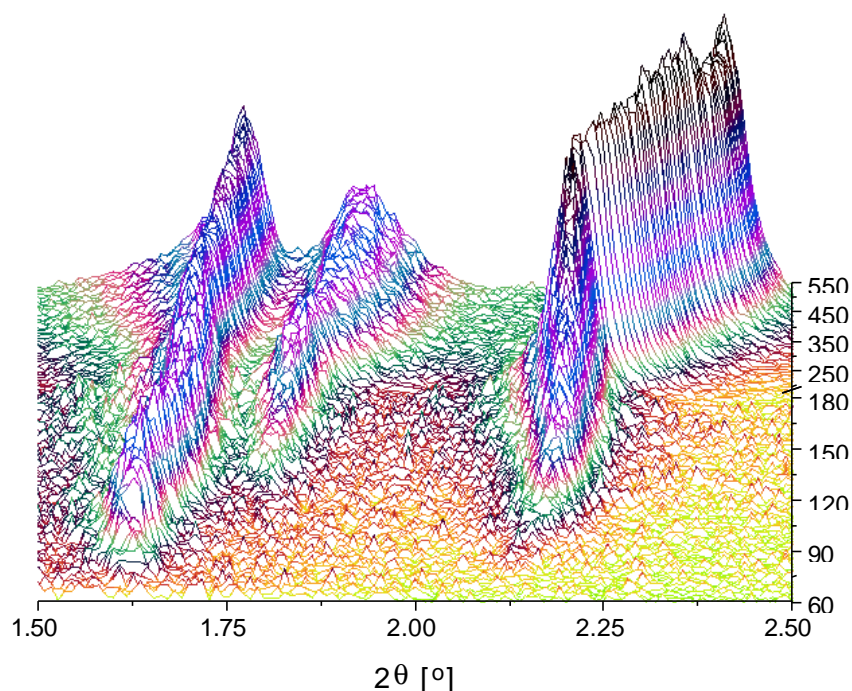
R. Schwarzenbacher, M. Kriechbaum, H. Amenitsch and P. Laggner,

Institute of Biophysics and X-Ray Structure Research, Austrian Academy of Sciences, Steyrergasse 17/VI, A-8010 Graz, Austria

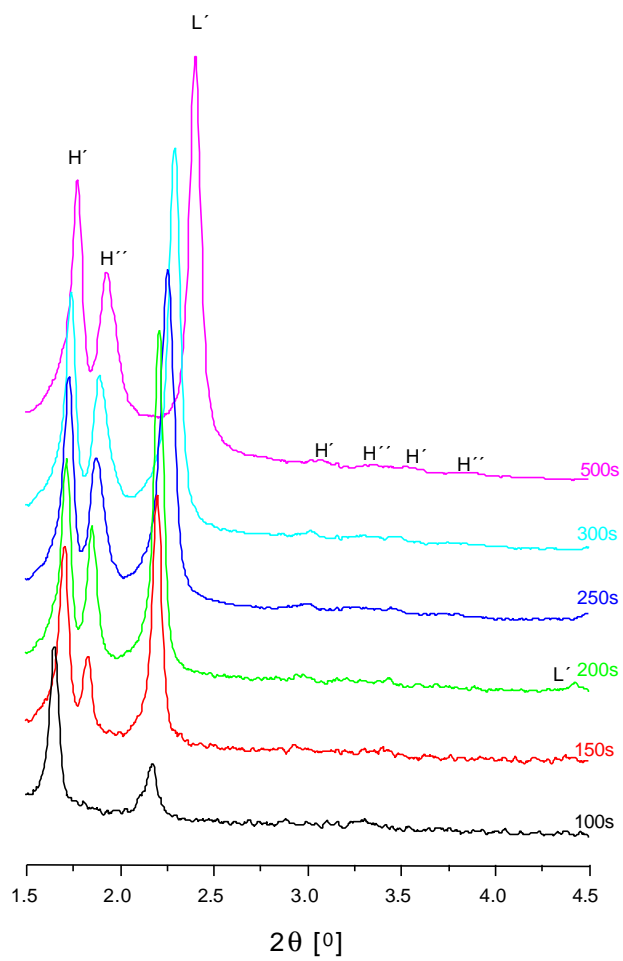
J. Blanchard and F. Schüth,

Dept. of Inorganic and Analytical Chemistry, Johann Wolfgang Goethe Universität, Marie Curie Str. 11, D-60439 Frankfurt am Main, Germany

The formation of hexagonal and lamellar surfactant-silicate mesophases at room temperature has been investigated by *in situ* synchrotron small angle X-ray scattering. Following chemicals were used in the experiments: water, ammonia, TEOS, CTAB, butanol and hexanol. Emphasis was given to the influence of butanol and hexanol on the surfactant-silicate phase behavior. The X-ray measurements were performed at the Austrian high flux SAXS beamline of the 2 GeV electron storage ring ELETTRA, Trieste, Italy. The experimental setup included a continuous flow reactor allowing a resolution in time as high as 0.3s, which allowed detailed information about the initial stages of silicate-surfactant mesophase formation. Depending on the reaction composition, one, two or three co-existing phases were observed. Furthermore, the observed structures were hexagonal or lamellar or a mixture of both phases. The results are discussed in terms of time-dependent changes in the concentration of co-surfactant not incorporated into the composite aggregates. Although many of the observed effects are paralleled by well known properties of aqueous surfactant solutions, important dissimilarities exist. Furthermore, the relative intensity of the high-order reflections are suggested to correspond to the degree of inter-aggregate condensation in the composite mesophase.



A



B

Fig. 1. SAXS patterns with HeOH (0.5 g) as co-surfactant prepared in the batch reactor (a) as a function of reaction time (note the discontinuity in the time axis after 185 s of mixing), (b) at various times after mixing of reactants. H' and H'' indicate the hexagonal phases and L' the lamellar phase.

## THERMAL BEHAVIOUR OF POLY-HYDROXYBUTYRATE GELS: A CALORIMETRIC AND SMALL ANGLE X-RAY SCATTERING STUDY

Attilio Cesàro<sup>1</sup>, Deborah Fabri<sup>1</sup>, Fabiana Sussich<sup>1</sup>, Gaio Paradossi<sup>2</sup>,  
H. Amenitsch<sup>3</sup> and S. Bernstorff<sup>4</sup>

1) Dip. Bioch., Biofis. Chim. delle Macromolecole, Università di Trieste, I-34127 Trieste

2) Dip. Scienze e Tecnologie Chimiche, Università di Roma "Tor Vergata", I-00173 Roma

3) AUSTRIAN ACADEMY OF SCIENCES, Inst. Biophysics and X-Ray Structure Res., Graz

4) Sincrotrone Trieste, SS14 per Basovizza, I-34012 Trieste

### Introduction

The aim of our recent work is to contribute to the understanding the thermodynamics and the kinetics of physical gelation of stereoregular biopolymers. Small angle X-ray scattering and calorimetric properties have been used to investigate the structural and thermal properties of polyhydroxybutyrate (PHB) gels in dimethylformamide (DMF). The dilute and semi-dilute mixed PHB/DMF system undergoes a phase separation on cooling at a temperature  $T_{gel}$ , producing a gel in which the crystalline fraction is of the order of 50-60% and the diffraction pattern is that of disperse nano-crystals, with the same unit cell of the pure crystalline PHB. Upon heating, two melting peaks are normally observed at  $T_{m1}$  and  $T_{m2}$  (always higher than  $T_{gel}$ ). Shapes of the peaks, temperatures and enthalpies of melting depend slightly on heating scan but on the procedure of gel preparation. The investigation has been carried out in a range of dilute solution mainly by high sensitivity scanning calorimetry. Gels of PHB in dimethylformamide, DMF, were formed under several conditions to clarify the thermo-reversibility of the gelation-dissolution process. Small angle X-ray scattering experiments have been made to evaluate the radius of gyration  $R_g$  of the dispersed nano-crystals as a function of concentration, and to follow the formation of the junction zones during the gelation. The time dependent scattering intensities have been collected with the aim of clarifying the distribution of the PHB cluster, which manifest clearly in the DSC experiments.

### Structural aspects and thermodynamics

Upon cooling of dilute and moderately concentrated (0.1%-20%) solutions of PHB in DMF from temperatures above 100°C to room temperature, the phenomenological observation of a turbidity is accomplished by the formation of a self-standing gel phase for concentrations larger than 1%. After quenching the optical activity of very dilute solutions (< 0.1%) deviates toward negative values with a sigmoidal shape, monitoring the ordering of the stereoregular chains. The formation of very disperse aggregated structures is also shown by the change in the viscosity as a function of time measured on the rapidly cooled solutions. Both phenomena are reversible, giving two-step sigmoidal melting profiles of the aggregated structure as a function of temperature. The overall dimension of these particles (about 5 nm), approximately evaluated from the peak broadness of diffraction data in the wide angle range, is found to correspond to the thickness of the lamella which is the basic structural unit in the gel phase. The importance of these results lies also in the findings that the polymer organisation in the gel phase is crystalline in nature and that the dimensions of the crystallites are rather small. Furthermore, once the contribution of the amorphous phase has been eliminated, the WAXS diffraction peaks obtained from the gel system congruently overlap those obtained from the pure crystalline PHB. More deep knowledge about the possible bimodal distribution of the crystalline nano-particles and their kinetic formation is being obtained from the analysis of the SAXS data on the nucleation and growth of the crystallites under controlled conditions and their subsequent melting. All the mixtures with low and moderate PHB concentration show thermograms with two melting endotherms on heating. However, peak size and shape vary significantly with composition, as results especially from the experiments carried out in the composition range between 0.025% and 15% w/w with scanning rate of 0.5 K min<sup>-1</sup>. A scrutiny of the two melting peaks shows that the endotherm at  $T_{m2}$  is sharper and larger than that at  $T_{m1}$  at low concentration, while sharpness and relative size is

progressively lost as the polymer concentration increases. The endotherm at  $T_{m1}$  seems to maintain a bell-shaped curve which is characteristic of the transition of independent (non-interacting) macrodomains like those occurring in the denaturation of globular proteins.

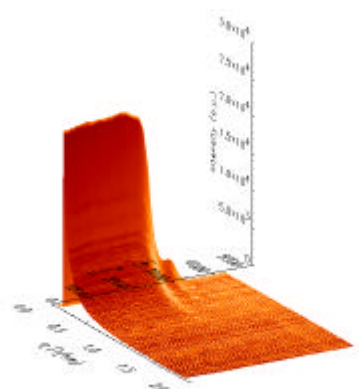


**Fig. 1.** Diffraction pattern of 1% PHB heated from 25 to 90 °C with a scan rate of 1 °C/min. The melting of the crystallites in two steps is visible in the pattern.

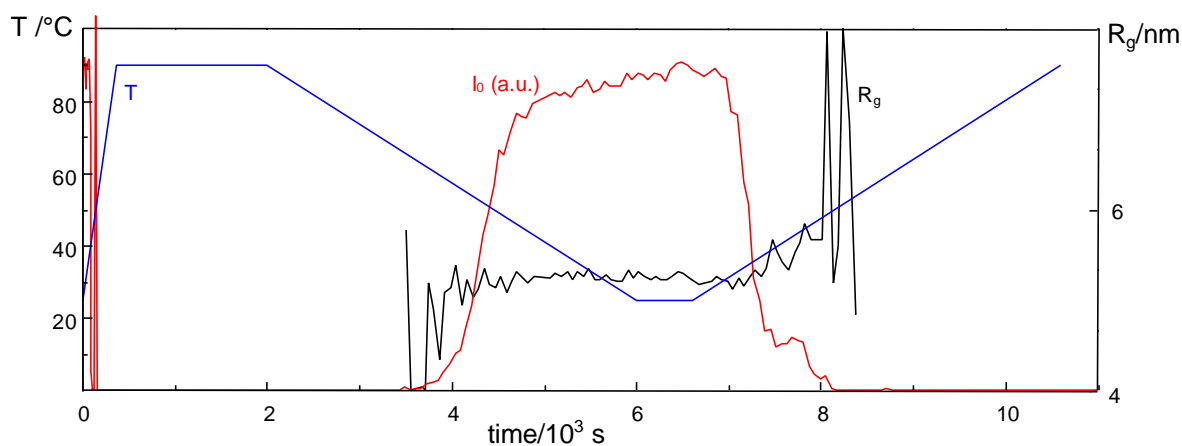


**Fig. 2.** Dependence of the radius of gyration  $R_g$  and of the forward intensity  $I_0$  of 1% PHB on the time during a temperature scan ( $T: 90 \rightarrow 25 \rightarrow 90$  °C). The formation occurs with constant size and with a continuously increasing crystalline fraction till the melting temperature of the crystallites is reached. After the melting of the primary fraction a melting of the secondary fraction starts, which has a slightly larger size than the primary one.

#### References:

- 1) A. Cesàro, S. Turchetto "Gel-sol Phase Transition of Poly(D-(-)- $\beta$ -hydroxybutyrate) in Dimethylformamide" *Thermochim. Acta* 1995, 269/270,307-317.
- 2) F. Bordi, C. Canetti, A. Cesàro, G. Paradossi "Dielectric properties of polyhydroxybutyrate gels in dimethylformamide" *Polymer*, 1996,37,3501-3507.
- 3) D. Fabri, J. Guan, A. Cesàro "Crystallisation and melting behaviour of polyhydroxybutyrate in dilute solution: toward an understanding of physical gels" *Thermochim. Acta* 1998,321,3-16.
- 4) A. Cesàro, D. Fabri, F. Sussich, G. Paradossi "Structural and Thermodynamic Features of Polyhydroxybutyrate Physical Gels" *Macromolecular Symposia*, (1999 in press).



# 5. Instrumentation

## CCD DETECTOR RESEARCH AND DEVELOPMENT

H. Amenitsch <sup>a</sup>, S. Bernstorff <sup>b</sup>, P. Ottonello <sup>c</sup>, G.A. Rottigni <sup>c</sup>, G. Zanella <sup>d</sup> and R. Zannoni <sup>d</sup>

<sup>a</sup>Inst. for Biophysics and X-ray Structure Research, Austrian Academy of Sciences, Steyrerg. 17, 8010 Graz, Austria

<sup>b</sup>Sincrotrone Trieste SCpA, Strada Statale per Basovizza 14 km 163.5, 34012 Trieste, Italy

<sup>c</sup>Dipartimento di Fisica dell'Universit  di Genova and Istituto Nazionale di Fisica Nucleare, Sezione di Genova, via Dodecaneso 33, 16146 Genova, Italy

<sup>d</sup>Dipartimento di Fisica dell'Universit  di Padova and Istituto Nazionale di Fisica Nucleare, Sezione di Padova, via Marzolo 8, 35131 Padova, Italy

During 1998 was tested an improved version of the CCD detector developed with support of INFN (SAXS-CCD experiment of „gruppo V“). This detector was designed according to the specific needs of the SAXS beamline, and for dynamic X-ray diffraction imaging [1].

In Fig.1 we can see a schematic drawing of the tested version. The useful input area is 75 x 75 mm<sup>2</sup> (106 mm diameter), the image intensifier is Proxitronic 2 MCP (40 mm diameter, fibre optic input and output, S20 photocatode, P20 output phosphor, 10 ns electronic gate), the CCD is 7896M-(H) Thomson (1024 pixel x 1024 pixel, 28 ms per frame, 4 outputs, 19µm x 19µm pixel size). The input area is covered by a removable Fibre Optic Plate with Scintillator (FOS). The FOS is Hamamatsu, coated with Gd<sub>2</sub>O<sub>2</sub>S:Tb, 30µm thick. The image processor is Matrox Genesis, which permits 64 MB processing memory on-board. The tested data rate is 25 frames/s, at 16 bits, with the possibility to synchronise the acquisition by an external trigger.

In Fig. 2 we can see a part of the diffraction figure obtained with the described detector from dry rat tendon collagen at room temperature, using 8 keV X-rays.

Other tests were addressed to detect X-ray diffraction patterns, accompanying structural changes in single muscle fibres, according to a planned acquisition protocol. The result of this application has evidenced a limit regarding the quantum efficiency, that is the single 8 keV X-photons are revealed at present with an efficiency of about 30 %.

In the light of this experience we are now working to improve this figure. The new version of the detector will have a more efficient X-ray converter, a detector design which reduces the light loss due to the input fiber optic taper and, if possible, a more efficient image intensifier.

[1] G. Zanella, R. Zannoni, *Design of CCD-based X-ray area detector in terms of DQE*, Nucl. Instr. and Meth. A (1998) 93-102.

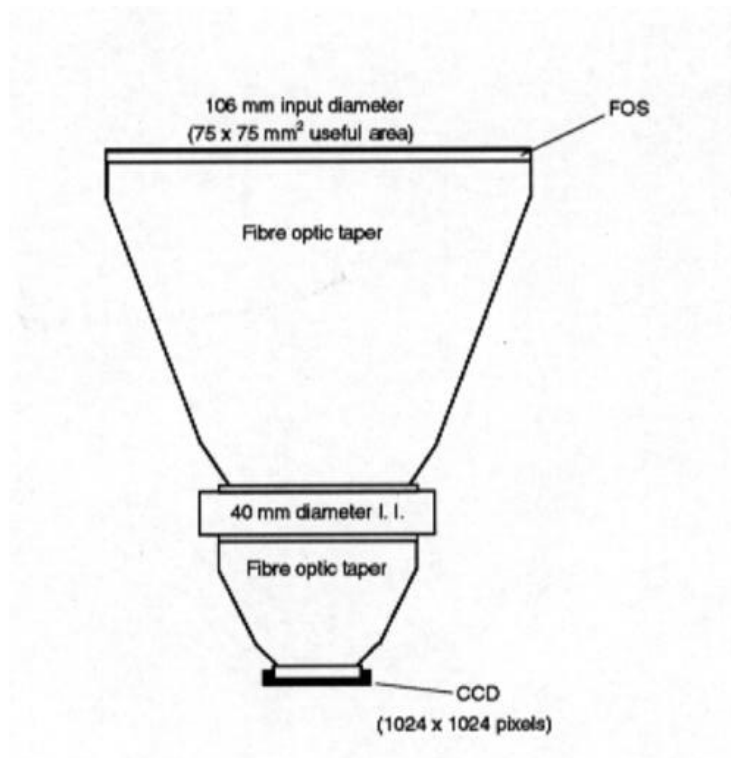


**Fig.1.** Schematic drawing of the detector

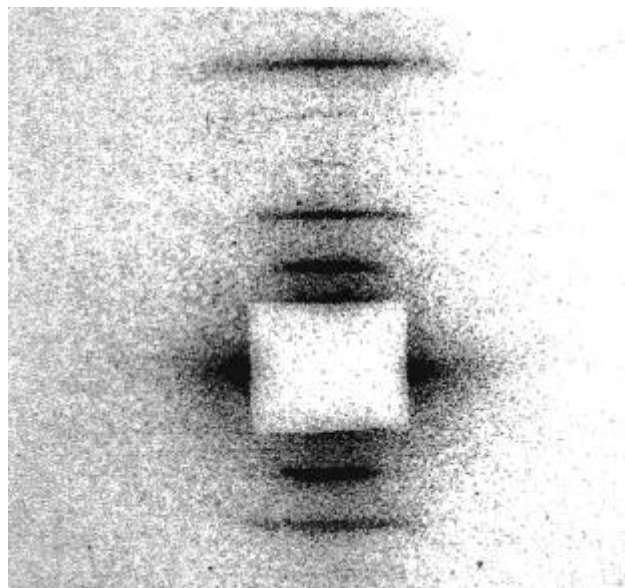


**Fig. 2.** Part of the 8 keV X-ray diffraction image of dry rat tendon collagen, obtained with the described CCD detector (8 bits negative printing)

# TIME-RESOLVED SMALL-ANGLE X-RAY SCATTERING STUDIES OF PRESSURE-JUMP INDUCED BAROTROPIC PHASE TRANSITIONS OF LIPIDS

M. Kriechbaum<sup>1</sup>, M. Steinhart<sup>2</sup>, P. Lagner<sup>1</sup>, H. Amenitsch<sup>1</sup>, and S. Bernstorff<sup>3</sup>

<sup>1</sup>Institute of Biophysics and X-Ray Structure Research, Austrian Academy of Sciences, Graz, Austria

<sup>2</sup>Institute of Macromolecular Chemistry, Academy of Sciences of the Czech Republic, Prague, Czech Republic

<sup>3</sup>Sincrotrone Trieste, Basovizza, Italy.

We have continued our time-resolved jump relaxation studies of barotropic phase transitions on phospholipid systems and have optimized the experimental setup of the p-jump technique (Fig.1) combined with time-resolved small-angle and wide-angle X-ray scattering with millisecond time resolution on the SAXS-beamline at ELETTRA using the high-pressure X-ray cell as described in the Annual Report 1996/1997.

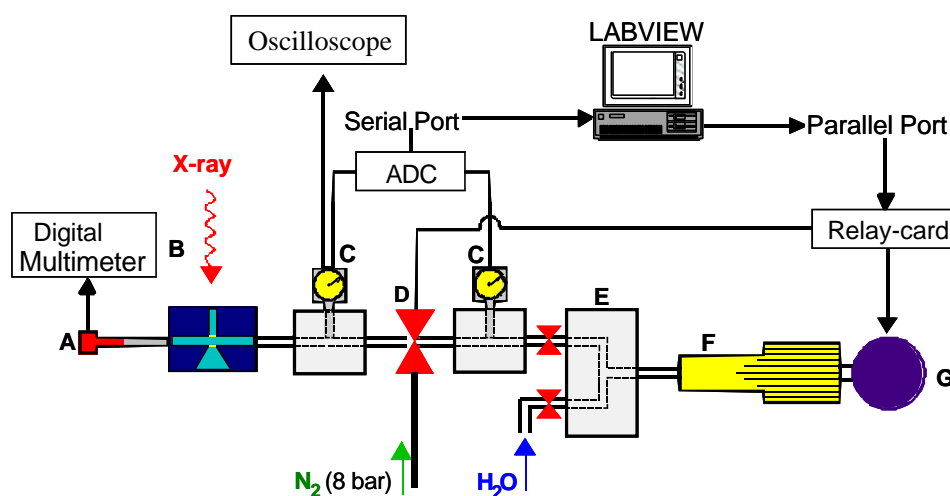


Fig1: **Set-up of the p-jump experiment:** Thermocouple (A), high pressure X-ray cell (B), pressure sensors (C). Two ‘pressure-circuits’ are separated by a pneumatic driven valve (D) and are kept at different pressure levels before activating a p-jump, which is accomplished by quickly opening the valve D, resulting in a quick pressure equilibration between both reservoirs within a few milli-seconds. Double-stem valve (E) and a motor(G)-driven pressure pump (F) are used for generating hydrostatic high pressures.

We have focused on barotropic phase transitions of the phospholipid DOPE (dioleoylphosphatidylethanolamine) within a temperature range of 5-70° C and a pressure range of 1-2000 bar using pressure jump amplitudes up to 1.5 kbar (0.15 GPa) within 10 ms, recorded by time-sliced X-ray diffraction patterns in the SAXS and WAXS region in typically 5/50/500 ms time-resolution following a p-jump. The example in Fig.2 shows that results with good statistics can already be obtained with 2/20/200 ms resolution in a single-shot experiment. Systematic variations of the p-jump amplitudes across the phase-boundaries in the p-T phase diagram have clearly shown that the kinetics, i.e. the occurrence, coexistence and life-time of non-equilibrium intermediates depend strongly on the magnitude of the ‘depth of the quench’ into the new phase.

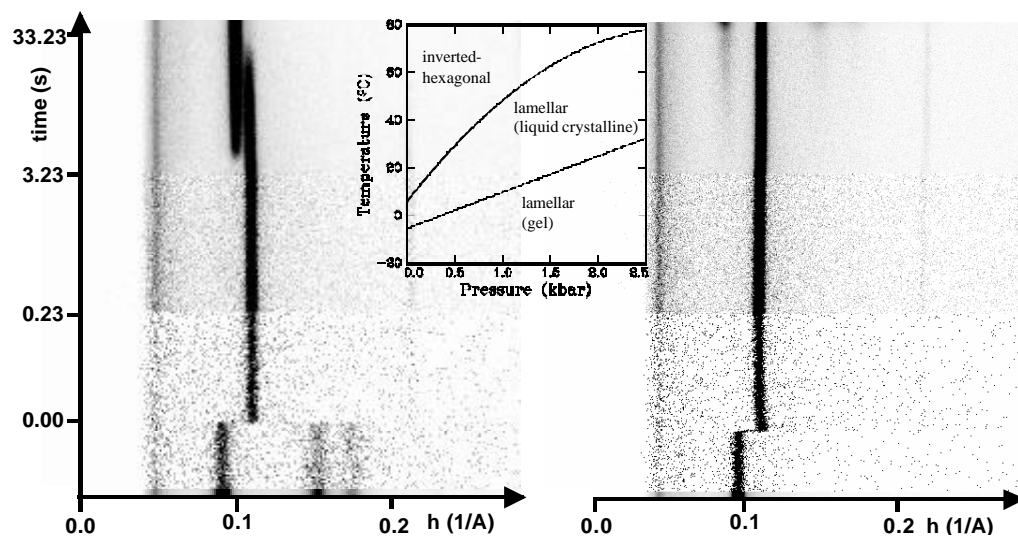


Fig. 2: **Time-resolved SAXS-data of two p-jump experiments of DOPE:** left: p-jump from 1 to 1550 bar (from the hexagonal to the lamellar-gel phase) and right: p-jump from 1550 to 90 bar (from the lamellar-gel to the hexagonal phase), both at 15°C and within 10 ms. The images show 512 frames with 1s (10x), 2ms (190x), 20ms (150x), 200ms (150x) and 1s (12x) time-resolution, respectively, from the bottom to the top (time-normalized, unsmoothed intensity-data obtained in a single-shot experiment, represented in a linear grey-scale). The insert shows the respective p-T phase-diagram of DOPE in excess water.

- (1) K.Pressl, M.Kriechbaum, M.Steinhardt and P.Laggner, *Rev.Sci.Instrum.* 68, 4588-4592 (1997).
- (2) M.Steinhardt, M.Kriechbaum, K.Pressl, H.Amenitsch, P.Laggner and S.Bernstorff, *Rev.Sci.Instrum.* 70, 1540-1545 (1999).

## A 1D STATE - OF -THE - ART GASEOUS IMAGING DETECTOR FOR ADVANCED SAXS STUDIES<sup>1</sup>

R.H. Menk<sup>a2</sup>, A. Sarvestani<sup>b</sup>, S. Bernstorff<sup>a</sup> and H. Amenitsch<sup>c</sup>

a ELETTRA, Sincrotrone Trieste, S.S.14, km 163.5, Basovizza, 34012 Trieste, Italy

b Fachbereich Physik, Universität-GH Siegen, 57068 Siegen, Germany

c IBR, Steyergasse 17, 8010 Graz, Austria

1 Work supported by the European Community (contract no. FMBICT980104).

2 Supported by the European Community (contract no. FMBICT961694).

The public investment in modern synchrotrons has resulted in a tremendous development of both the sources as well as the associated x-ray optics. Unfortunately the development of the X-ray detection devices has not kept pace with that of the synchrotron light sources. Thus it is often the detector performance that limits the final data quality (e.g. Kriechbaum *et al.*, 1989; Helliwell *et al.*, 1993) and prevents the full exploitation of the facilities. This applies especially to applications such as time-resolved small angle X-ray scattering (SAXS) or protein crystallography, where the requirements in terms of detector performance are exceptionally high. In the following a novel system is presented which bases on the principle of highly segmented gaseous detector. Although gaseous detectors are often considered as “classical” or “old fashioned“ devices, in combination with novel gas amplification structures such as the Micro-CAT (for a detailed description see Sarvestani *et al.*, 1998a) and sophisticated electronics they reveal unique features that make them a superior detection device and thus well suited for installation at modern beam lines.

In a close collaboration between the detector laboratories of the Sincrotrone Trieste and that of the Department of Physics, University Siegen, two gaseous prototype detectors suitable for the aforementioned applications in the energy range between 5 keV and 16 keV were developed. Both state-of-the-art detectors feature a high quantum efficiency (more than 70%) that can be adjusted by the appropriate gas mixture and the gas pressure (up to 5 bars) and a spatial resolution of about 200 $\mu$ m. The first one is a one dimensional integrating detector (in the following called ‘1D’ (for a detailed description see Menk *et al.*, 1998)) and the other is a two dimensional single photon counting pixel detector which is described elsewhere in this annual report (Besch *et al.*, 1997).

The 1D system is equipped with a novel gas gain structure, namely the Micro-CAT, which performs a charge amplification of the primary electrons by factors between 1 and  $10^4$ . The working principle of this structure is based on a strong increase of the electrical field in the vicinity of micro-holes and is very similar to that of other gas gain structures which have been developed in the past 5 years, such as CAT (Bartol *et al.*, 1996), MICROMEGAS (Giometaris *et al.*, 1996) or GEM (Sauli, 1997). The 1D records the deposited charge by charge integration. In this case the gas gain mechanism is used to adjust the total charge in the detector according to the incoming photon flux, so that for each single photon a signal is always generated which is significantly higher than the noise background of the integrating electronics. Hence, for almost all photon fluxes single photon precision can be obtained. The 2D is operated in single photon counting mode. Here the gas gain mechanism is used, to obtain the maximum intensity precision. The position resolution is obtained by collection the deposited and optionally amplified charge on a fine structure with gold-plated parallel strips.

Main and unique feature of the detector is its huge dynamic range ( $>10^8$ ) in a single frame at high rates ( $10^{12}$  photons/s $\cdot$ mm<sup>2</sup>) allowing measurements close to the direct beam. It enables for the first time a direct I<sub>0</sub> calibration while recording simultaneously SAXS pattern with a single photon precision at very reasonable readout times in the order of 0.1 ms (figure 1) as demonstrated at the SAXS beam line at Sincrotrone Trieste (see Amenitsch et al, Bernstorff et al). This is due to an innovative and novel combination of single photon counting devices and integrating detectors and is well reflected by the ( zero frequency ) detective quantum efficiency DQE (figure 2). A single photon counter for example has no inherent noise floor and thus for low rates a DQE value that is determined by the quantum efficiency of the device. For higher rates, however, dead time losses lead to an decrease of the DQE. Due to the inherent noise floor of an integrating detector the DQE value starts at zero for low photon flux and increases with increasing flux. The DQE approaches the quantum efficiency of the device for rates having a Poisson error somewhat larger than the noise of the integrator. Now the gas gain can be

utilized to increase the signal and thus the signal to noise rate leading to a shift of the DQE curve to lower photon fluxes.

Recording a 'hot spot' such as the direct beam and measuring at the same time weak diffraction signals with a single photon precision in the vicinity requires excellent spatial resolution. It was proven better than  $10^{-6}$  ( resolution limit of the measurement) for long range  $>5$  mm and thus is far beyond was reached with gaseous detectors so far. This valuable characteristics is mainly due to the shielding- and the gas amplification mechanism of the MircoCAT structure in combination with a low ion feedback and a strong suppression of optical photons generated in the avalanche.

Amenitsch, H., Rappolt, M., Kirchbaum, M., Mio, H., Laggner, P. & Bernstorff, S. (1998). *J. Synchrotron Rad.* 5, 506-508.

Bartol, F., Bordessoule, M., Chaplier, G., Lemonnier, M. and Megtert, S. (1996). *J. Phys. III France* 6, 337.

Bernstorff, S., Amenitsch, H. & Laggner, P. (1998). *J. Synchrotron Rad.* 5, 1215-1221.

Besch, H. J., Junk, M., Meißner, W., Sarvestani, A., Stiehler, R. & Walenta, A. H. (1997). *Nucl. Instr. and Meth. A* 392, 244-248.

Giomataris, Y., Rebourgeard, Ph., Robert, J.P. and Charpak, G. (1996). *Nucl. Instr. and Meth. A* 376, 29.

Helliwell, J. R., Ealick, S., Doing, P., Irving, T. & Szebenyi, M. (1993). *Acta Cryst. D* 49, 120-128.

Kriechbaum, M., Rapp, G., Hendrix, J. & Laggner, P. (1989). *Rev. Sci. Instr.* 60, 2541-2544.

Menk, R. H., Arfelli, F., Bernstorff, S., Pontoni, D., Sarvestani, A., Besch, H. J. & Walenta, A.H. (1998). *Nucl. Instr. and Meth. A* 422, 698-703.

Sarvestani, A., Besch, H. J., Junk, M., Meißner, W., Sauer, N., Stiehler, R., Walenta, A. H. & Menk, R. H. (1998a). *Nucl. Instr. and Meth. A* 410, 238-258.

Sauli, F. (1997). *Nucl. Instr. and Meth. A* 386, 531.

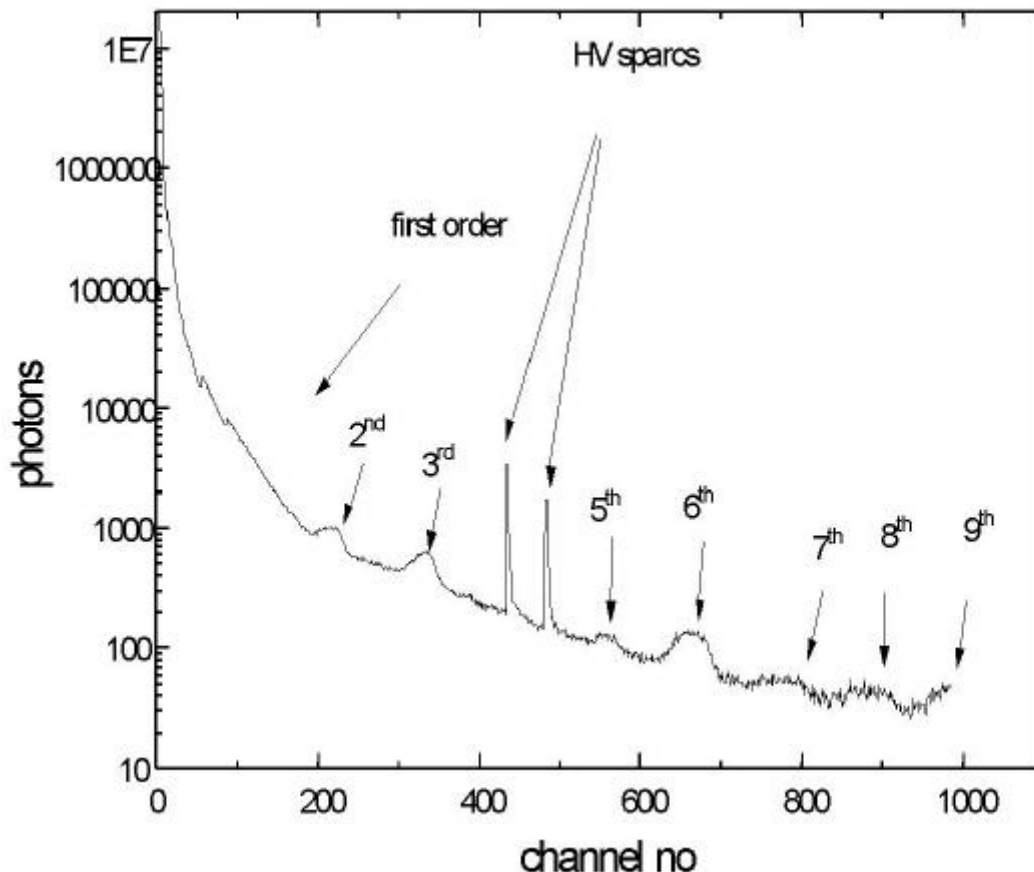


**Fig. 1.** Diffraction pattern of the rat tail tendon collagen recorded with the 1D with variable gas gain. The region close to the beam stop was imaged with ionization chamber mode while the 8<sup>th</sup> order was measured with a gas gain of 10000. The high voltage discharges (signed as HV sparks) occurred seldom (1 per minute or even less) and can be clearly distinguished from the diffraction peaks

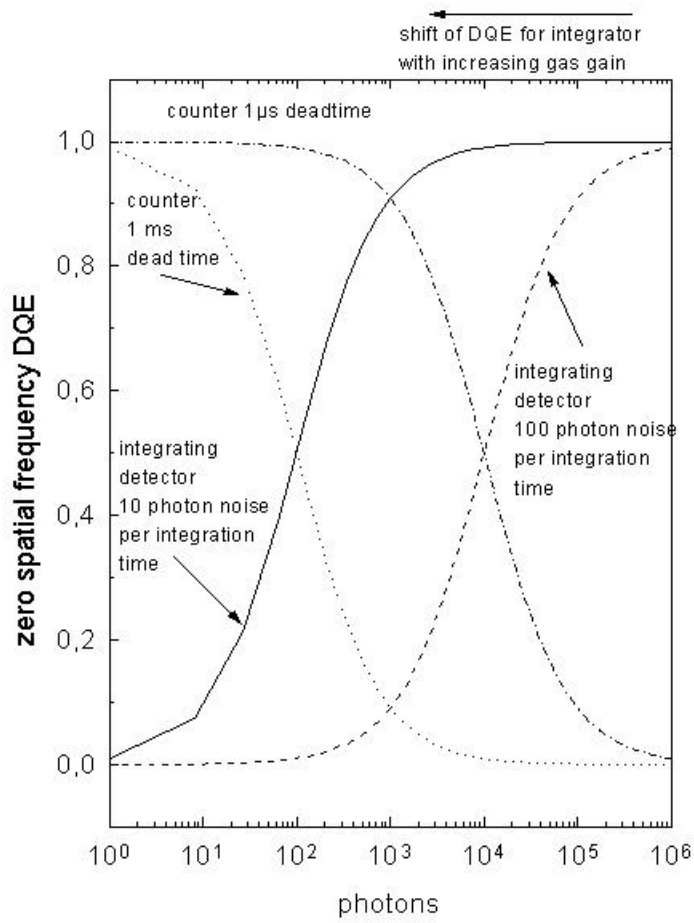


Fig. 2. DQE curves of single photon counting and integrating detectors

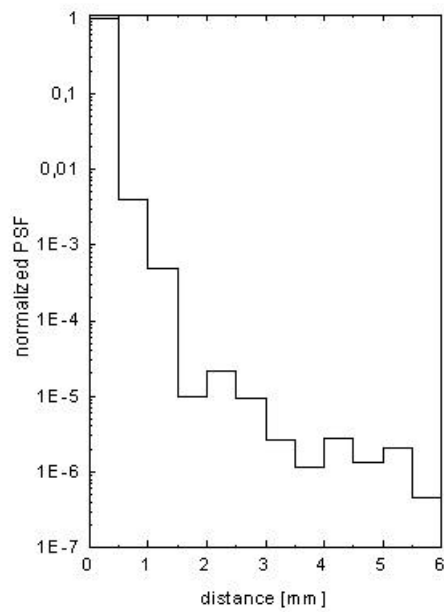


Fig.3. Long range point spread function of the detector



## DIFFRACTION TEST MEASUREMENTS WITH A PROTOTYPE OF A NOVEL 2D GASEOUS PIXEL DETECTOR

A. Sarvestani<sup>1</sup>, H. Amenitsch<sup>2</sup>, S. Bernstorff<sup>3</sup>, H.J. Besch<sup>1</sup>, R.H. Menk<sup>3</sup>, A. Orthen<sup>1</sup>, N. Pavel<sup>1</sup>, M. Rappolt<sup>2</sup>, N. Sauer<sup>1</sup>, A.H. Walenta<sup>1</sup>

<sup>1</sup>Fachbereich Physik, Universität-GH Siegen, 57068 Siegen, Germany

<sup>2</sup>IBR, Steyrergasse 17, Graz, Austria

<sup>3</sup>ELETTRA, Sincrotrone Trieste, S.S.14, km 163.5, Basovizza, 34012 Trieste, Italy

A prototype of a novel gaseous pixel detector has been developed which has already been introduced elsewhere [1,2]. Here, the latest results of the biological X-ray diffraction test measurements are presented. The detector provides in its current version an active area of 28 x 28 mm<sup>2</sup> with effectively 140 x 140 pixels. The position encoding is obtained by local interpolation using resistive charge division. This method combines the advantages of a pure pixel detector (i.e. high local and global count rates) with those of a projective system (i.e. low number of read out channels). A position resolution in the order of 300  $\mu$ m FWHM, a maximum intensity precision (due to single photon counting) and a local rate capability exceeding 1 MHz/mm<sup>2</sup> have already been demonstrated in previous measurements.

At the SAXS beamline at ELETTRA [3,4] measurements with three different biological diffraction samples have been performed using a monochromatic 8 keV beam and a camera length of 77 cm. The detector was operated with a xenon-CO<sub>2</sub> mixture at about 1.2 bar pressure which ensures for the drift length of 24 mm and the energy selected an absorption efficiency larger than 90 %, and reduces parallax sufficiently.

From the measured 2D diffraction pattern of the first sample, dry rat tail tendon collagen, the different orders of diffraction and their two-dimensional structure can clearly be detected (see Fig. 1). Unlike in case of 1D detectors this allows to determine precisely the alignment of the sample, thus excluding falsified diffraction profiles from oblique cuts. The same pattern was recorded at different fluxes proofing the intensity linearity up to a rate of 250 kHz (over the entire active area of the detector) which was the maximum rate obtained without changing the beamline optics.

A diffraction pattern of the second sample, a phospholipid, is shown in Fig. 2. Due to the limited detector area it has been composed out of 3 x 4 single images. The concentric diffraction rings up to the third order are clearly visible. The electron density which was calculated from this pattern is in good accordance with those from literature [5,6]. Eventually, the good time resolution of the detector was utilized in order to monitor the effect of radiation damage on the diffraction pattern parallel to the continuous measurement.

Finally a medium size protein crystal (unit cell:  $a = 53.3 \text{ \AA}$ ,  $b = 72.5 \text{ \AA}$ ,  $c = 72.8 \text{ \AA}$ ; space group: P2<sub>1</sub>2<sub>1</sub>2<sub>1</sub>) was selected. Oscillation patterns containing strong diffraction spots were recorded. Due to the single photon read out and storage a very high time resolution was obtained. Therefore, by knowing the constant angular speed of the sample rotation the continuously recorded data could be cut into very fine angular slices of widths as low as 0.001° allowing to determine the extremely small width of the rocking curve of 0.01° from a selected spot. In general, the fine angular slicing ability enhances distinctly the precision of the integrated intensities extracted from crystallography patterns.

Beside the demonstration of the suitability of this novel prototype detector for precise diffraction experiments also the reliability and robustness of the system have to be underlined. For the future a large scale detector is planned which would allow to record large 2D patterns with microsecond time resolutions.

- [1] H.J. Besch, M. Junk, W. Meißner, A. Sarvestani, R. Stiehler, A.H. Walenta, Nucl. Instr. and Meth. A392 (1997) 244.
- [2] A. Sarvestani, H. J. Besch, M. Junk, W. Meißner, N. Sauer, R. Stiehler, A. H. Walenta, R. H. Menk, Nucl. Instr. and Meth. A410 (1998) 238.
- [3] H. Amenitsch, M. Rappolt, M. Kirchbaum, H. Mio, P. Laggner, S. Bernstorff, J. Synchrotron Rad. 5 (1998) 506.
- [4] S. Bernstorff, H. Amenitsch and P. Laggner, J. Synchrotron Rad. 5 (1998) 1215.
- [5] V. Luzzati, A. Tardieu, D. Taupin, J. Mol. Biol. 64 (1972) 269.
- [6] K. Pressö, K. Jørgensen, P. Laggner, Bioch-Biophys. Acta 1325 (1997) 1.

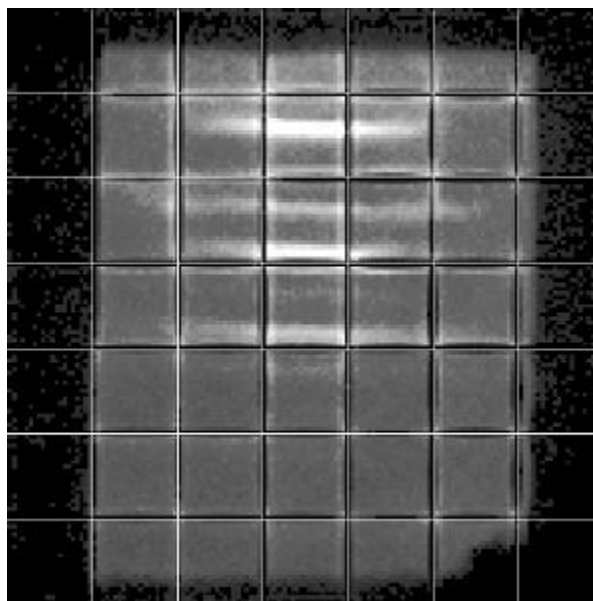


**Fig. 1.** Recorded diffraction pattern from a dry rat tail tendon collagen sample (full 28 x 28 mm<sup>2</sup> active area); the outer cells were blinded out by a collimator; the thin white lines indicate the cell borders at which slight distortions occur.

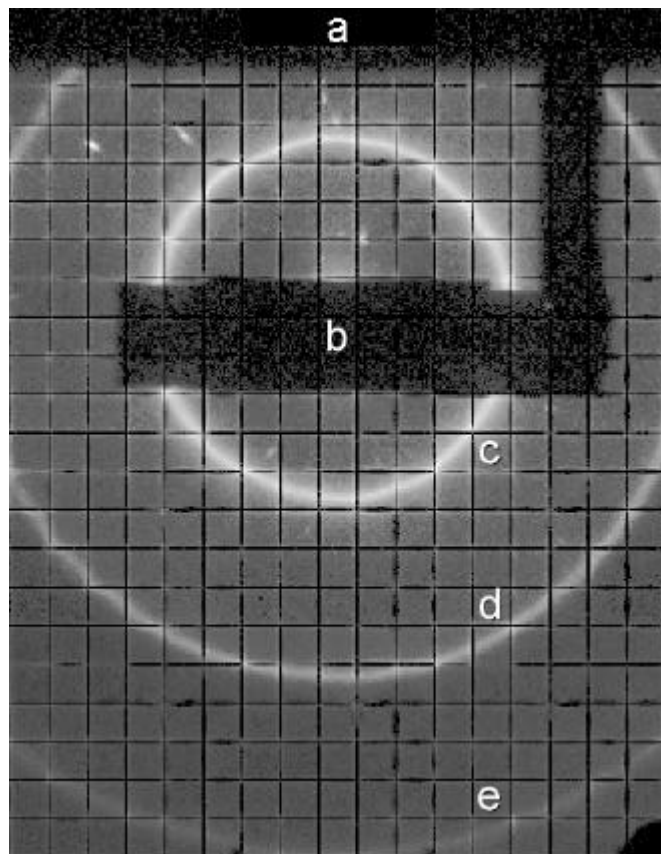


**Fig. 2.** Recorded diffraction pattern (logarithmic scale) from a phospholipid (1,2-Distearoyl-sn-Glycero-3-Phosphatidylcholin) sample; the pattern which corresponds to an area of 68 x 88 mm<sup>2</sup> (340 x 440 pixel) was acquired by composing 3 x 4 images which have been recorded separately; (a) shadow of the vacuum vessel, (b) shadow of the beam stop, (c) 1<sup>st</sup> order diffraction ring, (d) 2<sup>nd</sup> order diffraction ring, and (e) 3<sup>rd</sup> order diffraction ring. Again, at the cell borders slight distortions occur.

## SCANNING SAXS/WAXD WITH 20 mm SPATIAL RESOLUTION

I. Zizak<sup>1</sup>, O. Paris<sup>1</sup>, P. Roschger<sup>2</sup>, H. Amenitsch<sup>3</sup>, S. Bernstorff<sup>4</sup>, K. Klaushofer<sup>2</sup>, P. Fratzl<sup>1</sup>

- 1.) Erich Schmit Institut für Materialwissenschaft der ÖAW, Leoben & Institut für Materialphysik der Montanuniversität Leoben
- 2.) Ludwig Boltzmann Institut für Osteologie
- 3.) Institut für Biophysik und Röntgenstrukturforschung der ÖAW
- 4.) Sincrotrone Trieste, ELETTRA

Many complex materials providing optimized mechanical properties are hierarchically structured on different length scales down to the atomic or molecular level. Typical examples are biological tissues, such as bone, cartilage or wood. Investigation of the structure of such materials requires new experimental techniques in order to understand the interplay between mechanical properties and the structure at all levels of organization. A very promising attempt is the scanning of the specimen with a very narrow X-ray beam [1], taking SAXS (Small-Angle X-ray Scattering) and/or WAXD (Wide-Angle X-ray Diffraction) patterns for every scanning step. Such scanning experiments provide in principle structural information on three different length-scales: at the micrometer scale (absorption-image with a spatial resolution defined by the beam size), at the nanometer scale (SAXS) and/or at the scale of interatomic distances (WAXD).

In the last two years, we developed an experimental set-up at the SAXS beamline at ELETTRA, which allows us to perform extensive scans over large specimen areas in reasonable time. Using a laboratory x-ray source with pinhole geometry, the limited photon flux does not allow a reduction of the illuminated sample area below 200  $\mu\text{m}$  [1]. The high brilliance of synchrotron radiation sources opens the possibility to reduce the illuminated area to about 10  $\mu\text{m}$ . Note, that in order to obtain a certain spatial resolution, not only the beam area but also the sample thickness has to be proportionally reduced. Figure 1 shows schematically the experimental setup, we built at the SAXS beam-line at ELETTRA.

- To define the geometry of the irradiated area of the sample, we collimate the incoming X-ray beam with a set of pinholes. In most of our experiments, the size of the beam defining pinhole is 20 $\mu\text{m}$ , for strongly scattering samples it can be reduced to 10 $\mu\text{m}$ .
- The sample manipulator consists of positioning units (Newport), which perform linear motions normal to the beam with a precision of 1  $\mu\text{m}$ . A rotation of the sample around the vertical axis is also possible.
- To collect the scattering data from anisotropic samples an area detector is absolutely necessary. Since a high dynamic range is required we use a slow-scan CCD-detector (Bruker-AXS). Additionally a fast X-ray sensitive diode is used to perform a fast scanning experiment prior to the scattering experiments, monitoring only the transmission of the sample for large areas. This helps to identify the interesting regions where scattering scans are to be performed
- The whole system is fully remote controlled.

In our last visits to ELETTRA, we used this set-up to study the difference of mineral particles in bone and adjacent calcified cartilage which is described in the next contribution.

### References

- [1] Fratzl et al., *J. Appl. Cryst.* **30**, 765-769 (1997)

The project is supported by the Fonds zur Förderung der wissenschaftlichen Forschung FWF (project P11762-PHY).

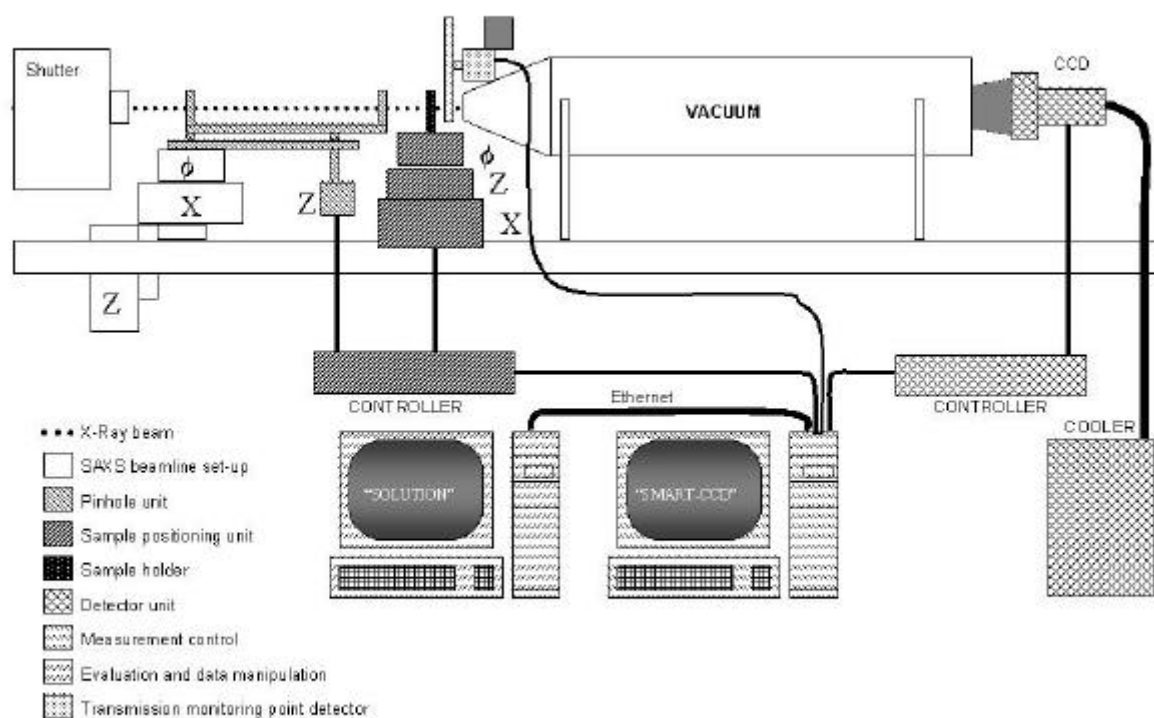


Fig. 1: Experimental set-up (Shaded are parts financed from FWF project)

# Publications

## Publications in 1998

H. Amenitsch, C.C. Ashley , M.A. Bagni , S. Bernstorff, G. Cecchi , B. Columbini and P.J. Griffiths

*Meridional X-ray diffraction intensity changes during sinusoidal length oscillations in skeletal muscle fibres of Rana temporaria.*

J.Physiol. 505 (1998) 88

H. Amenitsch, S. Bernstorff, M. Rappolt, Kriechbaum, H. Mio and P. Laggner

*First Performance Assessment of the SAXS Beamline at ELETTRA.*

J. Synchrotron Rad. 5 (1998) 506-508

S. Bernstorff, H. Amenitsch and P. Laggner

*High -Throughput Asymmetric Double-Crystal Monochromator of the SAXS Beamline at ELETTRA.*

J. Synchrotron Rad. 5 (1998) 1215-1221

H.J. Besch, M. Junk, W. Meissner, A. Sarvestani, N. Sauer, R. Stiehler, A. H. Walenta, E. Busetto, A. Lausi, R. H. Menk and R. Fourme

*Two dimensional gas pixel detectors for biological structure research.*

Proceedings of the 36th INFN ELOISATION Workshop on New Detectors, 17 November 1997, Erice, Sicily (1998)

V. Erokhin, S. Carrara, S. Bernstorff, H. Amenitsch and C. Nicolini

*Semiconductor Nanoparticles for Quantum Device.*

Nanotechnology 9 (1998) 158-161

V. Erokhin, S. Carrara, S. Guerzoni and C. Nicolini

*Synchrotron study of heat induced order in protein Langmuir-Blodgett films.*

Thin Solid Films (1998) 327-329, 636-638

P. Fratzl, K. Misof, I. Zizak, G. Rapp, H. Amenitsch and S. Bernstorff

*Fibrillar Structure and Mechanical Properties of Collagen.*

J. Structural of Biology 122 (1998) 119-122

Giacomini, Gorden, O'Neil, Van Kessel, Cason, Chapman, Lavendar, Gmur, Menk, Thomlinson, Zhong and Rubenstein

*Bronchial imaging in humans using xenon k-edge dichromography.*

NIM A 406 (1998) 473-478

T. Gog, R. Eisenhower, R.H.Menk and M.Tegze

*Multiple energy x-ray holography with atomic resolution.*

Journal of Electron Spectroscopy and related phenomena 92 (1998), 123-129

P.J. Griffiths, H. Amenitsch, C.C. Ashley, M.A. Bagni, S. Bernstorff, G. Cecchi, B. Colombini and G. Rapp

*Studies on the 14.5 nm meridional X-ray reflection during length changes of intact frog muscle fibres.*

Chapter 29 in "Mechanism of Work Production and Work Absorption in Muscle", ed. by Sugi and Pollack, Plenum Press, New York, 1998.

M. Horky, J. Baldrian, A. Sikora, M. Steinhart, P. Vlcek, H. Amenitsch and S. Bernstorff  
*Integral and nonintegral folding in poly(ethylene oxide)/poly(methyl methacrylate) blends.*  
Mater.Struct.Chem.Biol.Phys.Technol. 5 (1998) 272-273

M. Linari, M. Reconditi, L. Lucii, H. Amenitsch, S. Bernstorff, G. Piazzesi and V. Lombardi  
*Modulation of intensity of the M3 reflection by pharmacological and mechanical means in tetanized single fibres from frog skeletal muscle.*  
Pflügers Arch. 436 (1998) 18-35

M. Lohmann, H.J. Besch, W.R. Dix, O. Duenger, M. Jung and R.H. Menk  
*A high sensitive two line detector with large dynamic range for intravenous coronary angiography.*  
NIM A 419 (1998) 276-283

M. Lucic-Lavcevic, P. Dubcek, O. Milat, B. Etlinger, A. Turkovic, D. Sokcevic and H. Amenitsch  
*Nanostructure of sol-gel TiO<sub>2</sub> thin films on glass substrate measured by small angle scattering of synchrotron light.*  
Materials Letters 36 (1998) 56-60

M. Lucic-Lavcevic, A. Turkovic, D. Sokcevic, P. Dubcek, O. Milat, B. Etlinger, P. Laggner and H. Amenitsch  
*Grazing-Incidence Small Angle Scattering of Synchrotron Radiation on Nanosized TiO<sub>2</sub> Thin Films Obtained by Chemical Vapour Deposition and Spray Method.*  
Fizika A7 3 (1998) 119-132

D.V. Novikov, B. Adams, T. Heinrich, E. Kossel, G. Materlik, R.H. Menk and A. Walenta  
*X-Ray Holography for structural Imaging.*  
Journal of Synchrotron Radiation 5 (1998) 315-319

M. Rappolt, K. Pressl, G. Pabst and P. Laggner  
*L<sub>α</sub>-Phase Separation in Phosphatidylcholine-Water Systems Induced by Alkali Chlorides.*  
Biochim. Biophys. Acta 1372 (1998) 389-393

A. Sarvestani, H. J. Besch, M. Junk, W. Meissner, N. Sauer, R. Stiehler, A. H. Walenta and R. H. Menk  
*Study and Application of Hole Structures as Gas Gain Devices for Two Dimensional High Rate X-ray Detectors.*  
Nucl. Instr. and Meth. A 410 (1998) 238

A. Sarvestani, H. J. Besch, M. Junk, W. Meissner, N. Sauer, R. Stiehler, A. H. Walenta and R. H. Menk

*Gas amplifying hole structures with resistive position encoding: A new concept for a high rate imaging pixel detector.*

Nucl. Instr. and Meth. A 419 (1998) 444-451

R. Schwarzenbacher, M. Kriechbaum, H. Amenitsch and P. Laggner

*Characterization of the Nano-Structures in Liquid Crystalline Meso-Phases Present in the Ternary System Brij-35 / Dibutylether / H<sub>2</sub>O by Small- and Wide-Angle X-Ray Scattering.*

J. Phys. Chem. B 102 (1998) 9161-9167

R. Stiehler, M. Adamek, H. J. Besch, M. Junk, G. Menzel, E. Neuser, W. Meissner, A.

Sarvestani, N. Sauer, S. Volkov, A. H. Walenta and R. H. Menk

*A transient recorder system for applications in high rate detector systems.*

Nucl. Instr. and Meth. A 419 (1998) 711-714

A. Turkovic, M. Lucic-Lavcevic, A. Drasner, P. Dubcek, O. Milat, B. Etlinger, D. Sokcevic, H. Amenitsch and M. Rappolt

*Small angle X-ray scattering studies of nanophase TiO<sub>2</sub> thin films at ELETTRA.*

Materials Science & Engineering B54 (1998) 174-181.

M. Zehetbauer and P. Les

*Micromechanisms of Plastic Deformation in Metals.*

Metallic Materials 36 (3) (1998)

### **Publications until March 1999**

J. Baldrian, M. Horky, A. Sikora, M. Steinhart, P. Vlèek, H. Amenitsch and S. Bernstorff

*Time-resolved SAXS study of crystallization of poly (ethylene oxide) / poly (methyl methacrylate) blends.*

Polymer 40 (1999) 439-445

G. Balducci, L. Lucii, M. Linari, M. Reconditi, H. Amenitsch, S. Bernstorff, G. Piazzesi and V. Lombardi

*Structural aspects of after-stretch potentiation studied by time-resolved X-ray diffraction on single frog muscle fibers.*

Biophys. J. 76, A33/Su-Pos9, 1999

P. Laggner, H. Amenitsch, S. Bernstorff, P. Dubcek, M. Kriechbaum, R.H. Menk, M. Rappolt and G. Pabst

*Die Österreichische Kleinwinkelstation bei ELETTRA: Status und Experimente-Kinematographische Erfassung von Makromolekülen.*

Mitteilungsblatt der Österreichischen Physikalischen Gesellschaft, Nr. 1, p. 13-18, January 1999

M. Zehetbauer, T. Ungar, R. Kral, A. Borbely, E. Schafner, B. Ortner, H. Amenitsch and S. Bernstorff

*Scanning X-ray Diffraction Peak Profile Analysis in Deformed Copper Polycrystals by Synchrotron Radiation.*

Acta mater. 47 (1999) 1053

## **Publications, submitted**

P. Ågren, M. Lindén, J.B. Rosenholm, R. Schwarzenbacher, M. Kriechbaum, H. Amenitsch, P. Laggner, J. Blanchard and F. Schüth  
*Kinetics of Co-surfactant – Surfactant – Silicate Phase Behavior. 1. Short-chain Alcohols.*  
Submitted to J. Phys. Chem

P. Ågren, M. Lindén, J.B. Rosenholm, J. Blanchard, F. Schüth, R. Schwarzenbacher, M. Kriechbaum, H. Amenitsch and P. Laggner  
*Kinetics of Co-surfactant – Surfactant – Silicate Phase Behavior. 2. Short-chain Amines.*  
Manuscript in preparation.

H. Amenitsch, S. Bernstorff, A. Bigi, N. Roveri and J.S. Shah  
*D-Periodicity in Intramuscular Collagen.*  
Connective Tissue Research, in preparation.

H.Amenitsch, M. Kriechbaum, D. Lombardo, H. Mio, G. Pabst, M.Rappolt, P.Laggner and S. Bernstorff  
*The Small Angle X-Ray Scattering Beamline at ELETTRA: A New Powerful Station for Fast Structural Investigations on Complex Fluids with Synchrotron Radiation.*  
Nuovo Cimento, in press

J. Baldrian, M. Horky, M. Steinhart, A. Sikora , P. Vlcek, H. Amenitsch and S.Bernstorff  
*Time-resolved SAXS/WAXS study of polymer blend crystallization.*  
SPIE Proceedings of „4th Internat. Workshop on X-Ray Investigations of PolymerStructure, XIPS'98“, in print

T. Javorfi, Z. Cseh, I. Simidjiev, S. Borbely, H. Amenitsch, P. Laggner and G. Garab  
*Structure and dynamics of thylakoid membranes and lamellar aggregates of LHCII.*  
in prep.

P. Laggner, H. Amenitsch, M. Kriechbaum, G. Pabst and M. Rappolt  
*Trapping of Short-Lived Intermediates in Phospholipid Phase Transitions: The  $L_a^*$  Phase.*  
Faraday Discuss.111, in press.

R.H. Menk  
*Interface imaging and it's application to material and medical imaging.*  
Nucl. Instr. Meth. B, submitted.

R.H. Menk, F. Arfelli, S.Bernstorff, D. Pontoni, A.Sarvestani, H.J. Besch and A.H.Walenta  
*A fast 1-D detector for imaging and time resolved SAXS experiments.*  
Nucl. Instr. Meth. A , in press.

A. Sarvestani, H.J. Besch, R.H. Menk, N. Pavel, N. Sauer, C. Strietzel and A.H. Walenta  
*Study of the high rate performance of the MicroCAT detector.*  
Proceedings of the 6th International Conference of Advanced Technology in Particle Physics, Villa Olmo, Como, Italy, 5 - 9 Oct. 1998  
subm. to Nucl. Instr. and Meth. B (1998)



E. Schafler, M. Zehetbauer, P. Hanak, T. Ungar, T. Hebesberger, R. Pippan, B. Mingler, H.P. Karnthaler, S. Bernstorff and H. Amenitsch

*Fragmentation in Large Strain Cold Rolled Aluminium as observe by Synchrotron X-Ray Bragg Peak Profile Analysis (SXPA), Electron Back Scatter Diffraction (EBSD) and Transmission Electron Microscopy (TEM).*

Proc. NATO Adv.Res.Workshop "Investigations and Applications of Severe Plastic Deformation", Aug. 2-6 (1999, Moscow, Russia); to be published

E. Schafler, M. Zehetbauer, I. Kopacz, B. Ortner, S. Bernstorff, H. Amenitsch and T. Ungar  
*Local Dislocation Densities and Internal Stresses by High Lateral Resolution Peak Profile Analysis in Plastically Deformed Polycrystalline Nickel.*

Scripta Mater., in preparation

E. Schafler, M. Zehetbauer, I. Kopacz, I. Altpeter, B. Ortner, H. Amenitsch, S. Bernstorff and T. Ungar

*Messungen der Verteilung von Versetzungsdichten und inneren Spannungen in plastisch verformtem Ni mittels hochauflösender Synchrotron-Linienprofil-Analyse und magnetischer Mikroskopie.*

Scripta Mater., in preparation

M. Steinhart, M. Kriechbaum, K. Pressl, H. Amenitsch, P. Laggner and S. Bernstorff  
*High-Pressure Instrument for Small- and Wide-Angle X-ray Scattering. II: Time-Resolved Experiments.*

Rev. Sci. Instrum., submitted

A. Turkovic, P. Dubcek, Z. Crnjak-Orel and S. Bernstorff  
*Small angle scattering of synchrotron radiation on nanosized CeO<sub>2</sub> and CeO<sub>2</sub>-SnO<sub>2</sub> thin films obtained by sol-gel dip-coating method.*

Nanostructured Materials, in print

A. Turkovic, P. Dubcek, M. Gotic and S. Bernstorff  
*Grazing-incidence small-angle and wide-angle scattering of synchrotron radiation on nanosized CeO<sub>2</sub> thin films.*

Materials Science & Engineering B, in print

### **International Conferences and Workshops in 1998**

P. Ågren, M. Lindén, J.B. Rosenholm, J. Blanchard, F. Schüth, R. Schwarzenbacher, M. Kriechbaum, H. Amenitsch and P. Laggner  
*Real time study of the formation of ordered inorganic materials from organized molecular assemblies by in situ synchrotron SAXS.*

Spring seminar of the Graduate School of Materials Research, Turku, Finland, 3.6. 1998.

Poster presentation.

P. Ågren, M. Lindén, J. B. Rosenholm, R. Schwarzenbacher, M. Kriechbaum, H. Amenitsch, P. Laggner, J. Blanchard and F. Schüth

*In-Situ Synchrotron SAXS Study of the Formation of MCM-41 and MCM-50.*

18th European Crystallographic Meeting, Prague, Czech Republic, August 15-20, 1998, Poster presentation

P. Ågren, M. Lindén, J.B. Rosenholm, J. Blanchard, F. Schüth, R. Schwarzenbacher, M. Kriechbaum, H. Amenitsch and P. Laggner.

*In situ synchrotron SAXS study of the formation of MCM-41 and MCM-50.*

YKS-PKS Symposium, Helsinki, Finland, September 1998. Poster presentation.

P. Ågren, M. Lindén, J.B. Rosenholm, J. Blanchard, F. Schüth, R. Schwarzenbacher, M. Kriechbaum, H. Amenitsch, S. Bernstorff and P. Laggner

*Time resolved SAXS study of MCM-41 and MCM-50 in the phase of formation.*

Sixth User's Meeting, Sincrotrone Trieste, Trieste, Italy, November 30 – December 1, 1998.

Poster presentation.

P. Ågren, M. Lindén, J.B. Rosenholm, J. Blanchard, F. Schüth, R. Schwarzenbacher, M. Kriechbaum, H. Amenitsch and P. Laggner

*Kinetic study of the non-equilibrium co-surfactant- surfactant - silicate system.*

Autumn seminar of the Graduate School of Materials Research, Turku, Finland, 16.12. 1998.

Oral presentation.

H. Amenitsch

*SAXS Station at ELETTRA.*

Atominstut der Österreichischen Universitäten, 7.12.98

H. Amenitsch, C.C. Ashley, M.A. Bagni, S. Bernstorff, G. Cecchi, B. Colombini and P.J.Griffiths

*High time resolution X-ray diffraction measurements in living skeletal Muscle Cells of Frog.*

6th ELETTRA Users' Meeting, Trieste, Italien, 30.11.-1.12.98, Poster

H. Amenitsch, G. Balducci, S. Bernstorff, M. Linari, V. Lombardi, L. Lucii and G. Piazzesi  
*Mechanical and structural evidence for the mechanism of enhancement of force and shortening capability after stretch of active muscle.*

VI Convegno SILS Padova, 18-20 Giugno 1998

H. Amenitsch, S. Bernstorff, P. Dubcek, M. Kriechbaum, R. Menk, G. Pabst, M. Rappolt, R. Schwarzenbacher, M. Steinhart and P. Laggner

*Real-Time Monitoring of Macromolecular Assemblies in the State of Formation or Transition by Small- and Wide-Angle X-Ray Scattering (SWAXS) at ELETTRA.*

18th European Crystallographic Meeting, Prague, Czech Republic, August 15-20, 1998

H. Amenitsch, S. Bernstorff, P. Dubcek, M. Kriechbaum, R. Menk, G. Pabst, M. Rappolt, R. Schwarzenbacher and P. Laggner.

*Echtzeiterfassung von Makromolekülen im Zustand der Entstehung oder Transformation mit gleichzeitiger Klein- und Weitwinkelstreuung bei ELETTRA.*

Österreichische Physikalische Gesellschaft. 48th Annual Meeting 14.-18.9.1998. University of Graz, Austria.

H. Amenitsch, S. Bernstorff, M. Linari, V. Lombardi, L. Lucii, G. Piazzesi and E. Vannicelli.  
*Structural aspects of after-stretch potentiation studied by time-resolved X-ray diffraction on single fibres from frog skeletal muscle.*

6th ELETTRA Users' Meeting, Trieste, Italien, 30.11.-1.12.98, Poster

H. Amenitsch, R. Schwarzenbacher, M. Kriechbaum, P. Agren und P. Laggner  
*Statische und dynamische Roentgenstrukturuntersuchungen an Fluessigkristallen und MCM-41 nanokristallinen Phasen.*

48. Jahrestagung ÖPG, Graz, 14.-18.9.98, Vortrag

F. Arfelli, V. Bonvichini, A. Bravin, G. Cantatore, E. Castelli, L. Dalla Palma, M. Di Michele, R. Longo, R.H. Menk, A. Olivo, S. Pani, D. Pontoni, P. Poropat, M. Prest, L. Rigon, L. Rashevsky, G. Tromba, A. Vacchi and E. Vallazza,

*Diffraction imaging with Si analyzer crystal at Elettra.*

6th ELETTRA Users' Meeting, Trieste, Italien, 30.11.-1.12.98, Poster

J. Baldrian, M. Horky, M. Steinhart, A. Sikora, P. Vlèek, H. Amenitsch and S. Bernstorff

*Time-resolved SAXS/WAXS study of polymer blends crystallization.*

4th International Workshop on X-Ray Investigations of Polymer Structure XIPS98, Bielsko-Biala, Poland, 2-5 December, 1998, invited lecture

G. Balducci, L. Lucii, M. Linari, M. Reconditi, H. Amenitsch, S. Bernstorff, G. Piazzesi and V. Lombardi

*Structural aspects of after-stretch potentiation studied by time resolved X-ray Diffraction on single fibres from frog skeletal muscle.*

6th ELETTRA Users' Meeting, Trieste, Italien, 30.11.-1.12.98, Poster

S. Bernstorff

*Small and wide angle X-ray scattering at third generation synchrotron radiation centers: detector requirements for medical, biological and industrial applications.*

Satellite workshop of the Vienna Wire chamber conference, Vienna, Austria, 28.02.98, Talk

H.J. Besch, M. Junk, W. Meißner, A. Sarvestani, N. Sauer, R. Stiehler, A.H. Walenta, E. Busetto, A. Lausi, R.H. Menk and R. Fourme.

*Two-dimensional gas pixel detectors for biological structure research.*

36th INFN Eloisation Workshop on New Detectors. Erice, Sicily 1.-7. Nov. 1998.

S. Carrara, V. Erokhin and C. Nicolini

*Protein Langmuir-Blodgett Films Induced Order.*

6th ELETTRA Users' Meeting, Trieste, Italien, 30.11.-1.12.98, Poster

S. Carrara, V. Erokhin and C. Nicolini

*New materials for bioelectronics.*

I National Congress of National Institute of Biosystems and Biostructures (INBB), Venice, 25-28/12/98

A. Cesaro, D. Fabri, F. Sussich, G. Paradossi, H. Amenitsch and S. Bernstorff

*Thermal Behaviour of poly-hydroxybutyrate gels: a calorimetric and small angle X-ray scattering study.*

6th ELETTRA Users' Meeting, Trieste, Italien, 30.11.-1.12.98, Poster

P. Dubcek, B. Pivac, S. Bernstorff, H. Amenitsch, R. Tonini, F. Corni and G. Ottaviani

*Grazing Incidence Small Angle X-Ray Scattering Study of Irradiation Induced Defects in Silicon.*

18th European Crystallographic Meeting, Prague, Czech Republic, August 15-20, 1998,  
Poster

P. Dubcek, A. Turkovic, B. Etlinger, O. Milat, M. Lucic-Lavcevic, S. Bernstorff and H. Amenitsch

*Small Angle X-ray Scattering Study of TiO<sub>2</sub> of Thin Films at Grazing Angles.*

18th European Crystallographic Meeting, Prague, Czech Republic, August 15-20, 1998,  
Poster

P. Dubcek, A. Turkovic, B. Etlinger, O. Milat, M. Lucic-Lavcevic, S. Bernstorff and H. Amenitsch

*Small Angle X-ray Scattering Study of TiO<sub>2</sub> Thin Films at Grazing Angles.*

6th ELETTRA Users' Meeting, Trieste, Italien, 30.11.-1.12.98, Poster

A. Gamini, S. Paoletti, K. Bongaerts, E. Theunissen, H. Reynaers, H. Amenitsch and S. Bernstorff  
*SAXS Study on thermoreversible k-carrageenan gels by synchrotron radiation.*

6th ELETTRA Users' Meeting, Trieste, Italien, 30.11.-1.12.98, Poster

H. Grigoriew, A. G. Chmielewski, H. Amenitsch, S. Bernstorff and J. Domagala

*Time-resolved measurements of the system: cellulose membrane-water.*

6th European Powder Diffraction Conference (EPDIC-6), Budapest, Hungary, 22-25 .8.1998

A. Gupta, N. Bhagat, B. A. Dasannacharya, P. S. Goyal, G. Principi, A. Maddalena, H. Amenitsch and S. Bernstorff

*Study of nanocrystalline alloys produced by current annealing.*

6th ELETTRA Users' Meeting, Trieste, Italien, 30.11.-1.12.98, Poster

M. Horky, J. Baldrian and M. Steinhart

*Crystallization of poly(ethylene oxide)/poly(methyl methacrylate) mixtures*

*2nd Seminar: Student and Postgraduate Papers on Crystallography and Structure Analysis.*  
Prague 1997

Mater. Struct. Chem. Biol. Phys. Technol. 4(1997)25 Abstract (in Czech)

M. Horky, J. Baldrian, A. Sikora, M. Steinhart, P. Vlček, H. Amenitsch and S. Bernstorff

*Integral and nonintegral chain folding in poly(ethylene oxide) / poly(methyl methacrylate) blends.*

18th European Crystallographic Meeting, Prague, Czech Republic, August 15-20, 1998,  
Poster

M. Horky, J. Baldrian and M. Steinhart

*Crystallization of blends poly(ethylene oxide)/poly(methyl methacrylate).*

7th Annual Workshop 98, Technical University Prague 1998,

Proceedings p.489

M. Iacussi et al.

*Complessi Ternari DNA-Liposomi-Me<sup>++</sup>.*

XVII Convegno Interregionale Toscano-Umbro-Marchigiano-Abruzzese, Numana (AN),  
Italy, June 8-10 (1998)

M. Kriechbaum, M. Steinhart, P. Laggner, Y. Hiragi, H. Amenitsch and S. Bernstorff

*Time-resolved small-angle X-ray scattering of jump-relaxation and stopped-flow experiments of lipids and proteins.*

18th European Crystallographic Meeting, Prague, Czech Republic, August 15-20, 1998

M. Kriechbaum, P. Laggner, Y. Hiragi, H. Amenitsch and S. Bernstorff

*Time-Resolved Small-Angle X-Ray Scattering of Stopped-Flow Experiments of Protein Denaturations.*

6.Internatl.Conf. on Biophys. & Synchr. Radiation, Argonne, Illionois, USA, 4.-8..8.98, Poster

M. Kriechbaum, M. Steinhart, P. Laggner, H. Amenitsch and S. Bernstorff

*Time-Resolved Small-Angle X-Ray Scattering Studies of Pressure-Jump Induced Barotropic Phase Transitions of Lipids.*

6.Internatl.Conf. on Biophys. & Synchr. Radiation, Argonne, Ill. USA, 4.-8..8.98, Poster

M. Kriechbaum, M. Steinhart, P. Laggner, H. Amenitsch and S. Bernstorff

*Time-Resolved Small-Angle X-Ray Scattering Studies of Pressure-Jump Induced Barotropic Phase Transitions of Lipids.*

18th European Crystallographic Meeting, Prague, Czech Republic, August 15-20, 1998

M. Kriechbaum, P. Laggner, Hiragi, H. Amenitsch and S. Bernstorff

*Time-Resolved Small-Angle X-Ray Scattering Studies of Protein Denaturations Studied by Stopped-Flow Technique.*

6th ELETTRA Users' Meeting, Trieste, Italien, 30.11.-1.12.98, Poster

P. Laggner

*Die Synchrotronlichtquelle ELETTRA / Triest – Eine Großforschungsanlage mit Wirkung auf Österreich.*

"Auf nach Triest", Graz, 27.3.98, Vortrag

P. Laggner

*Röntgen-Videoclips über die Dynamische Formbildung aus Supramolekularen Lipid- und Tensidsystemen.*

Mini-Symposium GÖCH, Graz 16.4.98, Vortrag

P. Laggner

*New Frontiers in SAXS.*

18th European Crystallographic Meeting, Prague, Czech Republic, August 15-20, 1998, Vortrag

P. Laggner

*Small-Wide Angle X-Ray Scattering as a Tool in Thermoanalysis.*

3. Öst.Polymertage, Graz, 10.9.98, Vortrag

P. Laggner

*Stable and Transient States of Phospholipid Hydration.*

Int. Symp. on Self-Assembly of Amphiphilic Systems Dresden, BRD, 14.-18.9.98, Vortrag

P. Laggner, K. Pressl, G. Pabst, M. Rappolt and H. Amenitsch

*Stable and Transient States of Phospholipid Hydration.*

ECCS Summer School, Dubrovnik, Kroatien, 21.-25.9.98, Vortrag

P. Laggner

*Trapping of Short-Lived Intermediates in Phospholipid Phase Transition.*

Faraday Discussion No. 111, Bristol, U.K., 16.-18.12.98, Vortrag

P. Laggner

*New Frontiers in SAXS.*

4. Intern.School XIPS'98, Bielsko-Biala, Polen, 22.-5.12.98, Vortrag

P. Laggner, H. Amenitsch, S. Bernstorff, P. Dubcek, G. Pabst, M. Rappolt, A. Savoia, E. Busetto, L. Olivi, F. Zanini and A. Lausi

*Diffraction opportunities at ELETTRA.*

Workshop India-Italy on Utilisation of ELETTRA Synchrotrone, Calcutta, India, 10.11-13.11.98, Vortrag

E. Maccioni, P. Mariani, F. Spinozzi, S. Beretta, G. Chirico

*A SAXS study of association of BLG.*

6th ELETTRA Users' Meeting, Trieste, Italien, 30.11.-1.12.98, Poster

S. Mazumder, I.S. Batra, R. Tewari, S. Banerjee, A. Sequeira, H. Amenitsch and S. Bernstorff  
*Simple Temperature Dependent Phase Separation Behavior of a multicomponent Complex Alloy.*

6th ELETTRA Users' Meeting, Trieste, Italien, 30.11.-1.12.98, Poster

R.H. Menk

*Silicon detectors and their application to synchrotron and FEL experiments.*

Invited talk at the semiconductor seminar at DESY, Hamburg, Germany, 21.01.98

R.H. Menk

*New detector systems for novel imaging modalities.*

Invited talk at the satellite workshop of the Vienna Wire chamber conference, Vienna, Austria, 28.02.98

R.H. Menk, F. Arfelli, S. Bernstorff, A. Sarvestani, H.J. Besch and A.H. Walenta

*A fast 1-D detector for imaging and time resolved SAXS experiments.*

Symposium on: "Radiation Measurements and Applications", Ann Arbor, Michigan, USA, May 12-14, 1998

R.H. Menk

*Recent detector development at ELETTRA.*

Invited talk at the detector seminar at Brookhaven National Lab, New York, USA, 29.05.98

R.H. Menk

*Interference imaging and their applications to medical and material imaging.*

Invited talk at the 6th International Conference on Advanced Technology and Particle Physics Villa Olmo, Como, Italy, 5-9 October 1998 (8.10.98)

F.A. Sarvestani, H.J. Besch, R.H. Menk, N. Pavel, N. Sauer, C. Strietzel and A.H. Walenta

*Study of the high rate performance of the MicroCAT detector.*  
Proceedings of the 6th International Conference of Advanced Technology in Particle Physics,  
Villa Olmo, Como, Italy, 5 - 9 Oct. 1998

R.H. Menk

*Diffraction enhanced imaging.*

Invited talk at the Physik Kolloquium at the Universitaet Siegen, Germany, 5. 13.11.98

R.H. Menk, F. Arfelli, H. Amenitsch, S. Bernstorff, H.J. Besch, D. Pontoni, A. Sarvestani and  
A.H. Walenta

*A fast 1-d detector for imaging and time resolved SAXS experiments.*

Symposium on: "Radiation Measurements and Applications", Ann Arbor, Michigan, USA,  
May 12-14, 1998

R.H. Menk, F. Arfelli, H. Amenitsch, S. Bernstorff, H.J. Besch, D. Pontoni, A. Sarvestani and  
A.H. Walenta

*An integrating detector with single photon resolution for SAXS experiments.*

6th ELETTRA Users' Meeting, Trieste, Italien, 30.11.-1.12.98, Poster

T. Nawroth, I. Lauer, M. Rössle, H. Heumann, G. Goerigk, H. Amenitsch, S. Bernstorff, P.  
Boesecke, T. Narayanan and O. Diat

*Structural film of working FIATPase and ATP-synthase by time-resolved X-ray scattering.*

2nd Intern. Workshop on ATP-synthase and V-ATPase, 14.-18.5.1998, Osnabrück,  
proceedings FM7

T. Nawroth, I. Lauer, A. Neidhardt, K. Zwicker, O. Diat, T. Narayanan, P. Boesecke, H.  
Amenitsch, S. Bernstorff, M. Rössle and H. Heumann

*Structural film of working FIATPase and ATP-synthase obtained by time-resolved X-ray  
scattering of solution.*

Jahrestagung der Deutschen Gesellschaft für Biophysik, 21.-23.9.1998, Frankfurt/M.,  
proceedings 109

G. Pabst, M. Rappolt, H. Amenitsch, S. Bernstorff and P. Laggner.

*Realtime X-Ray Diffraction Studies of the Kinetics of Phase Transitions in Phospholipids.*

Scuola "Luce di Sincrotrone", Sardinien, Italy, Sept. 1998, Poster

G. Pabst, M. Rappolt, H. Amenitsch, S. Bernstorff and P. Laggner.

*Echtzeit Röntgendiffraktion zur Untersuchung der Kinetik von Phospholipid*

*Phasenübergängen.*

Österreichische Physikalische Gesellschaft. 48th Annual Meeting 14.-18.9.1998. University  
of Graz, Austria.

G. Pabst, M. Rappolt, H. Amenitsch, S. Bernstorff and P. Laggner

*Realtime X-Ray Diffraction Studies on the Formation of Intermediates in Phospholipids*

*Induced by Laser T-Jump.*

7th Annual CCP13/NCD Workshop, Daresbury / U.K., 12.-14.5.98

G. Pabst, M. Rappolt, H. Amenitsch, S. Bernstorff and P. Laggner

*Non-Equilibrium Perturbation Response-Kinetics of Phospholipid Bilayers in the Biologically  
Relevant  $L_{\alpha}$ -Phase.*

Faraday Discussion 111, Bristol, U.K. 16.-18.12.98, Poster

G. Pabst, M. Rappolt, H. Amenitsch, S. Bernstorff and P. Laggner  
*Non-Equilibrium Perturbation Response-Kinetics of Phospholipid Bilayers in the Biologically Relevant  $L_a$ -Phase.*

6th ELETTRA Users' Meeting, Trieste, Italien, 30.11.-1.12.98, Poster

M. Pisani, L. Saturni, P. Mariani and R. Caciuffo  
*The Effects of Hydrostatic Pressure on the Monoolein-Water.*

6th ELETTRA Users' Meeting, Trieste, Italien, 30.11.-1.12.98, Poster

M. Pregetter, H. Amenitsch, S. Bernstorff, R. Prassl and P. Laggner  
*Time-resolved x-ray diffraction of the core lipid transition of human Low Density Lipoproteins.*

6th ELETTRA Users' Meeting, Trieste, Italien, 30.11.-1.12.98, Poster

M. Rappolt

Forum Cosmeticum 19.-20.02.1998. SCC, DGK, GöCH. Roche Congress-Center, Basel, Switzerland. (passive participant).

M. Rappolt, H. Amenitsch, S. Bernstorff and P. Laggner.  
*Highly Resolving ( $< 10$  mK) Temperature-Gradient-Cell for X-ray Scattering Studies on Solutions.*

Österreichische Physikalische Gesellschaft. 48th Annual Meeting 14.-18.9.1998. University of Graz, Austria.

M. Rappolt, H. Amenitsch, S. Bernstorff and P. Laggner  
*Highly Resolving ( $< 10$  mK) Temperature-Gradient-Cell for X-Ray Scattering Studies on Solutions.*

6th ELETTRA Users' Meeting, Trieste, Italien, 30.11.-1.12.98, Poster

M. Roessle, E. Manakova, I. Lauer, T. Nawroth, S. Bernstorff, H. Amenitsch and H. Heumann

*Time resolved small angle scattering on motor proteins: The chaperonin system GroEL and GroES.*

6th ELETTRA Users' Meeting, Trieste, Italien, 30.11.-1.12.98, Poster

A. Sarvestani, M. Adamik, H. Amenitsch, S. Bernstorff, H.J. Besch, M. Junk, W. Meissner, R.H. Menk, A. Orthen, G. Pabst, N. Pavel, M. Rappolt, N. Sauer, R. Stiehler and A.H. Walenta

*A novel gaseous 2-d pixel detector for biological x-ray diffraction.*

6th ELETTRA Users' Meeting, Trieste, Italien, 30.11.-1.12.98, Poster

A. Sarvastani, H. Amenitsch, H.J. Bensch, S. Bernstorff, R.H. Menk, A. Orthen, N. Sauer and A.H. Walenta

*A two dimensional single photon counting pixel detector for modern SAXS experiments.*

6th ELETTRA Users' Meeting, Trieste, Italien, 30.11.-1.12.98, Poster

E. Schafler, M. Zehetbauer, I. Kopacz, I. Altpeter, B. Ortner, H. Amenitsch, S. Bernstorff and T. Ungar



*Messungen der Verteilung von Versetzungsdichten und inneren Spannungen in plastisch verformtem Ni mittels hochauflösender Synchrotron-Linienprofil-Analyse und magnetischer Mikroskopie.*

Annual Meeting of the Austrian Physical Society, Graz, Austria, Sept. 1998

R. Schwarzenbacher, K. Zeth, A. Gries, M.J. Chapman, R. Prassl and P. Laggner  
*Crystallization and Crystallographic Studies of the Human Plasma Lipoproteins, Low Density Lipoprotein (LDL) and Apolipoprotein-H.*

18th European Crystallographic Meeting, Prague, Czech Republic, August 15-20, 1998

R. Schwarzenbacher, K. Zeth, A. Gries, M. J. Chapman, R. Prassl and P. Laggner  
*Crystallization and Crystallographic Studies of the Human Plasma Lipoproteins, Low Density Lipoprotein (LDL) and Apolipoprotein-H.*

6th ELETTRA Users' Meeting, Trieste, Italien, 30.11.-1.12.98, Poster

A. Sarvestani, H.J. Besch, R.H. Menk, N. Pavel, C. Strietzel and A.H. Walenta

*Study of the high rate performance of the MicroCAT detectors.*

6th International Conference on Advanced Technology in Particle Physics. Villa Olmo. Como 5.-9. Oct. 1998.

E. Schafler, M. Zehetbauer, I. Kopacz, I. Altpeter, B. Ortner, H. Amenitsch, S. Bernstorff and T. Ungar

*Messungen der Verteilung von Versetzungsdichten und inneren Spannungen in plastisch verformtem Nickel mittels hochauflösender Synchrotron-Linienprofilanalyse und magnetischer Mikroskopie.*

48. Jahrestagung ÖPG, Graz, 14.-18.9.98, Poster

E. Schafler, M. Zehetbauer, T. Ungar, A. Borbely, R. Kral, B. Ortner, H. Amenitsch and S. Bernstorff

*Scanning X-Ray Diffraction Profile Analysis of Large Strain Deformed Cu by Synchrotron Radiatio.*

European Research Conference "Plasticity of Materials", Granada, Spain, April 25-30, 1998

M. Steinhart, M. Kriechbaum, M. Horiky, J. Baldrian, H. Amenitsch and P. Laggner

*Time-Resolved SWAXS Measurements of Effects Induced by Variation of Pressure.*

18th European Crystallographic Meeting, Prague, Czech Republic, August 15-20, 1998

M. Steinhart, M. Kriechbaum, H. Amenitsch and P. Laggner

*Time-Resolved SWAXS Measurements of Effects Induced by Variations of Pressure.*

ECM-18, Prag, Tschechien, 16.-20.8.98, Vortrag

A. Turkovic, M. Lucic-Lavcevic, D. Sokcevic, A. Drasner, P. Dubcek, O. Milat, B. Etlinger and H. Amenitsch

*Studij rasprsenja X-zraka pod malim kutem na nanofaznim TiO<sub>2</sub> tankim filmovima na ELETTRA.*

Zbornik sazetaka s V Susreta vakuumista Hrvatske i Slovenije, 20.05.1998., Institut "Ruder Boskovic", p.15-16, Lecture

A. Turkovic, P. Dubcek, Z. Crnjak-Orel and S. Bernstorff

*Grazing-incidence small-angle scattering of synchrotron radiation on nanosized CeO<sub>2</sub> and CeO<sub>2</sub>-SnO<sub>2</sub> thin films obtained by sol-gel dip-coating method.*

6th ELETTRA Users' Meeting, Trieste, Italien, 30.11.-1.12.98, Poster

A. Turkovic, M. Lucic-Lavcevic, O. Milat, P. Dubcek, S. Burnside, M. Gratzel and S. Bernstorff

*Rocking-angle scattering of synchrotron radiation on nanosized TiO<sub>2</sub> ordered and acidified thin films.*

6th ELETTRA Users' Meeting, Trieste, Italien, 30.11.-1.12.98, Poster

T. Ungar and M. Zehetbauer

*Internal Stresses and Microstructure at Large Strains in Cell-Forming Materials.*

European Research Conference "Plasticity of Materials", Granada, Spain, April 25-30, 1998, invited lecture

M. Zehetbauer

*Features & Models of Strengthening at Large Plastic Deformations.*

Institut f. Metallkunde u. Metallphysik, Rheinisch-Westfaelische Technische Hochschule, Aachen, Germany, Januar 1998, invited talk

M. Zehetbauer

*Micromechanisms of Plastic Deformation in Metals.*

2nd Intern.Coll."Materials Structure & Micromechanics of Fracture", (MSMF-2), Brno, Czech Republic, July 1-3, 1998, invited lecture

M. Zehetbauer

*Phaenomene und Modellierung der Verfestigung von Metallen bei starker plastischer Verformung.*

Institut f. Kristallographie und Festkoerperphysik, Technische Universitaet Dresden  
November 1998, invited talk

M. Zehetbauer, T. Ungar, E. Schafler, I. Kopacz, P. Hanak, I. Altpeter, S. Bernstorff and H. Amenitsch

*Investigation of Microstructure of Plastically Deformed Ni by means of Scanning X-Ray Bragg Peak Profile Analysis and Magnetic Microscopy.*

6th ELETTRA Users' Meeting, Trieste, Italien, 30.11.-1.12.98, Poster

I. Zizak, K. Misof, S. Bernstorff, H. Amenitsch and P. Fratzl,

*Struktur und Mechanische Eigenschaften von Kollagen.*

Institutseminar, Erich Schmid Institut, Leoben 17. 3. 1998, Vortrag

I. Zizak, K. Misof, S. Bernstorff, H. Amenitsch and P. Fratzl

*Struktur und mechanische Eigenschaften von Kollagen.*

48. Jahrestagung der ÖPG, 14-18. 9. 1998 Graz, Poster

I. Zizak, K. Misof, P. Roschger, H. Amenitsch, S. Bernstorff and P. Fratzl

*Scanning SAXS und WAXS investigations of bone-cartilage interface.*

Kampftseminar, Kapfenstein 26.9.1998, Vortrag

I. Zizak, K. Misof, P. Roschger, G. Rapp, H. Amenitsch, S. Bernstorff, D.J.S. Hulmes and P. Fratzl

*Synchrotron X-Ray Scattering Studies of the Elastic Properties of Type I Collagen.*  
6th ICCBMT, Vittel, 1.-6.11.1998, Poster

I. Zizak, O. Paris, P. Roschger, H. Amenitsch, S. Bernstorff and P. Fratzl

*Scanning SAXS and WAXS investigations of bone cartilage interfaces.*  
6th ELETTRA Users' Meeting, Trieste, Italien, 30.11.-1.12.98, Vortrag

### **Non-refereed Publications in 1998**

H. Amenitsch, C.C. Ashley, M.A. Bagni, S. Bernstorff, G. Cecchi, B. Colombini and P.J.Griffiths

*16 micro-second time resolution X-ray diffraction measurements in living skeletal muscle cells of the frog at the SAXS beamline of Elettra.*

ELETTRA News Number II, Number 26, August 31 (1998)

P.Fratzl, K. Misof, I. Zizak, G. Rapp, H. Amenitsch, S. Bernstorff

*In-situ Synchrotron X-Ray Scattering Study of the Tensile Properties of Collagen.*

ELETTRA News Number II, Number 25, July 30 (1998)

ELETTRA Highlights (1998)

M. Kriechbaum, P. Laggner, M. Steinhart, C. Krenn, H. Amenitsch, S. Bernstorff, G. Pabst and M. Rappolt

*300 MPa Jump-Relaxation Studies of Phase Transitions Investigated by Time-Resolved Small-Angle X-Ray Scattering in the ms range.*

ELETTRA Highlights (1998)

M. Kriechbaum, P. Laggner, M. Steinhart, C. Krenn, H. Amenitsch, S. Bernstorff, G. Pabst and M. Rappolt

*300 MPa p-Jump and 10 deg C T-Jump Relaxation Studies of Phase Transitions in Phospholipids Investigated by Time-Resolved Small-Angle X-Ray Scattering in the ms Range.*

ELETTRA News Number: 27 - September 30, 1998

G. Pabst, H. Amenitsch, C. Krenn, M. Rappolt, P. Laggner and S. Bernstorff

*Infrared-Laser T-jumps with  $10^4$  K/sec at the SAXS beamline.*

ELETTRA News Number II, Number 21, March 31th (1998)

and ELETTRA Highlights (1998)

G. Pabst, M. Rappolt, H. Amenitsch, S. Bernstorff and P. Laggner

*Non-Equilibrium Response-Kinetics of Phospholipid Bilayers in the Biologically Relevant La-Phase: A REAL-TIME, REAL-SPACE MOVIE.*

ELETTRA News Number: 29 - November 30, 1998

M. Rappolt, H. Amenitsch, S. Bernstorff and P. Laggner

*Highly resolving (<10 mK) Temperature-Gradient Cell for X-ray Scattering Studies on Solutions.*

ELETTRA News Number II, Number 23, May 29 (1998)  
and ELETTRA Highlights (1998)

### **Doctoral Theses**

Magdy Lucic-Lavcevic

*Rasprsenje X-zraka pod malim kutom na filmovima nanofaznog TiO<sub>2</sub> Sinchrotrone Source X-ray Scattering at Small Angle on Films of Nanophased TiO<sub>2</sub>.*

University of Zagreb, Department of Physics, Zagreb, Croatia, 29. XII 1998

Magdalena Pregetter

*Struktur und Dynamik von Lipiddomaenen in Low Density Lipoproteinen.*

TU Graz, Biochemie, TU Graz, Physik, Dr. techn. Promotion, December 1998

Erhard Schafner

*Untersuchung der mikrostrukturellen Entwicklung von hochverformten Metallen mittels Röntgen-Bragg-Profil-Analyse.*

Dissertation, Universitaet Wien, Austria, June 1998

## Author Index

ÅGREN, P.	98
ALTPETER, I.	41
AMENITSCH, H.	34 36 39 41 44 51 53 55 57 61 63 65 67 69 73 75 78 80 83 90 92 98 100 103 105 107 110 112
ASHLEY, C.C.	44
BAGNI, M.A.	44
BALDRIAN J.	34
BANERJEE, S.	36
BATRA, I.S.	36
BERNSTORFF, S.	34 36 39 41 44 51 53 55 61 63 69 75 78 80 83 85 90 92 94 100 103 105 107 110 112
BESCH, H.J.	110
BHAGAT, N.	92
BLANCHARD, J.	98
BONGAERTS, K.	51
BRADSHAW, J.	46
BRUNI, P.	88
CACIUFFO, R.	88
CARRARA, S.	85
CARSUGHI, F.	70
CECCHI, G.	44
CESARO, A.	73 100
CHMIELEWSKI, A.G.	90
CIUCHI, F.	77
COLOMBINI, B.	44
CORNI, F.	83
CSEH, Z.	53 55
DASANNACHARYA, B.A.	92
DARKES, M.	46
DEL SIGNORE, F.	48
DOMAGALA, J.	90
DUBCEK, P.	83 85 94
EROKHIN, V.	85
EVMENENKO, G.	51
FABRI, D.	100
FARKAS, R.	50
FAVILLA, R.	48
FRANCESCANGELI, O.	88
FRATZL, P.	78 80 112
FUNARI, S.S.	75
GAMINI, A.	51
GARAB, G.	53 55
GEBHARDT, R.	69
GOEL, P.S.	92

GRABNER, B.	80
GRIFFITHS, P.J.	44
GRIGORIEW, H.	90
GUPTA, A.	92
HANAK, P.	39 41
HEBESBERGER, T.	39
HEUMANN, H.	61 69
HORKY, M.	34
IACUSSI, M.	88
JÁVORFI, T.	53 55
KARNTHALER, H.P.	39
KLAUSHOFER, K.	78 112
KOPACZ, I.	41
KRIECHBAUM, M.	50 98 105
LAGGNER, P.	34 50 63 65 67 98 105
LAUER, I.	61 69
LINARI, M.	59
LINDEN, M.	98
LOHNER, K.	46 57
LOMBARDI, V.	59
LUCIC-LAVCEVIC, M.	94
LUCII, L.	59
MACCIONI, E.	48
MADDALENA, A.	92
MALHOTRA, N.	92
MARIANI, P.	48 70
MAURELLI, E.	88
MAZUMDER, S.	36
MENK, R.H.	107 110
MILAT, O.	94
MINGLER, B.	39
NAWROTH, T.	61 69
NICOLINI, C.	85
ORTHEN, A.	110
OTTAVIANI, G.	83
OTTONELLO, P.	103
PABST, G.	63 65
PADDEU, S.	85
PAOLETTI, S.	51
PARADOSSI, G.	100
PARIS, O.	78 80 112
PATERNOLLI, C.	85
PAVEL, N.	110
PIAZZESI, G.	59
PIPPAN, R.	39
PIVAC, B.	83
PRASSL, R.	50 67
PREGETTER, M.	67

PRINCIPI, G.	92
PRINCIVALLE, F.	73
RAPP, G.	75
RAPPOLT, M.	63 65 75 110
RHEYNAERS, H.	51
RICHTER, F.	75
ROMANZETTI, S.	70
ROSCHGER, P.	78 112
ROSENHOLM, J.B.	98
RÖBLE, M.	61 69
ROTTIGNI, G.A.	103
RUSTICHELLI, F.	70 77
SALVATO, B.	48
SARVESTANI, A.	107 110
SAUER, N.	110
SCHAFLER, E.	39 41
SCHWARZENBACHER, R.	98
SCHÜTT, F.	98
SEQUEIRA, A.	36
SPINOZZI, F.	48 70
STAUDEGGER, E.	46 57
STEINHART, M.	34 50 105
SUSSICH, F.	73 100
TEWARI, R.	36
THEUNISSEN, E.	51
TONINI, R.	83
TURKOVIC, A.	94
UNGAR, T.	39 41
VALKOVA, L.	85
VANNICELLI, M.E.	59
VLCEK, P.	34
WALENTA, A.H.	110
WHITE, J.W.	77
WOO, D.	75
YANG, B.	77
ZANELLA, G.	103
ZANNONI, R.	103
ZEHETBAUER, M.	39 41
ZIZAK, I.	78 80 112